Phototriggerable peptidomimetics for the inhibition of Mycobacterium turberculosis ribonucleotide reductase by targeting protein-protein binding

Christoffer Karlsson,[a] Magnus Blom,[a] Miranda Johansson (neé Varedian),[a] Anna Jansson,[b] Enzo Scifo,[c] Anders Karlén,[b] Thavendran Govender,[d] Adolf Gogoll[a*]

[a] Department of Chemistry BMC, Uppsala University, Box 576, S-751 23 Uppsala, Sweden
[b] Department of Medicinal Chemistry, Organic Pharmaceutical Chemistry, Uppsala University, Box 574, S-751 23 Uppsala, Sweden
[c] Department of Cell and Molecular Biology, Structural Biology, Uppsala University, Box 597, S751 24 Uppsala, Sweden
[d] Catalysis and Peptide Research Unit, University of KwaZulu Natal, Durban 4000, South Africa

Contents

1. Syntheses

3'-Bromocinnamic acid (10).[1] A mixture of compound **9** (10.354 g, 56.0 mmol), malonic acid (9.317 g, 89.5 mmol), piperidine (16 drops) and pyridine (5.6 ml) was refluxed (105 °C, 100 min). Ice and HCl (conc., 12 ml) was added. The white precipitate that formed was filtered off and washed with HCl (1 M, 40 ml). The filtrate was recrystallised from EtOH (50 ml), the crystals were washed with cold MeOH (~0 °C, 2×20 ml) and HCl (1 M, 2×40 ml) and were put on vacuum over night. Yield: 6.480 g, 66 %; white crystals; Tm: 180-182°C (lit. 178-182 °C); ^{1}H NMR: (500 MHz, CDCl$_3$) δ = 6.47 (d, J = 16.1 Hz, 1H, CHCOOH), 7.30 (d, J = 7.8 Hz, 1H,ArH), 7.48 (d, J = 7.8 Hz, 1H, ArH), 7.55 (d, J = 7.8 Hz, 1H, ArH), 7.70 (m, 2H, ArH, CHCHCOOH) ppm; ^{13}C NMR: (125 MHz, CDCl$_3$) δ = 121.0, 123.7, 127.7, 131.5, 131.7, 133.9,138.0, 144.2, 169.6 ppm.

Methyl 3'-bromocinnamate (11).[1] A mixture of compound **10** (2.010 g, 8.9 mmol), HCl (12 M, 1 drop) and MeOH (6 ml) was heated in a microwave cavity (130 °C, 50 min). The solvent was evaporated. Yield: 2.143 g, 100 %; white crystals; ^{1}H NMR: (500 MHz, CDCl$_3$) δ = 3.82 (s,3H, CH$_3$), 6.45 (d, J = 16.0 Hz, 1H, CHCOOH), 7.28 (m, 5H, ArH, CHCHCOOH) ppm; ^{13}C NMR: (125 MHz, CDCl$_3$) δ = 51.8, 119.2, 123.0, 126.6, 130.3, 130.7, 133.0, 136.4, 143.1, 166.9 ppm.

Methyl 3'-bromodihydrocinnamate (12).[1] MeOH (10 ml) and EtOAc (20 ml) was added dropwise to a mixture of compound **11** (1.000 g, 4.1 mmol), NaBH$_4$ (471 mg, 12.4 mmol) and Ni(OAc)$_2$ · 4 H$_2$O (1.548 g, 6.2 mmol). The mixture was kept under H$_2$ atmosphere (1 bar) and stirred at r.t. for 45 min. The solvent was evaporated, which yielded a black residue. The residue was taken up in DCM (100 ml) and was washed with H$_2$O (dist., 100 ml). The aqueous phase was washed with DCM (3×100 ml). The combined organic phases were dried (Na$_2$SO$_4$), filtered through Celite and evaporated. Yield: 1.131 g, 100 %; white crystals; ^{1}H NMR: (500 MHz, CDCl$_3$) δ = 2.64 (t, J = 7.6 Hz, 2H, β-CH_2), 2.95 (t, J = 7.6 Hz, 2H, α-CH_2), 3.69 (s, 3H, CH$_3$), 7.15 (m, 4H, ArH) ppm; ^{13}C NMR: (125 MHz, CDCl$_3$) δ = 30.4, 35.2, 51.6, 122.4, 126.9, 129.3, 130.0, 131.3, 142.7, 172.8 ppm.

3'-bromohydrocinnamic acid (13).[2] Compound **12** (529 mg, 2.2 mmol) and NaOH (87 mg, 2.2 mmol) was dissolved in EtOH (22 ml). The solution was refluxed for 2 h. The solvent was removed and the white residue was dissolved in water. HCl (conc., 12 ml) was added to pH ≈ 1. The solution was extracted with ether (3×100 ml) and the combined organic phases were dried over Na$_2$SO$_4$, filtered and evaporated. Yield: 480 mg; 99 %; white crystals; ^{1}H NMR: (500 MHz, CD$_3$OD) δ = 2.68 (t, J = 7.5 Hz, 2H, β-CH_2), 2.93 (t, J = 7.5 Hz, 2H, α-CH_2), 7.15 (m, 2 H, ArH), 7.37 (m, 2 H, ArH) ppm; ^{13}C NMR: (125 MHz, CD$_3$OD) δ = 30.3, 35.3, 127.1, 128.7, 129.7, 130.2, 131.5, 142.6, 178.2 ppm.

N-Boc-2-(3'-bromophenyl)-ethylamine (14).[1] A solution of compound **13** (365 mg, 1.5 mmol), NaN$_3$ (683 mg, 10.5 mmol), Bu$_4$NBr (73 mg, 0.23 mmol), ZnBr$_2$ (11 mg, 0.05 mmol) and di-*tert*-butyl dicarbonate (360 mg, 1.7 mmol) in THF (15 ml) was stirred at 40 °C for 48h. NaNO$_2$ (10 % aqueous solution, 30 ml) and EtOAc (30 ml) was added to the reaction mixture and it was stirred at r.t. for 20 min. The organic phase was evaporated and purified by flash column chromatography (gradient eluent: EtOAc/pentane, 0:1, 1:19, 1:9, 1:4). Yield: 108 mg; 24 %; colourless oil; ^{1}H NMR (500 MHz, CDCl$_3$) δ = 1.43 (s, 9H, tBu), 2.76 (t, J = 7.0Hz, 2H, α-CH$_2$), 3.35 (br t, J = 7.0 Hz, 2H, β-CH$_2$), 4.56 (br s, 1H, NH), 7.12 (dm, J = 7.7 Hz, 1H,ArH-6), 7.17 (ddd, J = 7.7, 7.7, 0.9 Hz, 1H, ArH-5), 7.34 (m, 2H, ArH-2, ArH-4) ppm; ^{13}C NMR (125 MHz, CDCl$_3$) δ = 28.3, 34.8, 41.5, 79.3, 122.5, 127.4, 129.4, 130.0, 131.8, 141.3, 155.7 ppm.

N-Boc-(3-vinylphenyl)-ethylamine (15).[1] Two vials, each containing a mixture of compound **14** (662 mg, 2.2 mmol), Pd(PPh$_3$)$_2$Cl$_2$ (46 mg, 0.07 mmol), LiCl (234 mg, 5.5 mmol), tributylvinyltin (970 μl, 3.3 mmol) and DMF (1.4 ml) were heated in a microwave cavity (130 °C, 25 min). The mixtures were pooled, filtered through Celite and washed with DCM. Flash column chromatography (eluent: EtOAc/pentane, 1:4) was performed on the filtrate. Yield: 859 mg, 79 %; yellow oil; ^{1}H NMR: (500 MHz, CDCl$_3$) δ = 1.43 (s, 9H, tBu), 2.78 (t, J = 6.9 Hz, 2H, α-CH$_2$), 3.36 (br t, J = 6.9 Hz, 2H, β-CH$_2$), 4.49 (br s, 1H, NH), 5.24 (dd, J$_Z$ =10.9, Jgem = 0.9 Hz, 1H, CHC*H*$_2$), 5.75 (dd, J$_E$ = 17.6, J$_{gem}$ = 0.9 Hz, 1H, CHC*H*$_2$), 6.72 (dd, J$_E$ = 17.6, J$_Z$ = 10.9 Hz, 1H, C*H*CH$_2$), 7.08 (m, 1H, Ar-H), 7.24 (m, 3H, Ar-H) ppm; ^{13}C NMR: (125MHz, CDCl$_3$) δ = 28.3, 36.0, 41.6, 79.1, 113.9, 124.2, 126.6, 128.2, 128.7, 136.7, 137.7, 139.1,155.8 ppm; Alternative synthesis of compound **8**: 2-(3-Vinylphenyl)-ethylamine (62 mg, 0.42 mmol) and di-*tert*-butyl dicarbonate (108 mg, 0.49 mmol) was dissolved in DCM (1.3 ml). K$_2$CO$_3$ (176 mg, 1.2 mmol) was dissolved in H$_2$O (dist., 1.3 ml) and was added to the DCM solution. The mixture was stirred at r.t. for 46 h. The organic phase was dried over Na$_2$SO$_4$ and the solvent was evaporated. Yield: 91 mg, 90 %; yellow oil.

E-1-(3-(N-Boc-(2-aminoethyl))phenyl)-2-(O-methyl hydrocinnam-3'-yl)-ethene (16).[1] Compound **15** (89.0 mg, 0.360 mmol), compound **12** (96.2 mg, 0.396 mmol), Pd(OAc)$_2$ (4.0 mg, 0.018 mmol), tri-*o*-tolyl-phosphine (11.0, mg, 0.036 mmol) and Et3N (0.150 ml, 1.080 mmol)was dissolved in DMF (1.8 ml) and microwaved (120 °C, 30 min). The brownish reaction mixture was filtered through Celite into a separatory funnel and was washed with DCM (25ml). The red solution was washed with HCl (1 M, 25 ml), which afforded a peach colouredemulsion that was washed with NaHCO$_3$ (aq, sat, 25 ml). The combined organic phases weredried over MgSO$_4$, filtered and evaporated. Flash column chromatography (eluent: EtOAc/pentane, 1:9) was performed on the red oil. Yield: 45 mg; 31 %; colorless crystals; ^{1}H NMR (500 MHz, CDCl$_3$) δ = 1.44 (s, 1H, tBu), 2.67 (t, J = 8.0 Hz, 2H, C*H*$_2$COOH), 2.83 (br t, J =7.0 Hz, 2H, C*H*$_2$CH$_2$NH), 2.98 (t, J = 8.0 Hz, 2H, C*H*$_2$CH$_2$COOH), 3.41 (br t, J = 7.0 Hz, 2H,C*H*$_2$NH), 3.67 (s, 3H, Me), 4.57 (br s, 1H, NH), 7.12 (m, 4H, Ar-H), 7.30 (m, 2H, Ar-H), 7.35 (m,4H, Ar-H) ppm.

E-1-(3-(2-aminoethyl)phenyl)-2-(O-methyl hydrocinnam-3'-yl)-ethene (17).[1] Compound **16** (2.924 mg, 7.14 mmol) was dissolved in TFA (15 ml) and DCM (15 ml). The solution was stirred at r.t. for 20 min and was then evaporated. Crude yield: 2.204 g; 100 %; yellow oil; ^{1}H NMR (CDCl$_3$, 500 MHz) δ = 2.69 (t, J = 7.8 Hz, 2H, C*H*$_2$COOH), 2.96 (t, J = 7.8 Hz,2H, C*H*$_2$CH$_2$NH), 3.02 (t, J = 6.9 Hz, 2H, C*H*$_2$CH$_2$COOH), 3.39 (br t, J = 6.9 Hz, 2H, C*H*$_2$NH), 3.69(s, 3H, Me), 7.32 (m, 12H, Ar-H, NH$_2$) ppm.

E-1-(3-(N-Fmoc-(2-aminoethyl))phenyl)-2-(O-methyl hydrocinnam-3'-yl)-ethene (18).[1] Compound **17** (2.204 g, 7.14 mmol) and 9-fluorenylmethyl chloroformate (2.032 g, 7.85 mmol) was dissolved in 1,4-dioxane (75 ml) and Na$_2$CO$_3$ (10 %, aq, 75 ml). The heterogeneous mixture was stirred at r.t. for 24 hours and was then extracted with DCM. The organic phase was dried (Na$_2$SO$_4$), filtered and evaporated. Crude yield: 3.754 g; 100 %; white crystals; ^{1}H NMR (400 MHz, CDCl$_3$) δ = 2.66 (t, J = 7.5 Hz, 2H, C*H*$_2$COOH), 2.86 (br t, J =6.7 Hz, 2H, C*H*$_2$CH$_2$NH), 2.98 (t, J = 7.5 Hz, 2H, C*H*$_2$CH$_2$COOH), 3.50 (br t, J = 6.7 Hz, 2H, C*H*$_2$NH), 3.68 (s, 3H, CH$_3$), 4.22 (br t, J = 7.0 Hz, 1H, Fmoc-CH), 4.40 (br d, J = 7.0 Hz, 2H, Fmoc-CH$_2$), 4.83 (br s, 1H, NH), 7.08 (m, 4H, ArH), 7.39 (m, 10H, ArH), 7.56 (m, 2H, Fmoc-ArH), 7.75 (m, 2H, Fmoc-ArH) ppm; ^{13}C NMR: (100 MHz, CDCl$_3$) δ = 30.9, 35.6, 36.1, 42.1,47.2, 51.6, 66.6, 119.9, 124.5, 124.7, 125.0, 126.5, 126.9, 127.00, 127.04, 127.6, 128.1, 128.4, 128.82, 129.84, 128.9, 137.4, 137.6, 139.1, 140.9, 141.2, 143.9, 156.2, 178.3 ppm.

E-1-(3-(N-Fmoc-(2-aminoethyl))phenyl)-2-(hydrocinnam-3'-yl)-ethene (2).[1]
Compound **18** (3.754 g, 7.14 mmol) was dissolved in DCM (220 ml) and HCl (conc., 15 ml) was added. The solution was refluxed at 120 °C for 17 hours, with a NaOH trap connected to the reflux condenser to trap HCl (g). The reaction mixture was extracted with DCM and the combined organic phases were dried (Na_2SO_4), filtered and evaporated, yielding a yellow solid. Flash chromatography was performed (eluent: EtOAc/pentane/AcOH, 33:66:1). Yield: 1.887 g; 34 %; white crystals; ^{1}H NMR (500 MHz, $(CD_3)_2SO$) δ = 2.55 (t, J = 7.6 Hz, 2H, CH_2COOH), 2.74 (t, J = 7.1 Hz, 2H, CH_2CH$_2$NH), 2.83 (t, J = 7.6 Hz, 2H, CH_2CH$_2$COOH), 3.26 (brt, J = 7.1 Hz, 2H, CH_2NH), 4.19 (t, J = 6.9 Hz, 1H, Fmoc-CH), 4.28 (d, J = 6.9 Hz, 2H, Fmoc-CH$_2$),7.09 (dm, J = 7.7 Hz, 1H, ArH), 7.13 (dm, J = 7.6 Hz, 1H, ArH), 7.20 (m, 2H, CH=CH), 7.26 (dd,J = 7.5, 7.5 Hz, 1H, ArH), 7.27 (dd, J = 7.5, 7.5 Hz, 1H, ArH), 7.30 (ddd, J = 7.6, 7.4, 1.2 Hz, 2H, Fmoc-ArH), 7.39 (ddm, J = 7.6, 7.6 Hz, 2H, Fmoc-ArH), 7.43 (m, 4H, ArH), 7.65 (dm, J = 7.4 Hz, 2H, Fmoc-ArH), 7.86 (dd, J = 7.6, 1.2 Hz, 2H, Fmoc-ArH) ppm; ^{13}C NMR: (100 MHz,$(CD_3)_2SO$) δ = 30.6 (α-CH$_2$), 35.4 (α'-CH$_2$), 35.5 (β-CH$_2$), 41.8 (β'-CH$_2$), 46.8 (Fmoc-CH), 65.3 (Fmoc-CH$_2$), 120.1 (Ar-C), 121.4 (Ar-C), 124.3 (Ar-C), 125.2 (Ar-C), 126.3 (Ar-C), 126.9 (Ar-C), 127.0 (Fmoc-Ar-C), 127.3 (Ar-C), 127.6 (Fmoc-Ar-C), 128.0 (Ar-C), 128.3 (Ar-C), 128.4(Ar-C), 129.0 (Fmoc-Ar-C), 137.0 (Ar-C), 137.5 (Ar-C), 139.4 (Fmoc-Ar-C), 139.9 (Ar-C), 140.7 (Fmoc-Ar-C), 141.5 (Ar-C), 144.0 (Fmoc-Ar-C), 156.1 (OCONH), 174.0 (COOH) ppm; IR: 3340, 2943, 1691 cm-1; MS (ESI, positive ion mode, 30 eV) m/z (%) = 1058.2 (2) [2M+Na]$^+$, 719.4 (10) [M+Na+Fmoc-COO]$^+$, 540.2 (100) [M+Na]+, 179.0 (50) [Fmoc-COO]$^+$; MS (ESI, negative ion mode, 30 eV) m/z (%) = 1033.6 (26) [2M-H]$^-$, 293.8 (100), [M+2Cl]$^{2-}$.

2. Computational details

2.1. Experimental details of calculations

Calculations were performed using the Maestro 9.0.109 interface. Local energy minimization of structures was performed with MacroModel (OPLS 2005, H_2O solvent, PRCG, number of steps ≤ 10 000). Conformational searches were performed on local minima using MCMM (2 000 · N steps [N = number of rotatable bonds], minimization conditions as above, number of torsion rotations in each step chosen randomly between 1 and N-1). Unique structures within a 21.0 kJ/mol energy window were saved. Maximal atom deviation for comparison of structural similarity was 0.5 Å, comparing all heavy atoms. The population of each conformation was calculated using the Boltzmann distribution (equation 1).

$$p_i = \frac{g_i * e^{-\frac{E_i}{k_B T}}}{\sum_i g_i * e^{-\frac{E_i}{k_{BT}}}}$$

Equation 1. For each state i, p_i is the population, g_i is the degeneracy and E_i is the potential energy.

The extent of intramolecular hydrogen bonding between peptide chains was then calculated from the populations of all conformations with appropriate hydrogen bonds. Enzyme docking studies were performed with Glide on the RNR dimerization site, both in standard precision mode and in extra precision mode.

2.2. Comparison of conformational search methods

To assess which method would be best to use in conformational searching of the new peptidomimetics,five different methods were employed in searching the conformational space of one molecule. The molecule used was Ac-Trigger-Glu-NHMe and the methods were MCMM (with three different sets of parameters), LMOD and Mixed mode. The method parameters are summarised in table A1. The difference between LMOD, MCMM and mixed mode is described in section 1.5.4. For all methods, the force field used was OPLS 2005, with water solvation model. The miminisation method was PRCG with a maximum number of steps of 10 000. Structures within 21.0 kJ/mol (5.0 kcal/mol) of the global minimum were kept. The maximum atom deviation of structure comparison was 0.5 Å. MCMM was first run with default parameters as defined in Maestro. The number of torsion rotations in each Monte Carlo step is picked at random in a defined interval. Default is 1-5, but the conformational space should be searched more effectively when varying the number of torsion rotations between 1 and N-1, where N is the total number of rotatable bonds in the molecule.14 Therefore, a second MCMM was performed with those parameters (abbreviated "MCMM MCNV"). The default number of Monte Carlo steps is 2000 steps per rotatable bond. To examine the results of a more thorough search, a third MCMM with 3000 steps per rotatable bond was performed (abbreviated "MCMM MCNV 3000").

Table S 1: Parameters for the different search methods.

Abbreviation	Description	Maximum #torsion rotations	#steps per rotatable bond	LMOD move (Å)	Probability of MCMM move
MCMM	Monte Carlo Multiple Minima	5	2000	N/A	1
LMOD	Low Mode	N/A	2000	2.5 – 5.0	0
Mixed	Mixed Mode	5	2000	3.0 – 6.0	0.5
MCMM MCNV	MCMM, #torsion rotations 1 - (N-1)	12	2000	N/A	1
MCMM MCNV 3000	MCMM, #torsion rotations 1 - (N-1), 3000 steps per rotatable bond	12	3000	N/A	1

All methods found roughly the same number of conformers, except for LMOD, which found significantly less. This can be seen in figure A1, which shows the number of conformers within a given energy window. The CPU time required for each search is shown in figure A2 MCMM finished within nine hours, whereas LMOD requires about double that time. The mixed mode search took over 32 hours, *i.e.* triple the time of MCMM. Increasing the number of torsion rotations did not affect CPU time considerably. On the other hand, an increase in the number of steps resulted in a proportional increase in CPU time. The average duplication rate (*i.e.* how many times each conformer is found in average) is shown in figure A2 as well as the standard deviation of the duplication rate. The duplication rate is similar for all methods except LMOD, which has a much higher duplication. MCMM with more steps have a slightly

higher duplication rate than MCMM with fewer steps. Figure A2 shows the acceptance rate (*i.e.* how many of the minimized structures that are within the energy window). It is similar for all methods, except LMOD, which have a much lower acceptance. This reflects the fact that LMOD does not find as many conformers, because more structures are rejected by energy (because they are outside the energy window, hence low acceptance) and more structures are rejected by similarity to a previous structure (because the structure has been found before, hence high duplication). This indicates that the conformers found by LMOD do not represent the whole of conformational space, but only a local region of it.

Number of conformers found
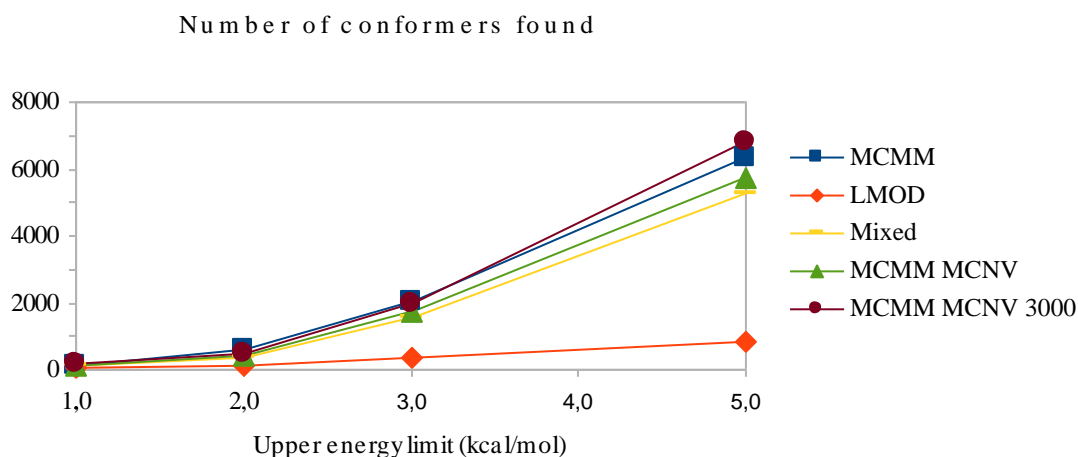
Figure S 1:The number of conformers (lower than 1, 2, 3 and 5 kJ/mol) found by each search method.

Figure A3 shows the duplication rate for the two conformers with the lowest energies. When increasing the number of torsion rotations for the MCMM search, a new global minimum was found, although the second minimum was not found in that search. Both minima were found by the MCMM with more steps. The mixed mode search also found both the lower minima, and with a duplication of three for both, whereas the other methods only found them once or twice. Since the duplication rates are so low, it is hard to say with much certainty which method is the best in finding the lowest-energy conformers. Normally one would like to have a much higher rate of duplication of the lowest-energy conformers, but this molecule is rather large and flexible, which could explain why each conformer is not found as many times as desirable. In conclusion, MCMM and mixed mode give comparable results, although the former is three times faster. LMOD is much less capable of searching the conformational space than the other methods, at least for this particular molecule. Using many torsional rotations is advisable, and increasing the number of steps might be necessary in order to find all the low-energy conformations. However, in the study of the peptidomimetics, it is not quite necessary to find every possible conformer, but it is enough to find a reasonably good representation of the conformational space for qualitative evaluation. The most time effective method would therefore be MCMM with an increased number of torsion rotations and with 2000 steps per rotatable bond. This was the method used for searching the peptidomimetics.
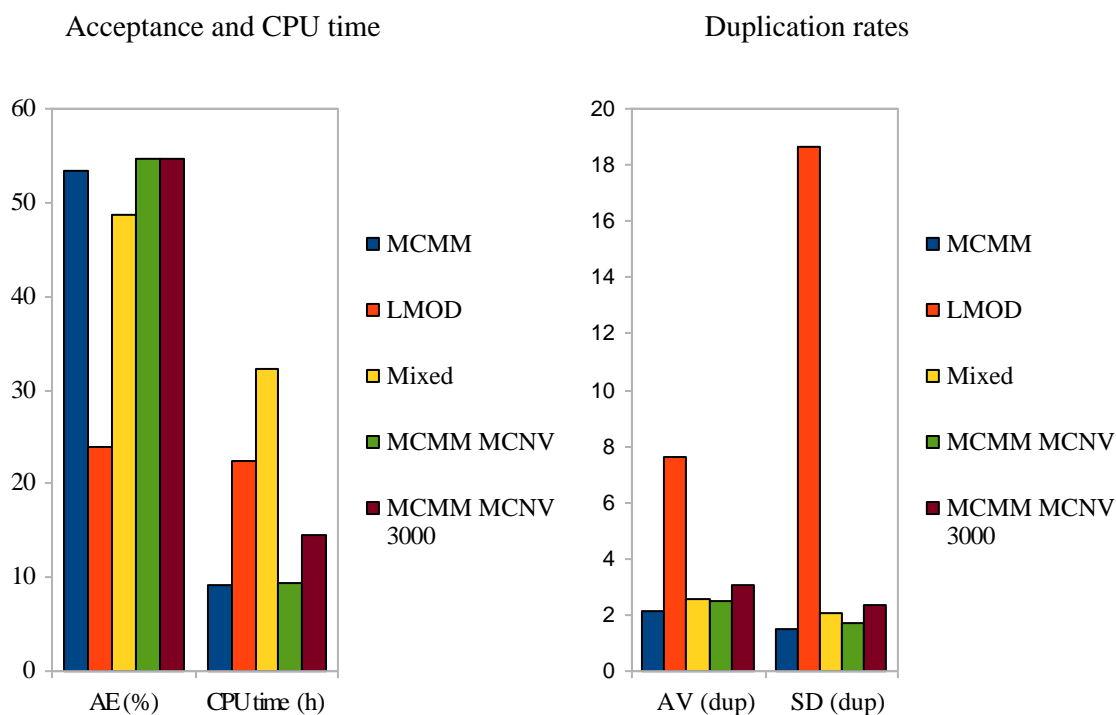
Figure S 2: Various data for the different search methods. Left: The acceptance rate (AE) and CPU timerequired for each method. Right: The average duplication rates (Av(dup)) and the respective standarddeviations (SD(dup)).
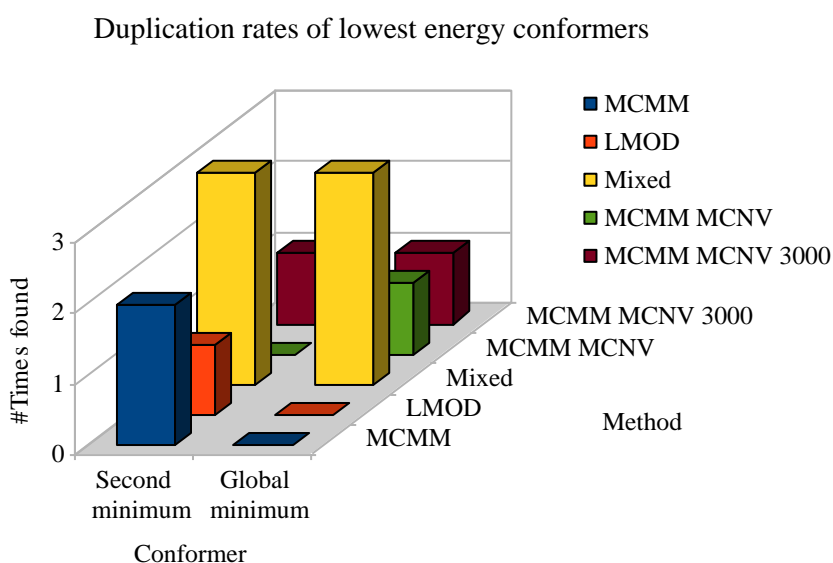
Figure S 3: The duplication rate, i.e. the number of times that the different search methods found the two lowest energy conformers

Peptidomimetic cluster structure comparison

As described, all conformers from the conformational searches of the peptidomimetics were clustered with XCluster. For every peptidomimetic, the structures in each cluster with the lowest energy are overlayed below. To the right are the clusters with populations over 10 % and to the left are clusters with populations between 1 % and 10 %. Clusters with populations below 1 % are omitted here. The population of each cluster (identified by colour) can be

found in the corresponding tables, together with the total population of clusters > 10 % and > 1 %. Double lines in the tables divide the clusters in the left and right images, respectively. Molecules in the *E* configuration are directly below the *Z* form. All structures are drawn with the N-terminal to the left and the C-terminal to the right. Atom colours are described in the table below.

Table S 2: Atom colours of peptidomimetic clusters.

Atom	Colour
C	According to cluster
O	Red
N	Blue
H	Not shown

Ac-Trigger-Phe-OH

Z
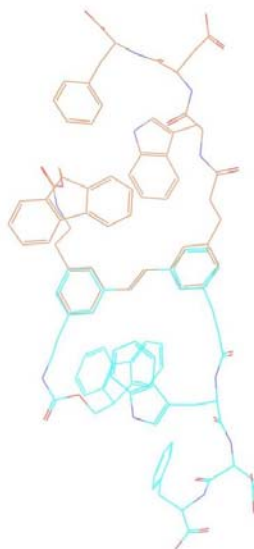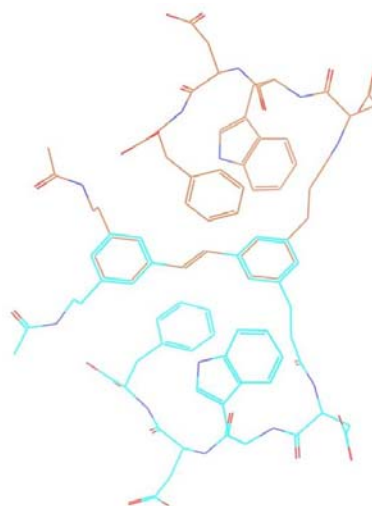
Clusters to the left account for 96.7 % of the population. All shown clusters account for 98.9 % of the population.
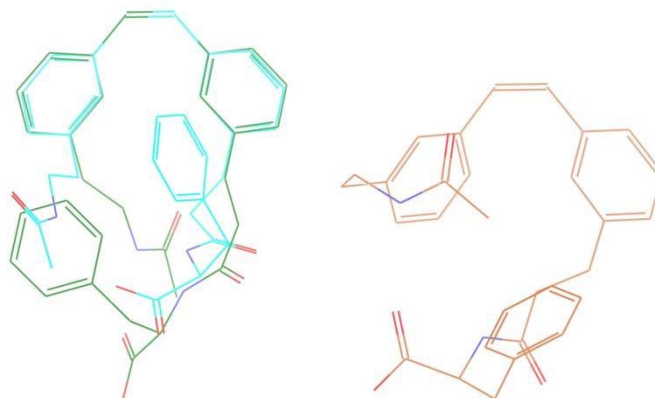
Cluster number	1	3	2
Population	74.8%	21.9%	2.2%
Colour	Cyan	Dark green	Brown

E

Clusters to the left account for 83.4 % of the population. All shown clusters account for 100.0 % of the population.
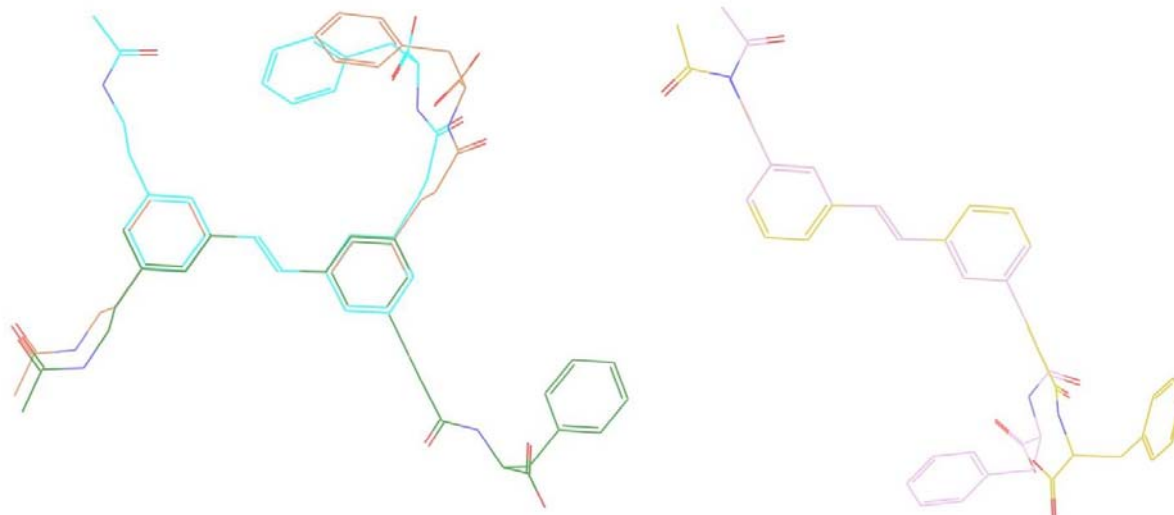
Cluster number	4	1	2	6	5
Population	33.8%	24.9%	24.7%	8.6%	8.0%
Colour	Dark green	Cyan	Brown	Pink	Orange

Fmoc-Trigger-Phe-OH

Z

Clusters to the left account for 83.9 % of the population. All shown clusters account for 95.2 % of the population.
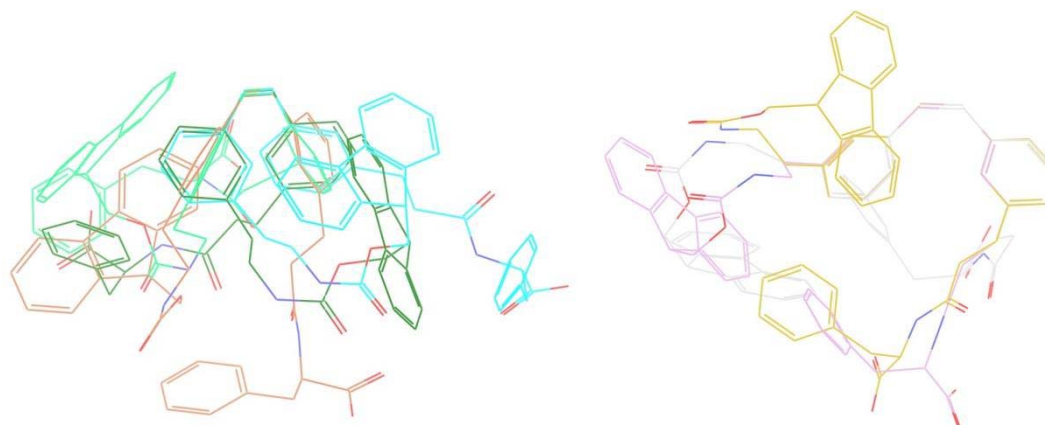
| Cluster number	17	1	28	99	30	67	41
Population	31.9%	21.4%	17.7%	13.0%	8.8%	1.5%	1.0%
Colour	Brown	Cyan	Dark green	Mint green	Orange	Grey	Pink

E

All shown clusters account for 95.0 % of the population. All shown clusters account for 97.4 % of thepopulation.
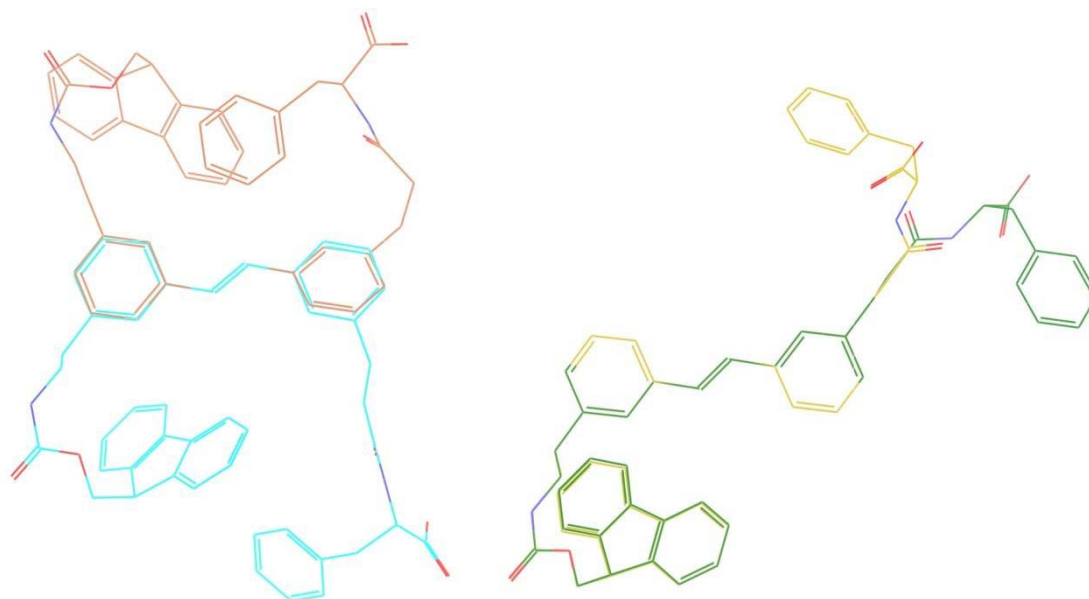
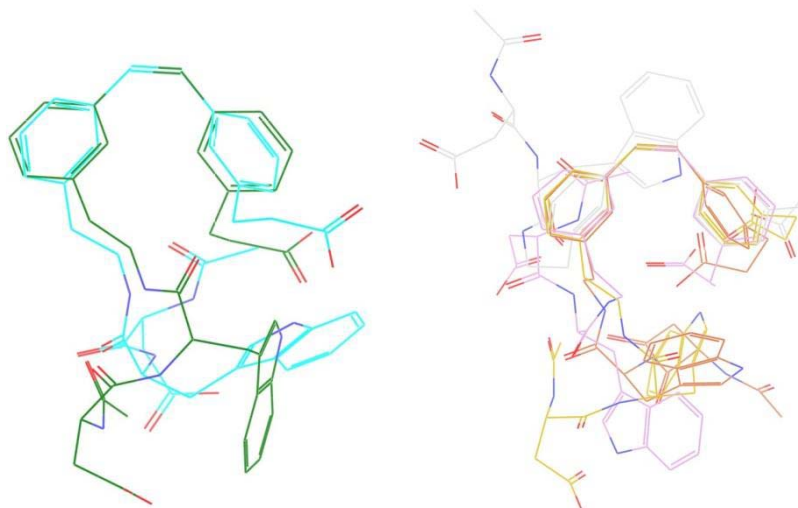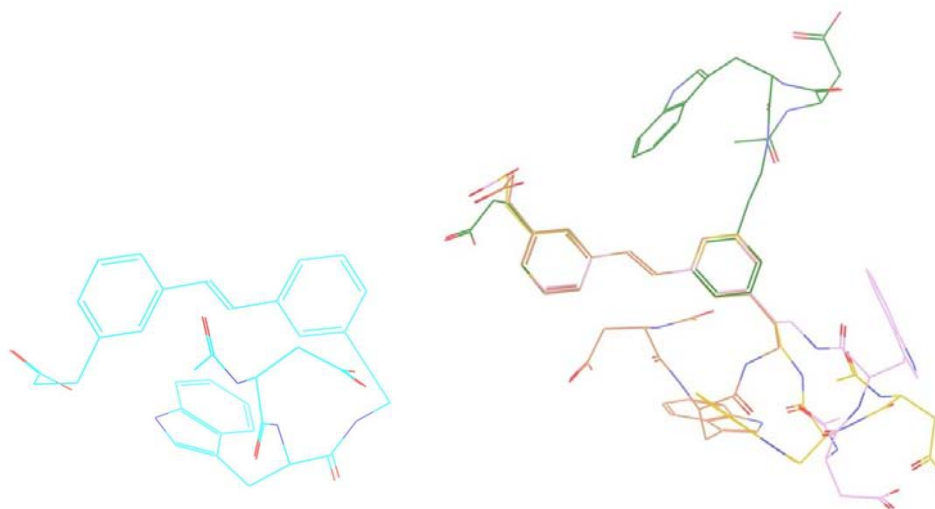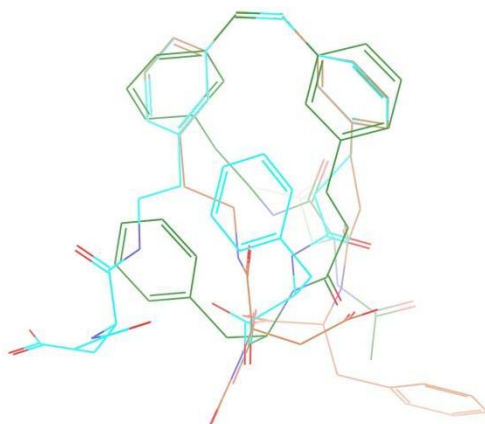| Cluster number	1	2	14	9
Population	62.9%	32.1%	1.2%	1.1%
Colour	Cyan	Brown	Orange	Dark green

Ac-Trigger-Asp-Phe-OH

Z

Clusters to the left account for 88.5 % of the population. All shown clusters account for 98.8 % of the population.
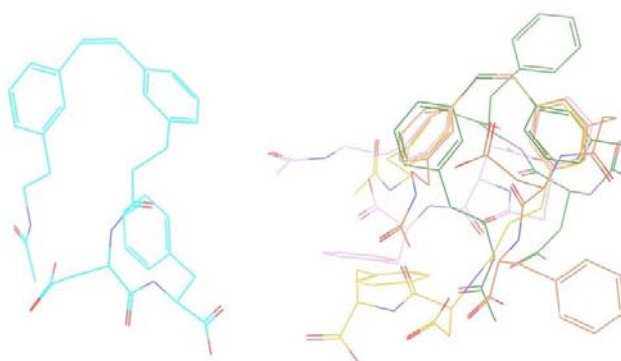
Cluster number	1	4	8	2	30
Population	88.5%	4.2%	2.6%	2.0%	1.6%
Colour	Cyan	Dark green	Orange	Brown	Pink

E

All shown clusters account for 63.0 % of the population. All shown clusters account for 98.4 % of the population.
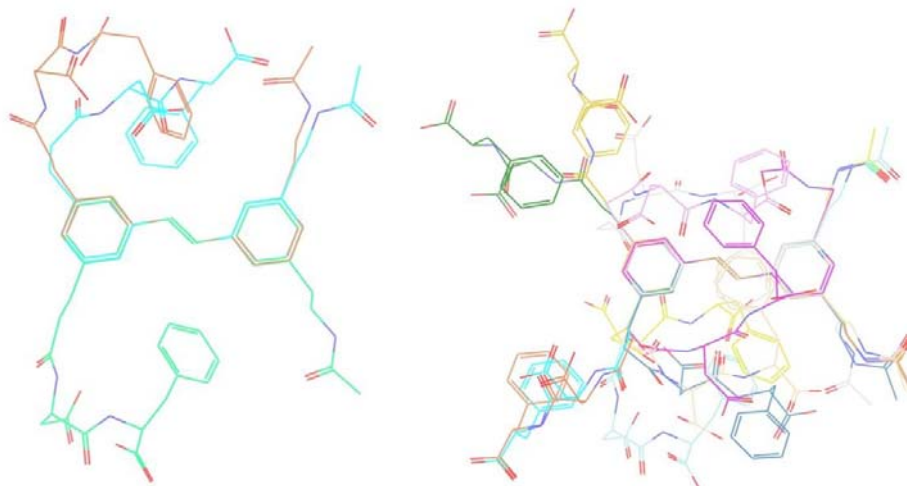
Cluster number	1	16	2	21	11	10	26
Population	37.9%	13.2%	11.9%	6.8%	5.0%	4.3%	4.2%
Colour	Cyan	Mint green	Brown	Pale blue	Pink	Orange	Cyan

| Cluster number	29	17	9	30	12	24	26
Population	3.5%	2.9%	2.6%	1.8%	1.7%	1.5%	1.2%
Colour	Brown	Marine blue	Dark green	Dark green	Grey	Purple	White

Fmoc-Trigger-Asp-Phe-OH

Z

Clusters to the left account for 78.3 % of the population. All shown clusters account for 95.8 % of thepopulation.
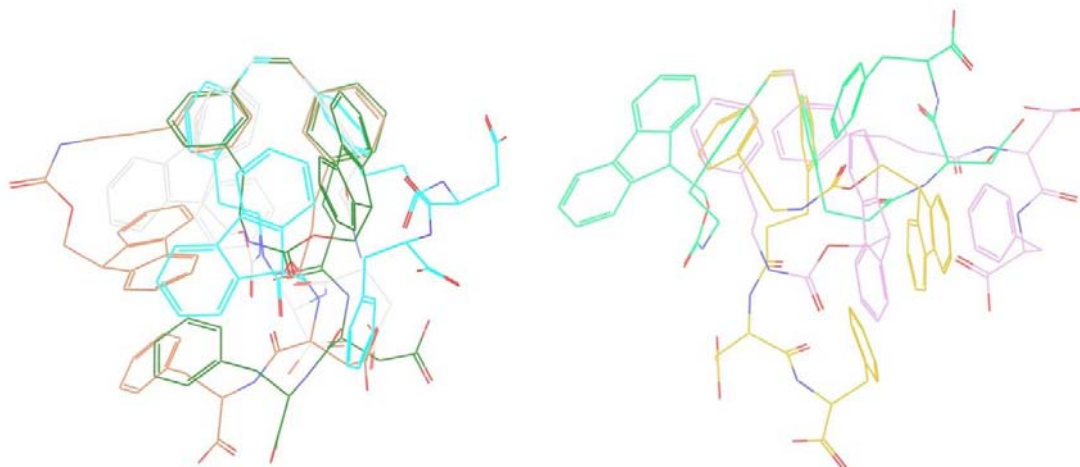
Cluster number	1	6	3	34	25	16	70
Population	26.7%	22.5%	15.6%	13.5%	8.8%	7.5%	1.2%
Colour	Cyan	Dark green	Brown	Grey	Pink	Orange	Mint green

E
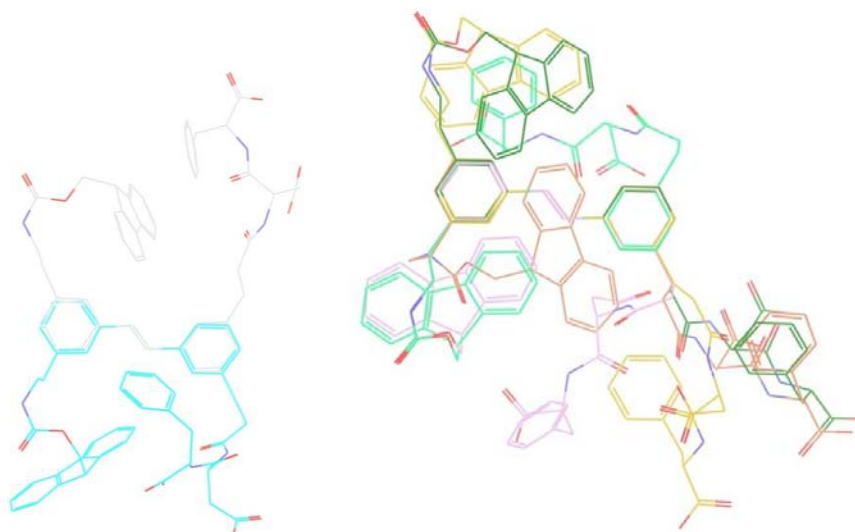
Cluster number	16	1	11	31	2	4	3
Population	53.5%	30.5%	4.3%	4.2%	2.2%	1.1%	1.0%
Colour	Grey	Cyan	Pink	Mint green	Brown	Orange	Dark green

Ac-Trigger-Trp-Asp-Phe-OH

Z

Clusters to the left account for 85.8 % of the population. All shown clusters account for 98.4 % of the population.
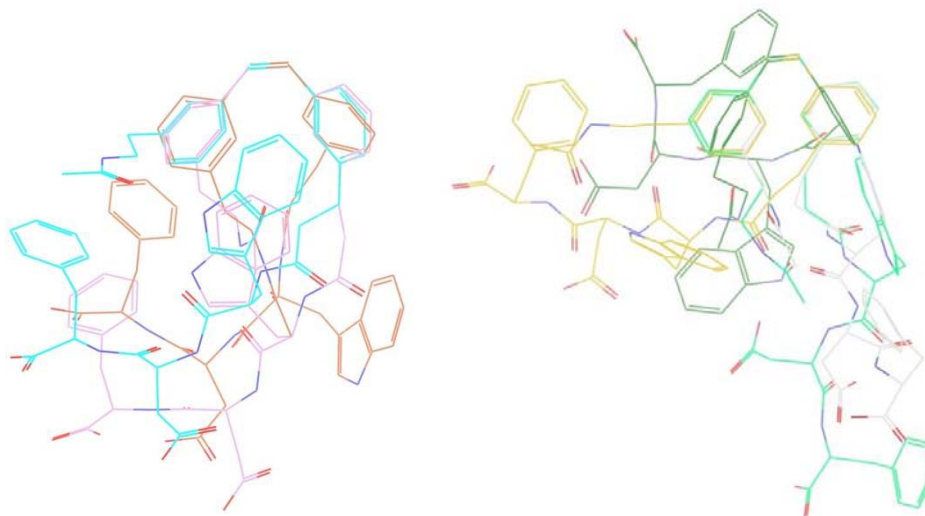
Cluster number	8	2	1	4	23	3	25
Population	37.6%	27.6%	20.6%	6.4%	3.8%	1.4%	1.0%
Colour	Pink	Brown	Cyan	Orange	Grey	Dark green	Mint green

E
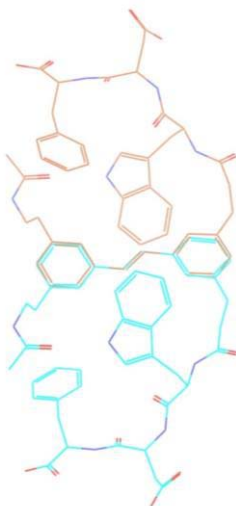
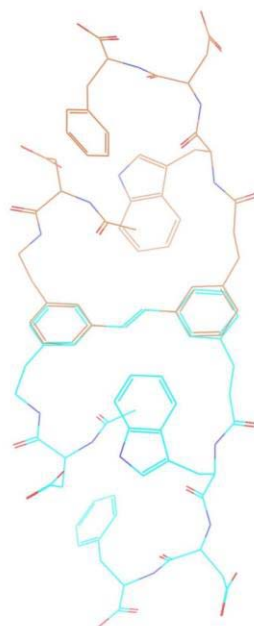| Cluster number	1	7
Population	81.1%	17.1%
Colour	Cyan	Brown

Fmoc-Trigger-Trp-Asp-Phe-OH

Z

Clusters to the left account for 85.6 % of the population. All shown clusters account for 99.9 % of the population.
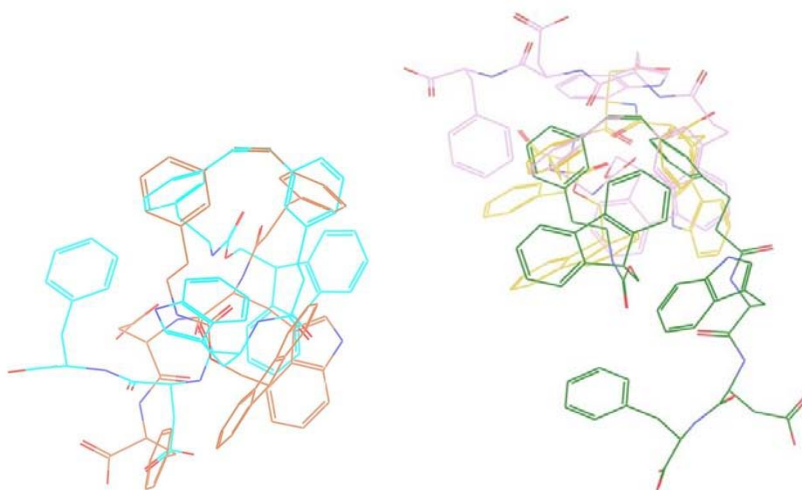
Cluster number	1	2	5	4	6
Population	62.5%	23.1%	9.9%	2.7%	1.8%
Colour	Cyan	Brown	Orange	Dark green	Pink

E

All shown clusters account for 100.0 % of the population. (There are no clusters with populations 1 – 10%.)

Cluster number	1	2
Population	79.7%	20.3%
Colour	Cyan	Brown

Ac-Trigger-Asp-Trp-Asp-Phe-OH

Z

Clusters to the left account for 84.4 % of the population. All shown clusters account for 92.1 % of the population.
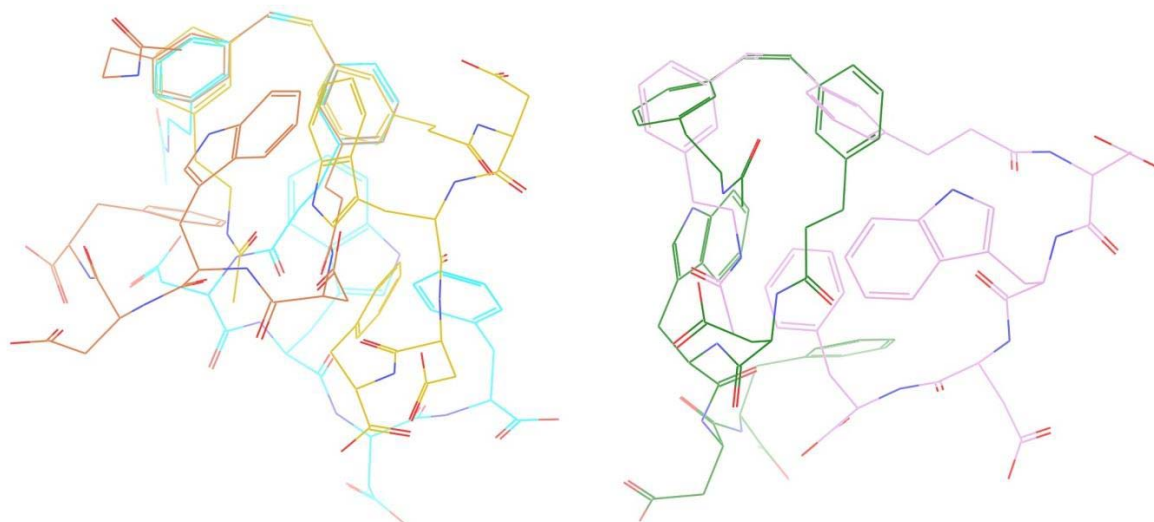
Cluster number	1	11	2	20	3
Population	53.2%	16.1%	15.1%	4.6%	3.1%
Colour	Cyan	Orange	Brown	Pink	Dark green

E

All shown clusters account for 99.7 % of the population. (There are no clusters with populations 1 – 10%.)

Cluster number	1	4
Population	63.6%	36.1%
Colour	Cyan	Brown

Ac-Trp-Trigger-OH

Z

Clusters to the left account for 80.1 % of the population. All shown clusters account for 96.6 % of the population.
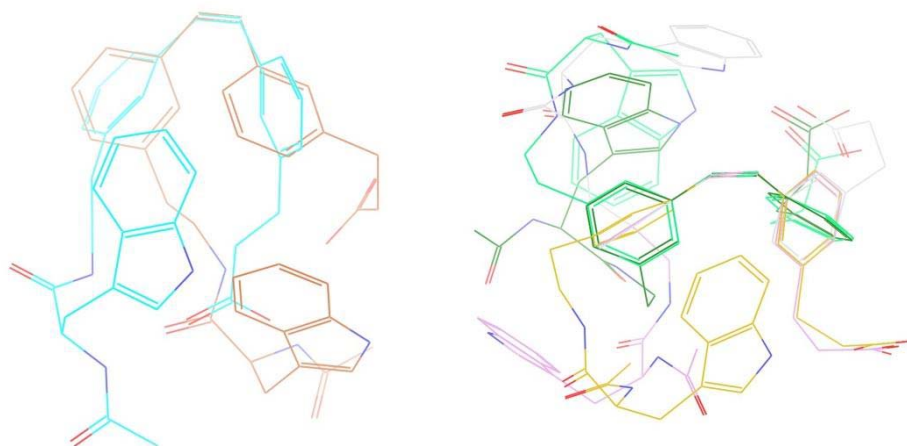
Cluster number	2	1	14	31	11	34	23
Population	43.3%	36.8%	6.8%	4.4%	2.5%	1.7%	1.1%
Colour	Brown	Cyan	Orange	Grey	Dark green	Mint green	Pink

E

Clusters to the left account for 96.3 % of the population. All shown clusters account for 98.3 % of the population.
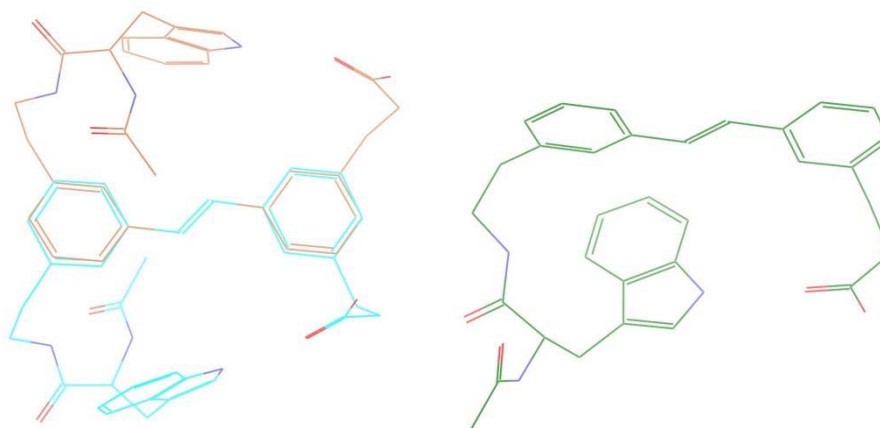
Cluster number	1	2	3
Population	66.2%	30.1%	2.0%
Colour	Cyan	Brown	Dark green

Ac-Asp-Trp-Trigger-OH

Z

Clusters to the left account for 83.5 % of the population. All shown clusters account for 93.9 % of the population.

Cluster number	1	3	2	7	23	10
Population	54.6%	28.9%	4.0%	3.2%	2.0%	1.2%
Colour	Cyan	Dark green	Brown	Orange	Grey	Pink

E

Clusters to the left account for 91.4 % of the population. All shown clusters account for 98.8 % of thepopulation.

Cluster number	1	5	7	8	3
Population	91.4%	2.8%	2.0%	1.6%	1.0%
Colour	Cyan	Dark green	Orange	Pink	Brown

Ac-Asp-Trigger-Phe-OH

Z

All shown clusters account for 96.6 % of the population. (There are no clusters with populations 1 – 10%.)

Cluster number	2	1	5
Population	43.0%	39.0%	14.6%
Colour	Brown	Cyan	Dark green

E

Clusters to the left account for 94.0 % of the population. All shown clusters account for 98.8 % of the population.
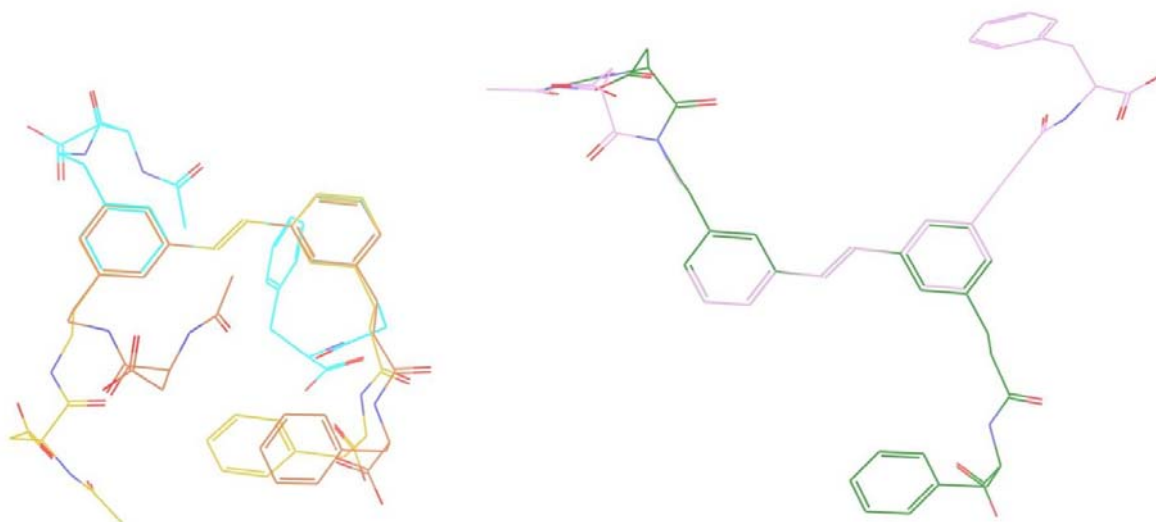
Cluster number	2	1	12	15	10
Population	59.0%	17.7%	17.3%	2.9%	1.9%
Colour	Brown	Cyan	Orange	Pink	Dark green

Ac-Asp-Trigger-Asp-Phe-OH

Z

Clusters to the left account for 97.3% of the population. All shown clusters account for 99.3 % of the population.
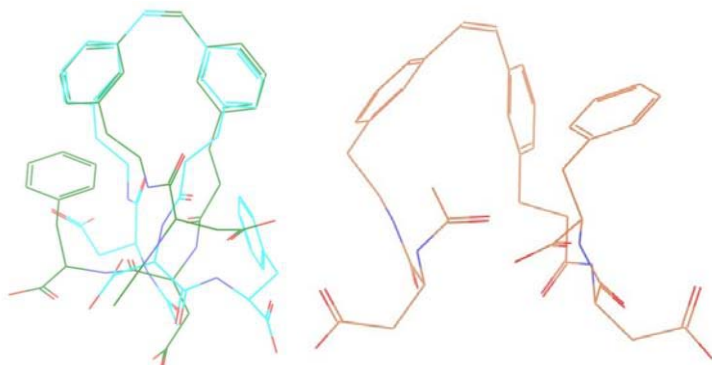
Cluster number	1	6	2
Population	66.1%	31.2%	2.1%
Colour	Cyan	Dark green	Brown

E

Clusters to the left account for 65.8 % of the population. All shown clusters account for 97.0 % of the population.
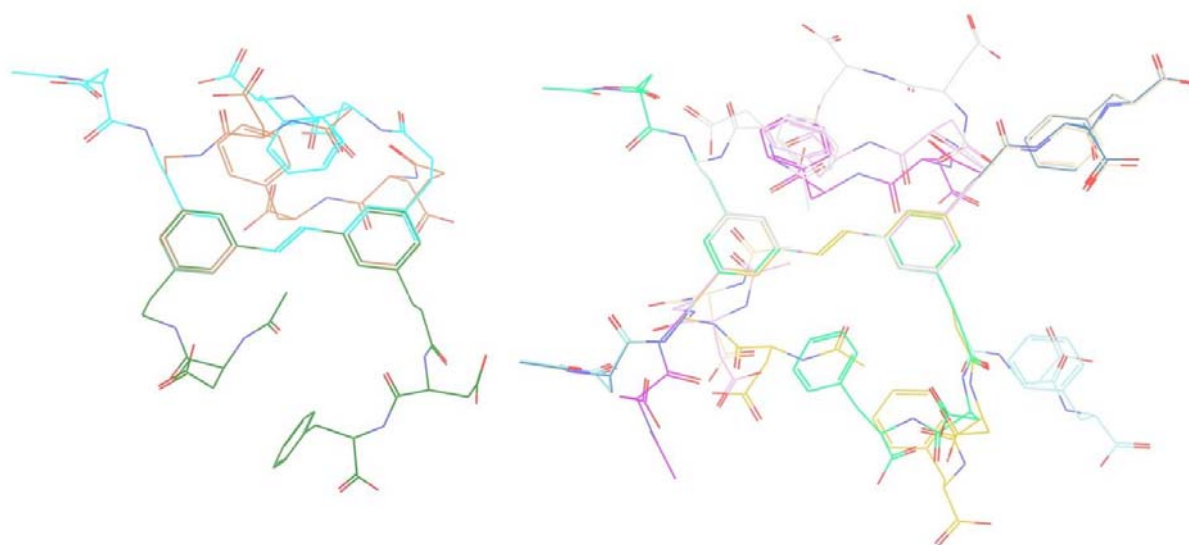
Cluster number	1	7	2	8	10	25	20	44	39	33	14
Population	30.7%	18.3%	16.8%	7.7%	7.1%	6.3%	3.7%	2.4%	1.8%	1.4%	1.0%
Colour	Cyan	Dark green	Brown	Orange	Pink	Marine blue	Mint green	Purple	Pale blue	White	Grey

Ac-Asp-Trigger-Trp-Asp-Phe-OH

Z

Clusters to the left account for 80.5 % of the population. All shown clusters account for 96.7 % of the population.
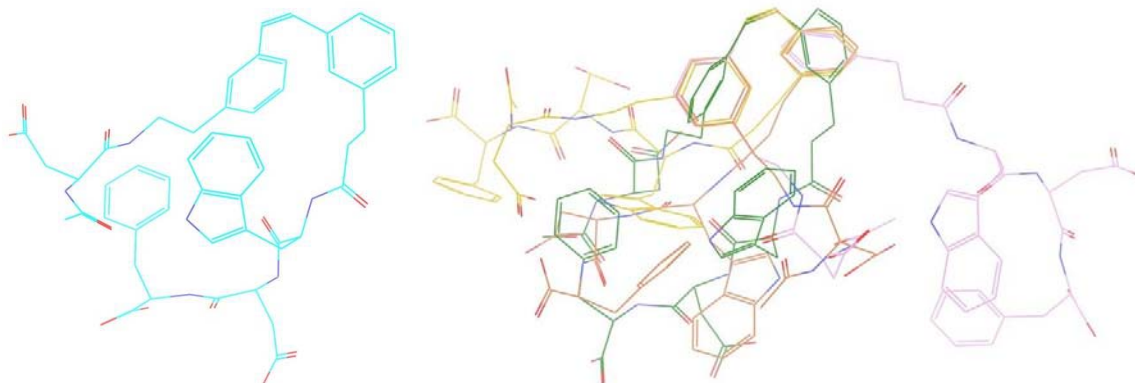
Cluster number	1	3	2	4
Population	80.5%	7.2%	7.1%	1.9%
Colour	Cyan	Dark green	Brown	Orange

E

All shown clusters account for 99.6 % of the population. (There are no clusters with populations 1 – 10%.)

Cluster number	1	4
Population	88.2%	11.4%
Colour	Cyan	Brown

Evaluation of results from calculations

Conformational searches were performed on several shorter analogues of the inhibitory heptapeptide, with a stilbene moiety inserted. The results from those searches were evaluated by comparing the extent of intramolecular hydrogen bonding between the peptide chains attached to the stilbene phototrigger. In some cases the overall geometry of the peptidomimetics was only slightly affected by the isomerization of the stilbene moiety, *i.e.* the extent of hydrogen bonding is the same in the *Z* and *E* peptidomimetics. In other cases, however, the peptide chains could only interact when the stilbene moiety was in the *Z* configuration. This means that the extent of hydrogen bonding was large in the *Z* peptidomimetics, but small in the *E* peptidomimetics. In these cases, the peptidomimetic adopts a folded geometry in the *Z* form, and a more extended geometry in the *E* form. Using this correlation, the overall geometry of the peptidomimetics could be evaluated simply by calculating the extent of hydrogen bonding. Comparing this to examination of the individual low energy conformations of each peptidomimetic, it appears that the extent of hydrogen bonding was indeed a good measurement for the overall geometry in these cases. The hydrogen bonding of each peptidomimetic is shown in table Table S 3 and Figure 6.

In five of the peptidomimetics, isomerizing the stilbene moiety (the "trigger") from *Z* to *E* had a large impact on the overall geometry, according to the calculations. These peptidomimetics were Ac-Trigger-Phe-OH, Ac-Trigger-Asp-Phe-OH, Fmoc-Trp-Asp-Phe-OH, Ac-Asp-Trigger-Phe-OH and Ac-Asp-Trigger-Asp-Phe-OH. Docking studies were performed to see whether they could bind to the RNR dimerization site. All five peptidomimetcs had the possibility of binding in both the *Z* and the *E* configurations.

Table S 3: The data presented in Figure 6, i.e. the percentage of the peptidomimetics in each configuration that has hydrogen bonds between the side chains. Peptidomimetics with a large difference has bold figures.

Peptidomimetic	*Z*	*E*	Difference
Ac-Trigger-Glu-NHMe (Model compound)	65.8 %	7.8 %	58.0 %
Ac-Trigger-Phe-OH	91.7 %	0.0 %	**91.7 %**
Fmoc-Trigger-Phe-OH	11.6 %	0.0 %	11.6 %
Ac-Trigger-Asp-Phe-OH	81.1 %	20.0 %	61.1 %
Fmoc-Trigger-Asp-Phe-OH	12.2 %	0.2 %	12.0 %
Ac-Trigger-Trp-Asp-Phe-OH	82.5 %	95.6 %	-13.1 %
Fmoc-Trigger-Trp-Asp-Phe-OH	84.8 %	3.1 %	**81.7 %**
Ac-Trigger-Asp-Trp-Asp-Phe-OH	78.9 %	84.9 %	-6.0 %
Ac-Trp-Trigger-OH	95.9 %	94.0 %	1.9 %
Ac-Asp-Trp-Trigger-OH	93.4 %	75.2 %	18.2 %
Ac-Asp-Trigger-Phe-OH	98.8 %	0.0 %	**98.8 %**
Ac-Asp-Trigger-Asp-Phe-OH	97.7 %	0.1 %	**97.6 %**

3. Docking study

Five peptidomimetics (in both *Z* and *E* forms) were docked to the dimerisation site of the RNR R2 subunit, using Glide. Each docking pose is shown below, *Z* to the left and *E* to the right. The peptidomimetics are shown in gray (blue nitrogens, red oxygens) and the enzyme iscoloured according to residue type (blue: positive, red: negative, white: hydrophobic, pink: aromatic, yellow: polar).

Ac-Trigger-Phe-OH
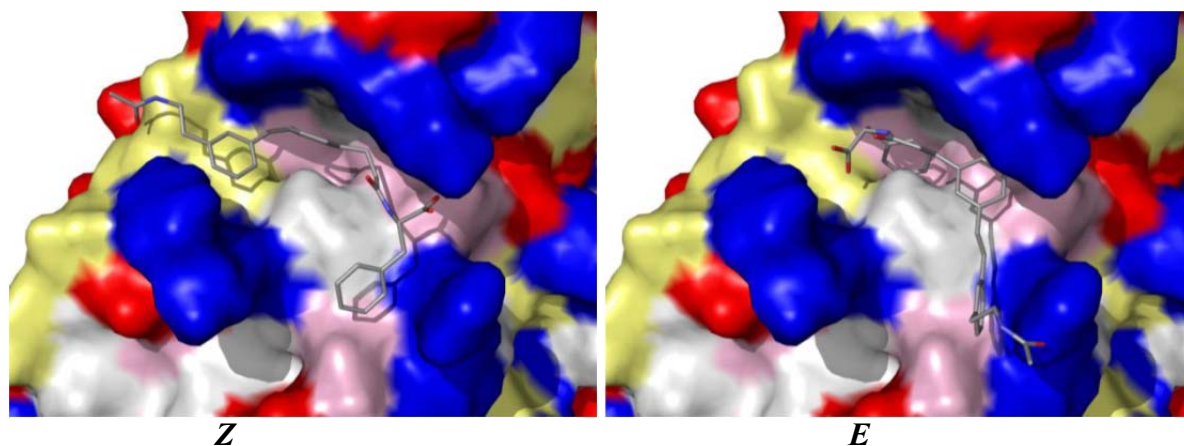
Ac-Trigger-Asp-Phe-OH
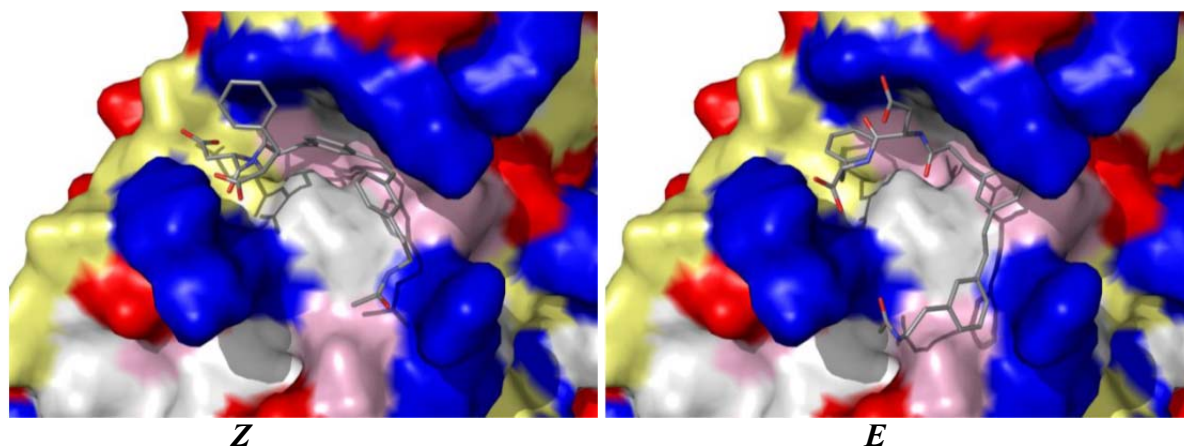
Fmoc-Trigger-Trp-Asp-Phe-OH

Figure S 4: Docking studies.
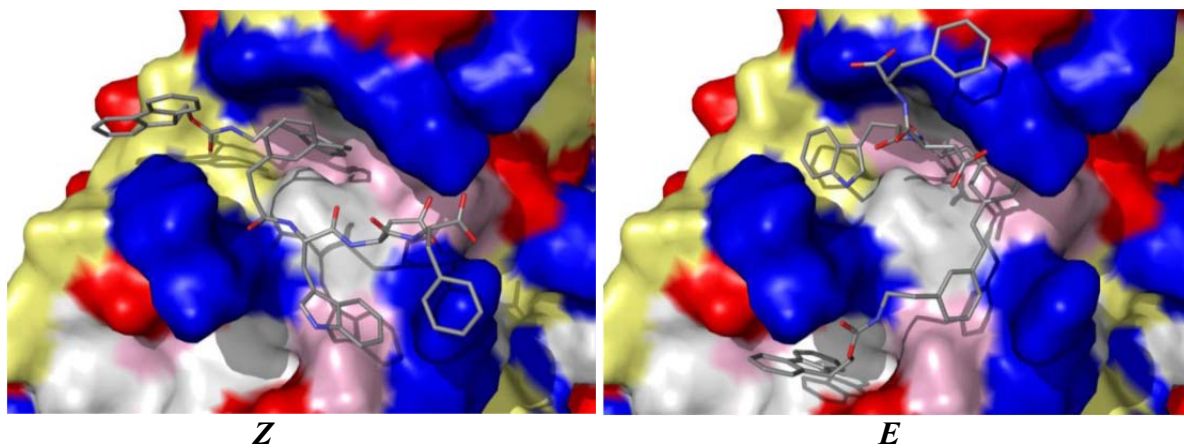
Ac-Asp-Trigger-Phe-OH
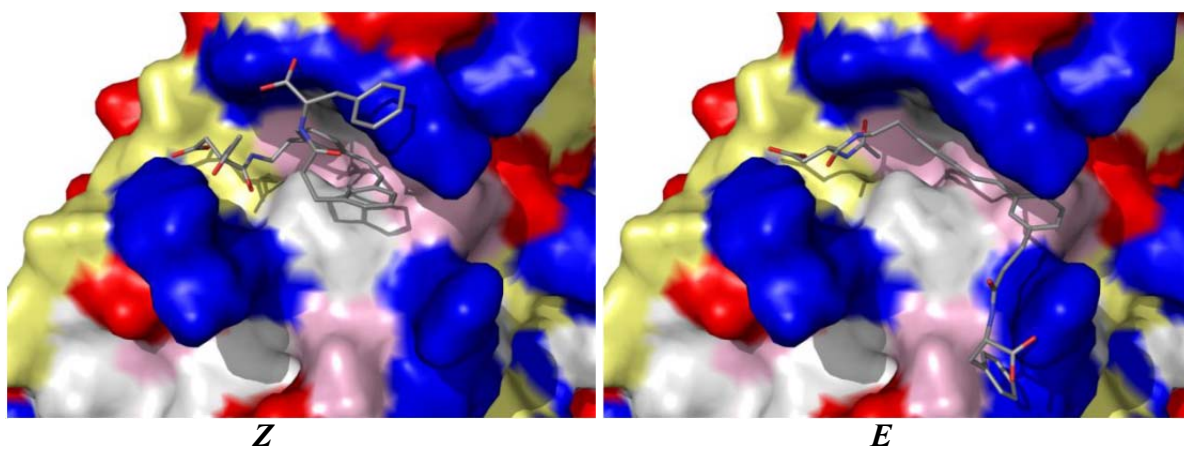
Ac-Asp-Trigger-Asp-Phe-OH
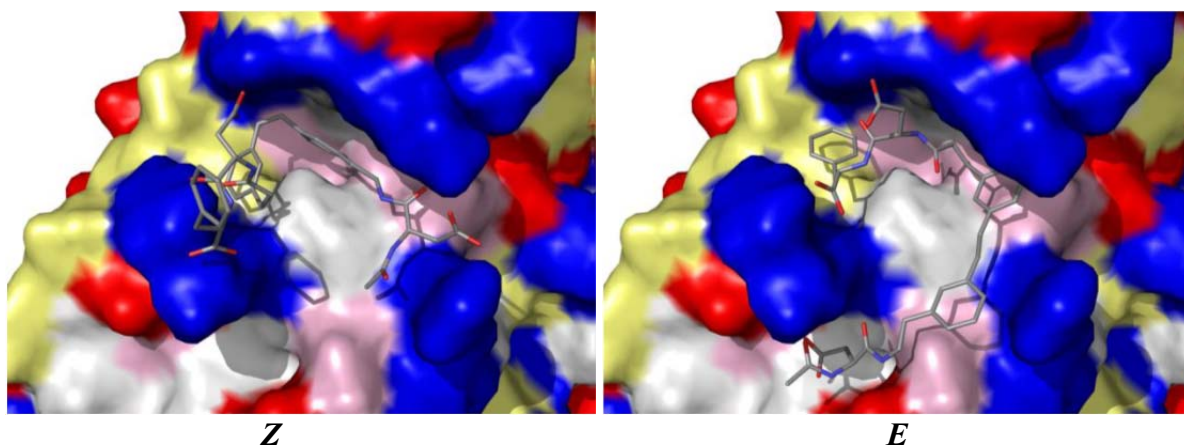
Figure S 5: Docking studies.

4. Photoisomerization

Formation of the *Z*-isomer of stilbene derivatives **3** through **8** can conveniently be monitored by ^{1}H NMR spectra, where the chemical shift of the olefinic protons decreases from approx. 7.2 (*E*-isomer) to around 6.6 (*Z*-isomer) ppm (Figure S 14, Figure S 15, Figure S 16, Figure S 19, Figure S 40, Figure S 53). The $^3J_{HH}$ coupling constant between these protons, measured on the ^{13}C satellites in case of **4**, **5**, **7** and **8**, decreases from 16.4 Hz (*E*-isomer) to 12.4 Hz (*Z*-isomer). This is very similar to the photoisomerization of *E*-stilbene (Figure S 6).[4]
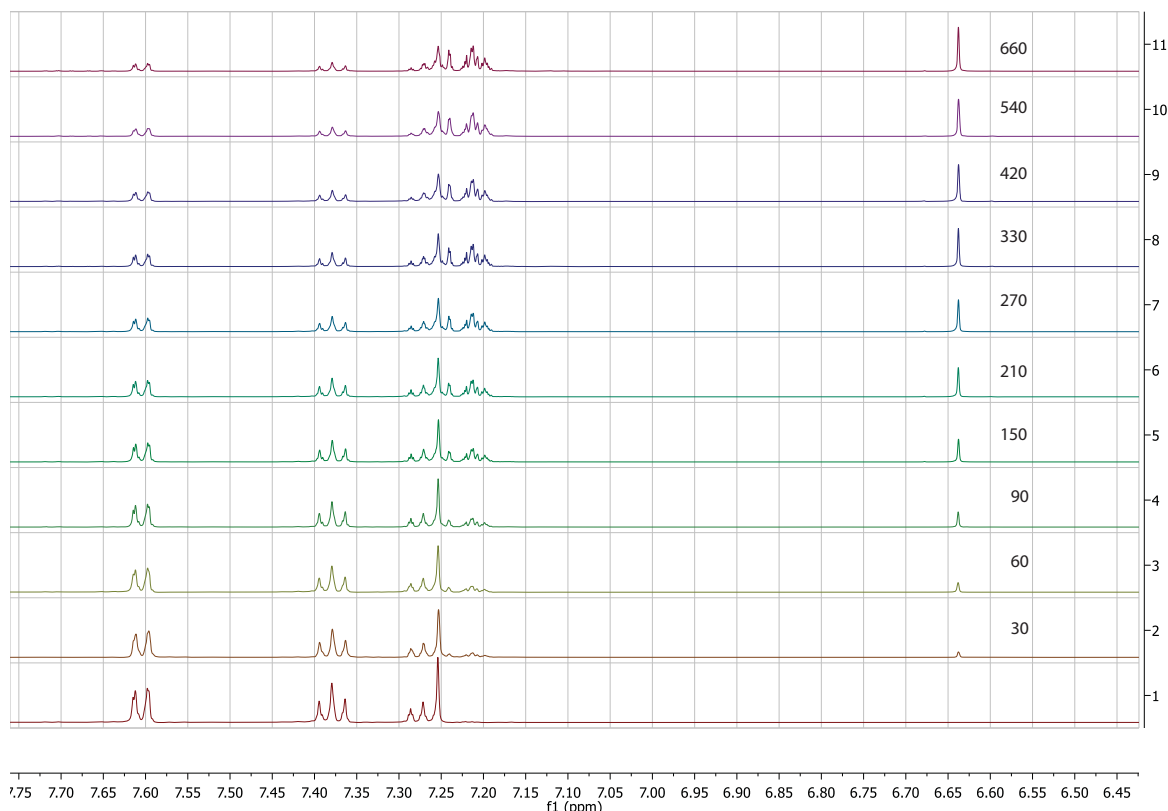
Figure S 6: ^{1}H NMR spectra illustrating the $E \rightarrow Z$ photoisomerization of stilbene after 30 to 660 minutes of irradiation, bottom: E-stilbene (500 MHz, CDCl$_3$ solution).

5. Binding assay[3]

In fluorescence polarization, light from two channels is measured: light parallel to the plane of the emitted light ($I^=$) and light perpendicular to the plane same. ($I^\perp$). These are used to calculate anisotropy (A).

$$A = \frac{I^= - I^\perp}{I^= + 2I^\perp}$$

Two binding models were used in order to evaluate the affinites of compounds **6-8**, the direct binding (1) and complete competitive binding (2).

$$(1) \quad R + L_s \ \underset{K_{D1}}{\rightleftharpoons} \ RL_s$$

$$(2) \quad R + L_s + L \ \underset{K_{D1}}{\rightleftharpoons} \ RL_s + L$$

$$\Big\updownarrow K_{D2}$$

$$RL + Ls$$
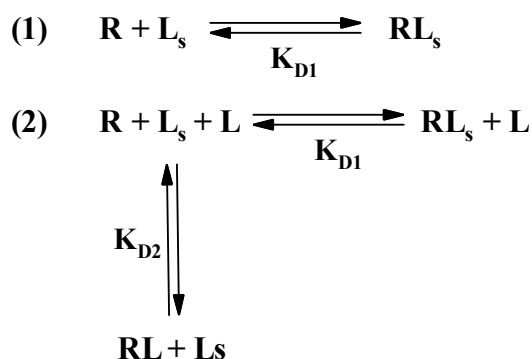
The following definitions are used: R, free enzyme; L, free unlabelled ligand (compounds **6-8**); L_s, free labelled ligand (dansylated heptapeptide); K_{D1}, dissociation constant between free enzyme and the probe; K_{D2}, dissociation constant between free enzyme and compounds **6-8.**

Direct binding model

This 2-state equilibrium binding model is expressed by the following equations:

$$K_{D1} = \frac{R \ast L_S}{R L_S}$$

$$R_T = R + RL_S$$

$$L_{ST} = L_S + RL_S$$

$$F_{SB} = \frac{L_S}{L_{ST}}$$

F_{SB} is the fraction of probe bound to the receptor. The equations above can be solved with a physiologically meaningful root for F_{SB} using the equation below:

$$F_{SB} = \frac{K_{D1} + L_{ST} + R_T - \sqrt{(K_{D1} + L_{ST} + R_T)^2 - 4L_{ST}R_T}}{2L_{ST}}$$

R_T is the total concentration of receptor used. In order to calculate a value for K_{D1}, the relationship described above is linked to the experimentally measured anisotropy through the following equation where A_{obs} is the observed anisotropy; A_B is the anisotropy of the completely bound probe and Q is a corrective factor.

$$A_{OBS} = \frac{QF_{SB}A_B + (1 - F_{SB})A_F}{1 - (1 - Q)F_{SB}}$$

The experiments were conducted with a constant concentration of probe and a varied concentration of the receptor.

Complete competitive model

To describe the 3-state complete competitive model used to evaluate compounds **6-8** the following sets of equations are needed:

$$K_{D2} = \frac{R * L}{RL}$$

$$R_T = R + RL_S + RL$$

$$L_T = L + RL$$

These can be solved for a physiologically meaningful root for F_{SB} using the equation below:

$$F_{SB} = \frac{2\sqrt{(a^2 - 3b)}\cos\left(\frac{d}{3}\right) - a}{3K_{D1} + 2\sqrt{(a^2 - 3b)}\cos\left(\frac{d}{3}\right) - a}$$

Where

$$a = K_{D1} + K_{D2} + L_{ST} + L_T - R_T$$

$$b = (L_T - R_T)K_{D1} + (L_{ST} - R_T)K_{D2} + K_{D1}K_{D2}$$

$$c = -K_{D1}K_{D2}R_T$$

$$d = arccos\left(\frac{-2a^3 + 9ab - 27c}{2\sqrt{(a^2 - 3b)^3}}\right)$$

The anisotropy is measured with constant concentrations of receptor and probe and varied concentration for the competing ligand (**6-8**).

6. MS Data
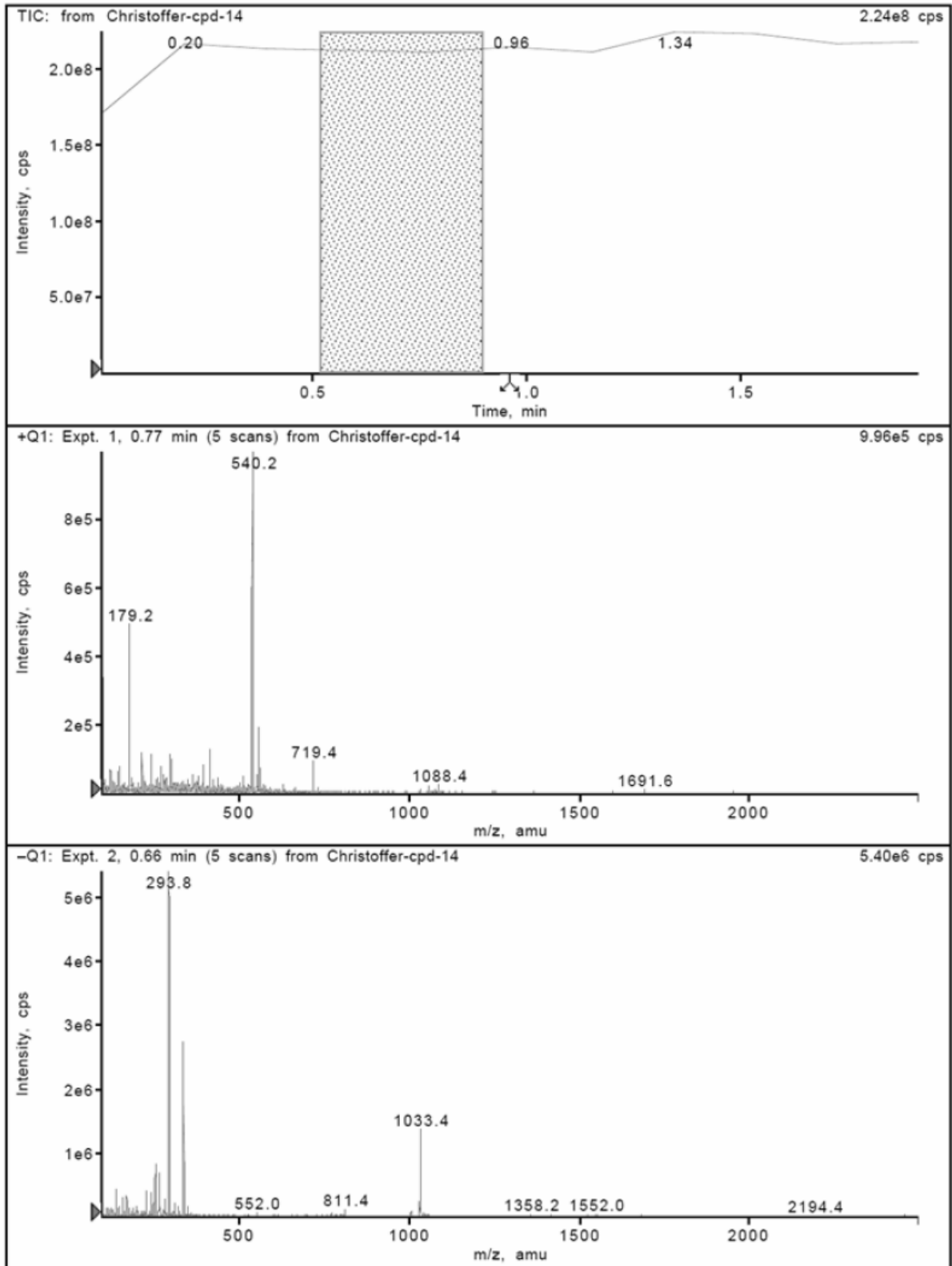
Figure S 7: MS of Compound **2**
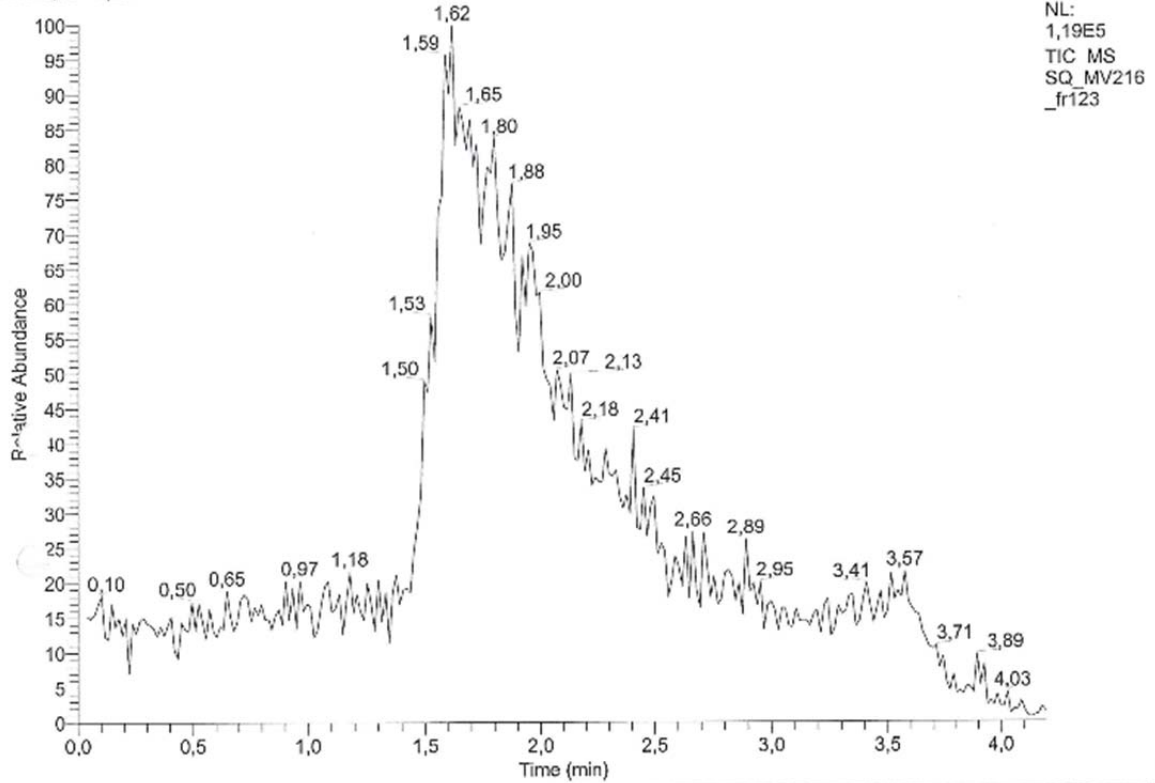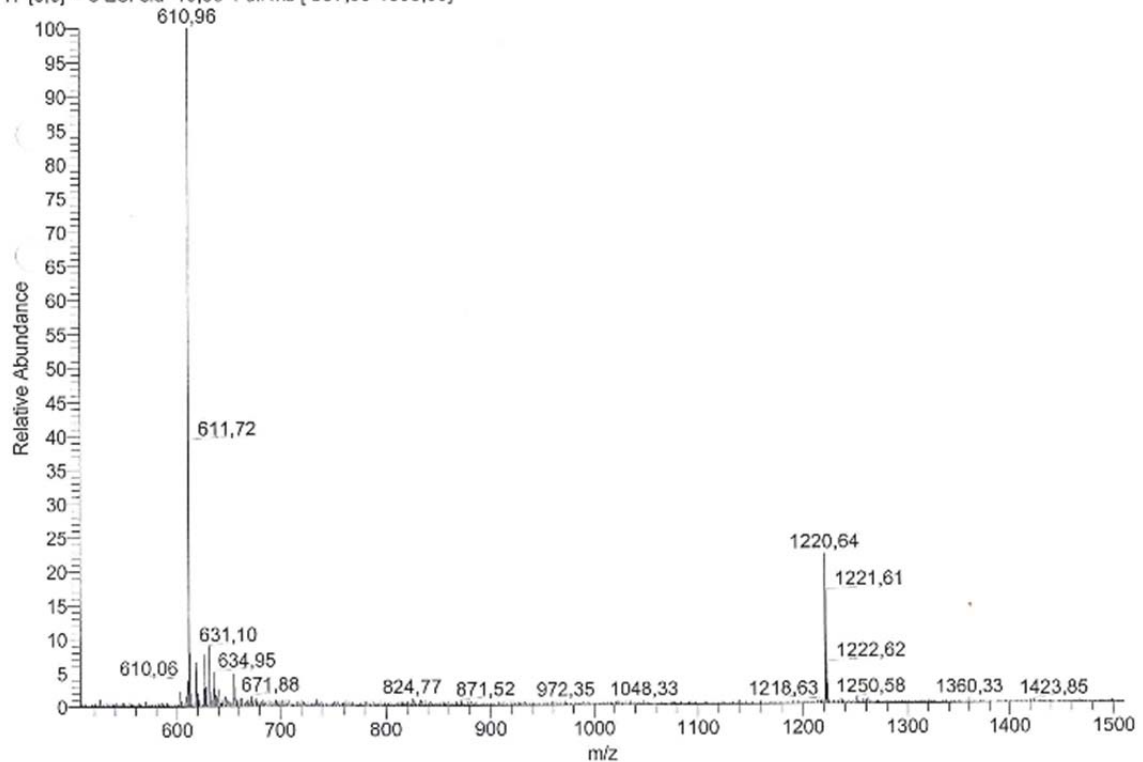
Figure S 8: MS of Compound **3**
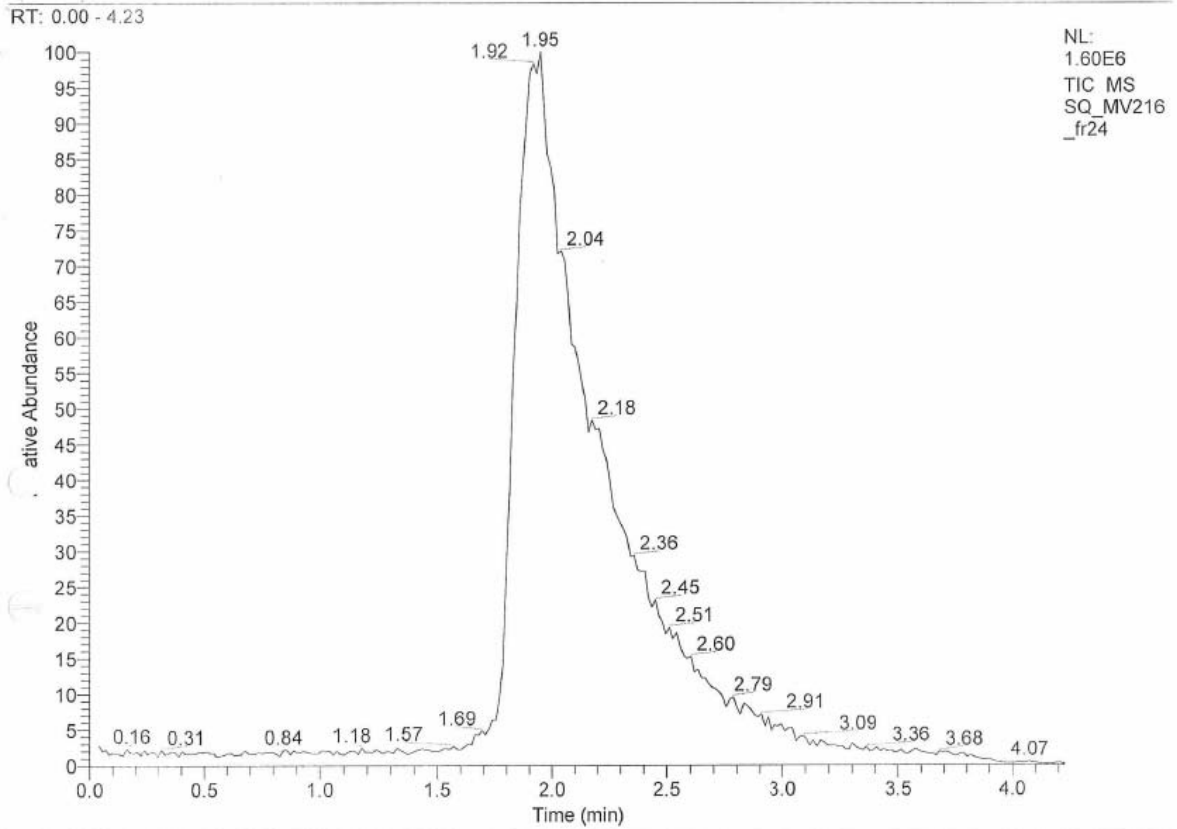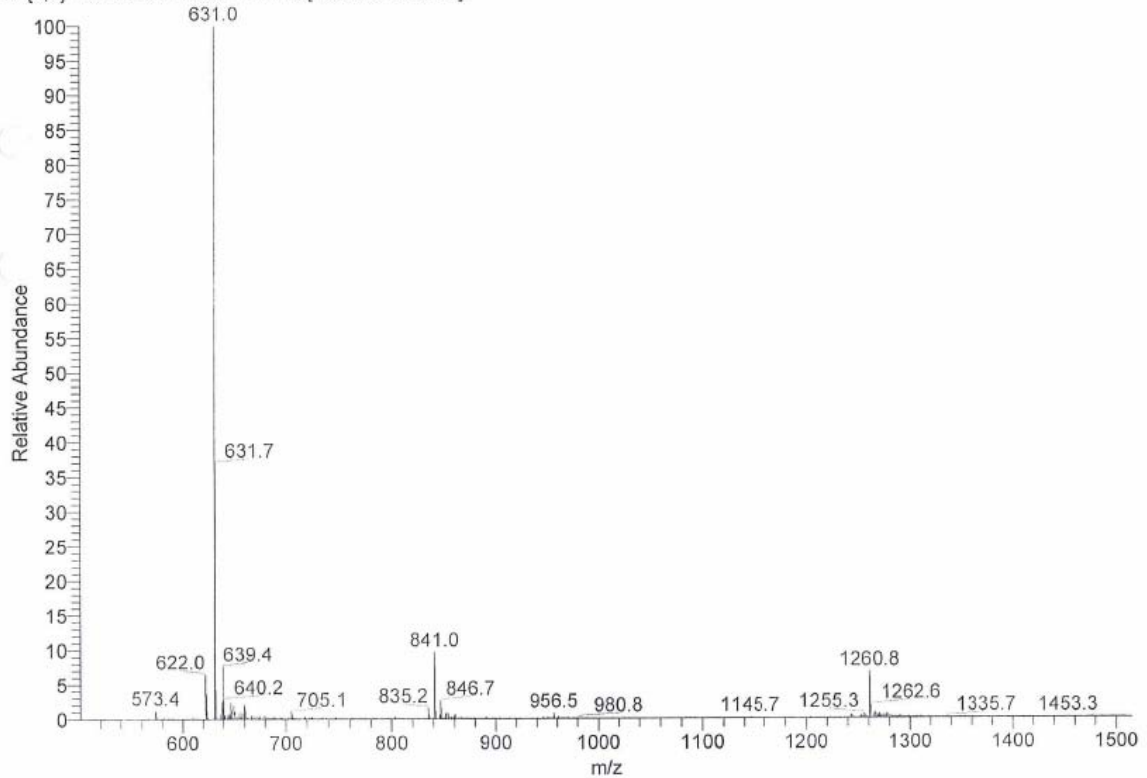
Figure S 9: MS of Compound **4**
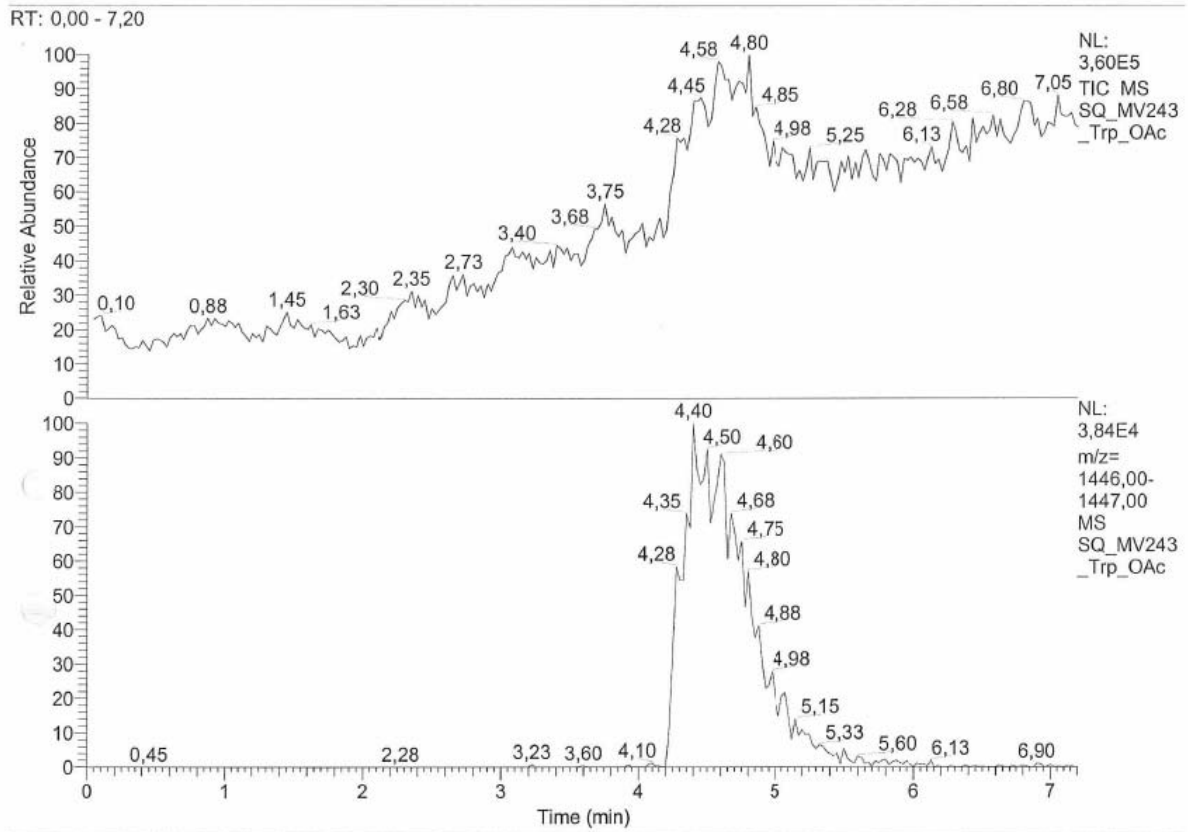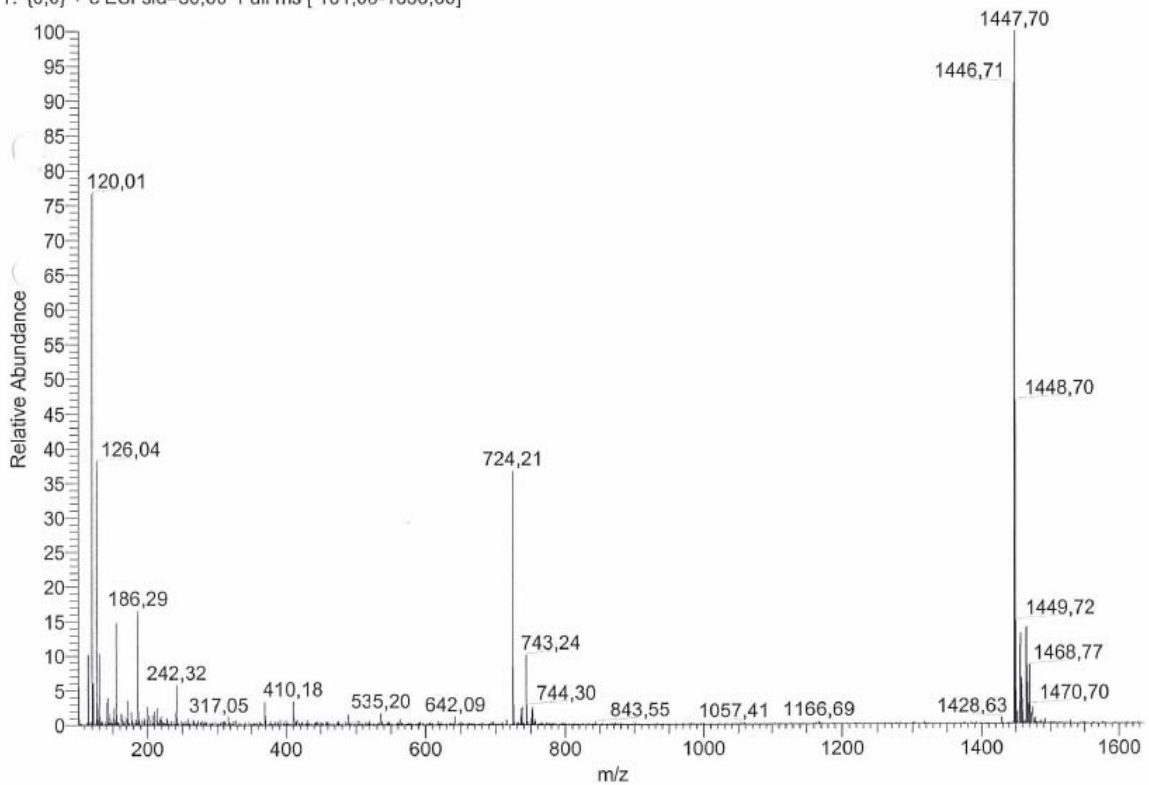
Figure S 10: MS of Compound **5**
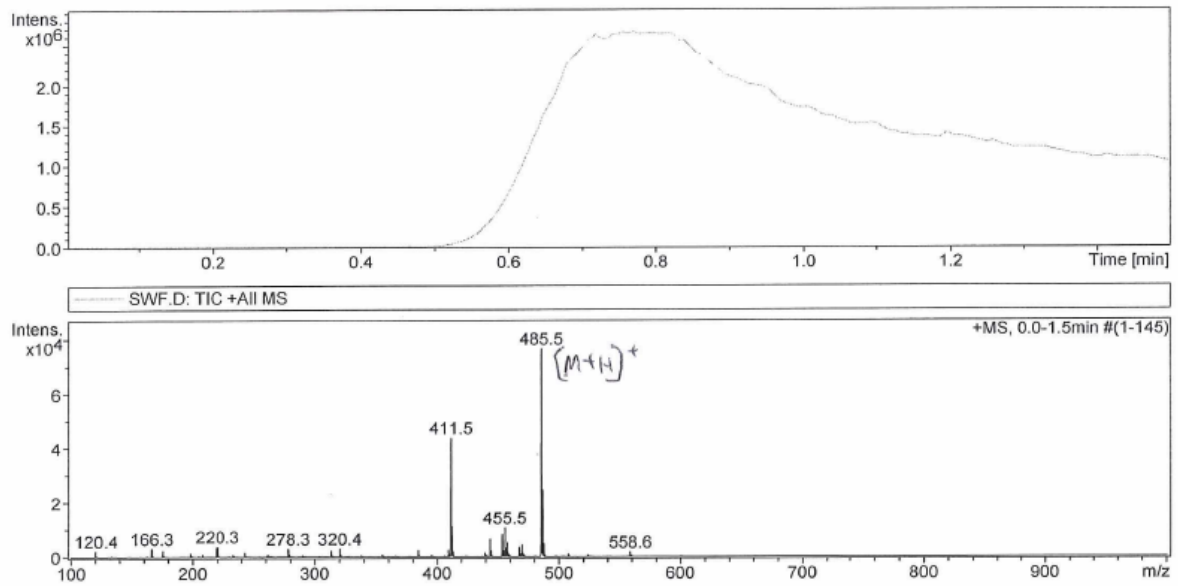
Figure S 11: MS of Compound **6**
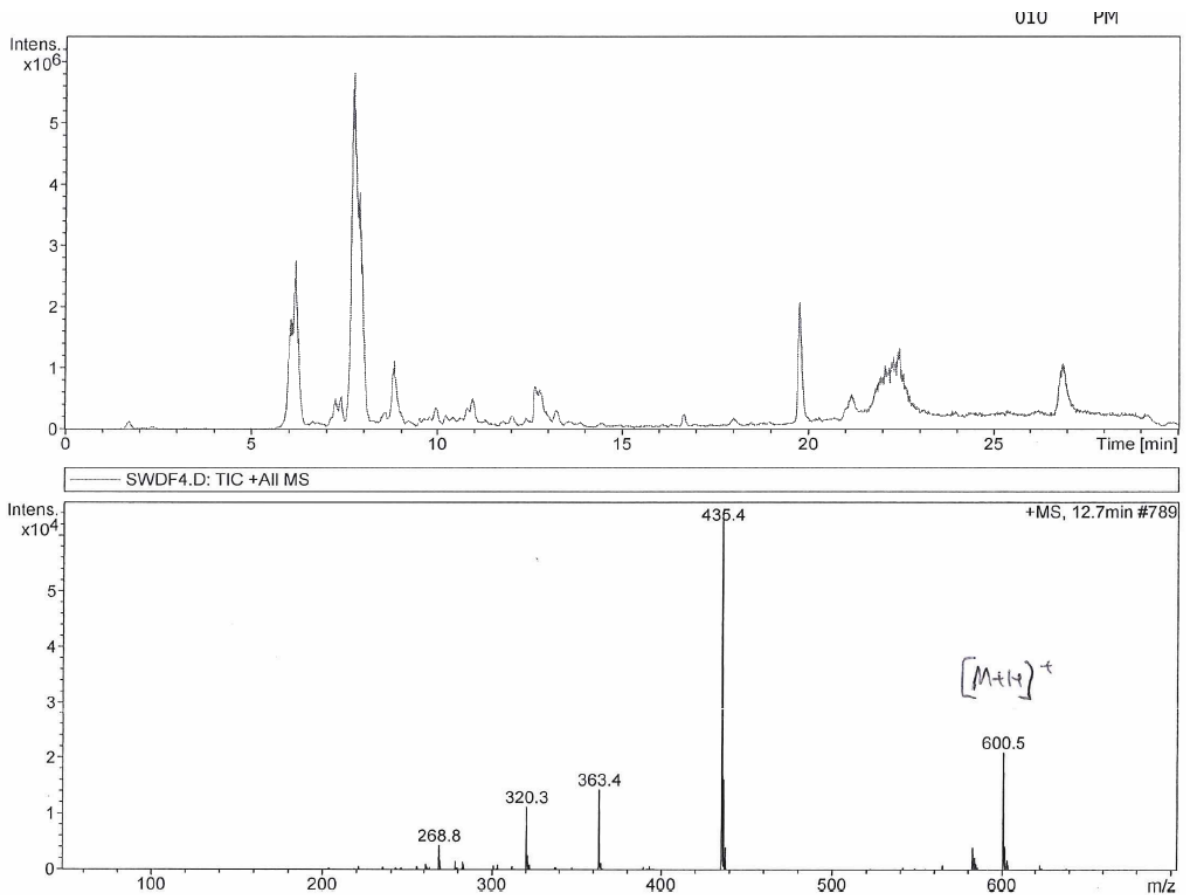
Figure S 12: MS of Compound **7**
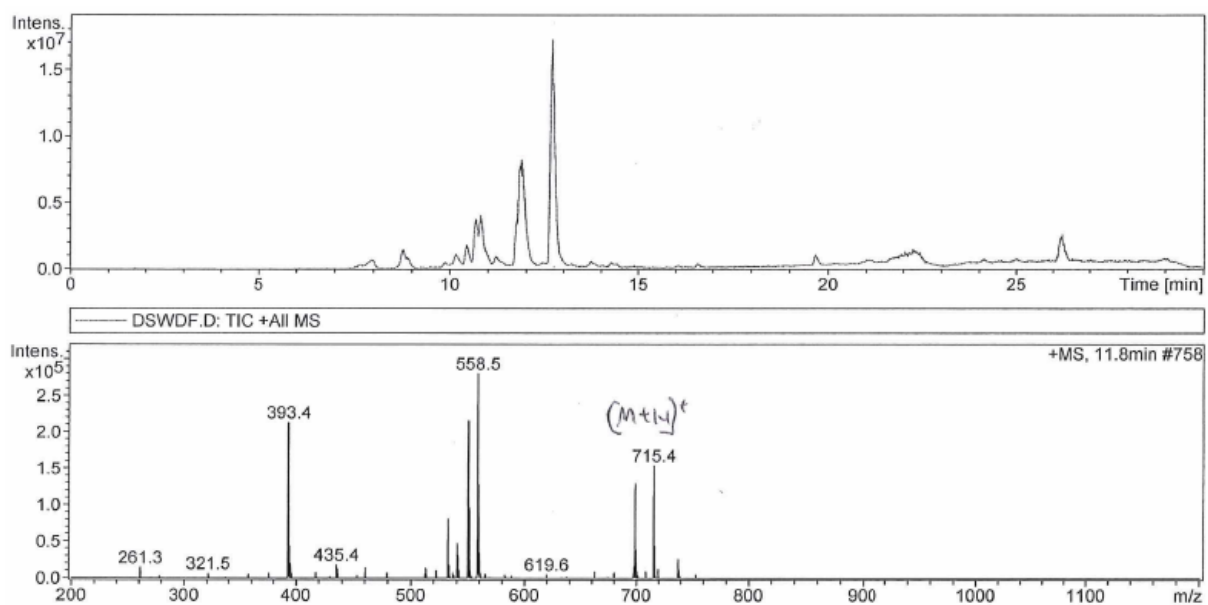
Figure S 13: MS of Compound **8**

7. NMR data

7.1. Photoisomerization of 3 – 5
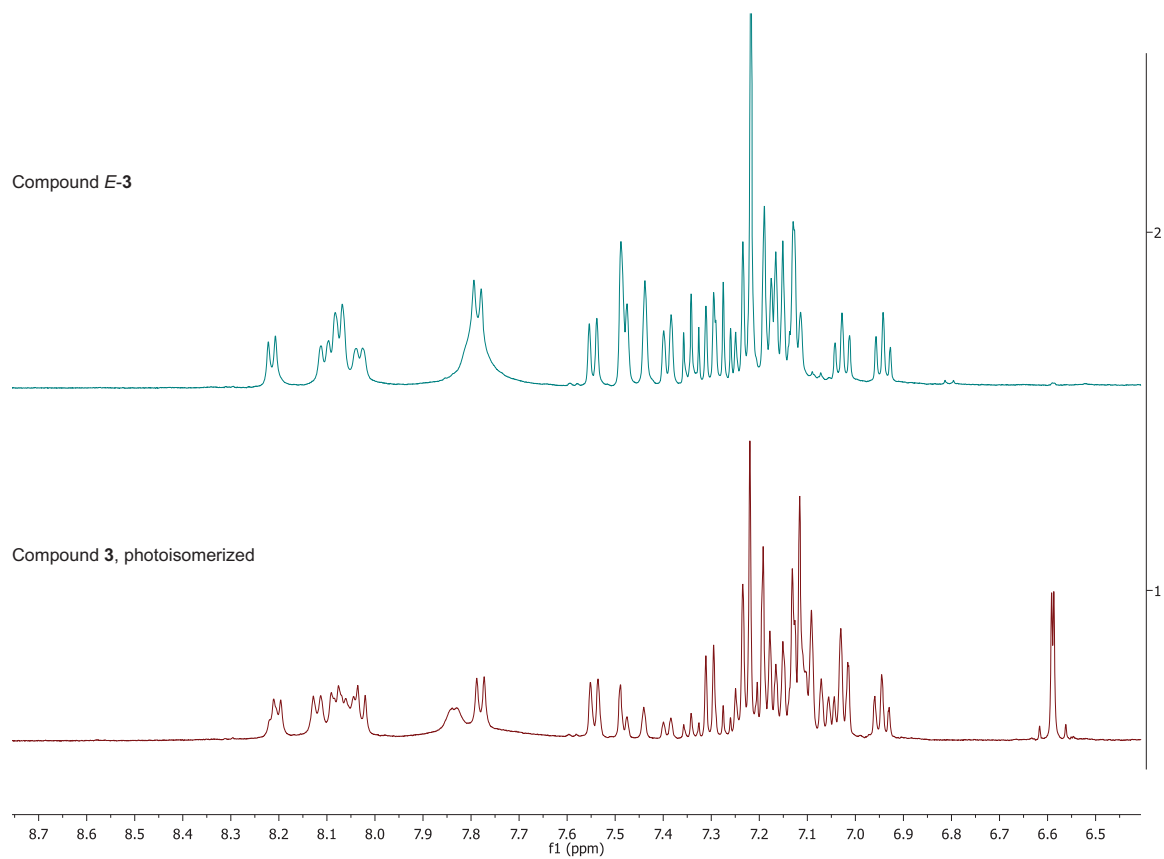
Figure S 14: Expansion of ^{1}H NMR spectrum of photoisomerized compound **3** (500 MHz, DMSO-d$_6$ solution). Top: *E*-isomer, bottom: photoisomer mixture.
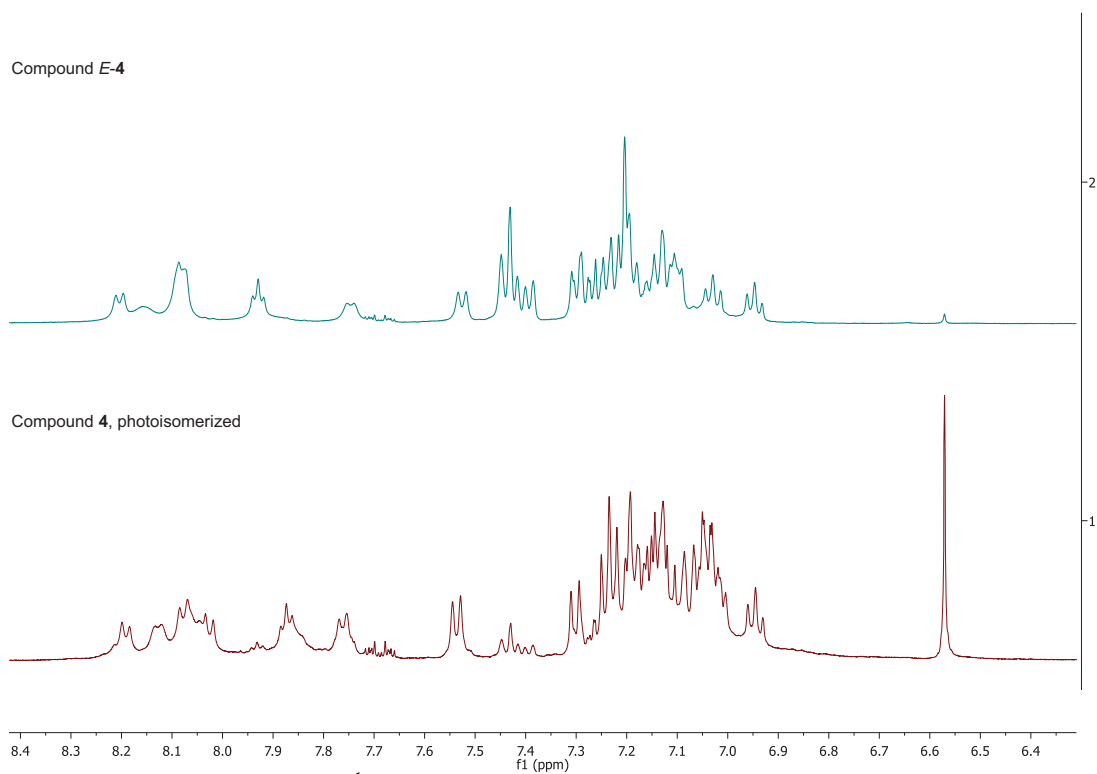
Figure S 15: Expansion of ^{1}H NMR spectrum of photoisomerized compound **4** (500 MHz, DMSO-d$_6$ solution). Top: *E*-isomer, bottom: photoisomer mixture.
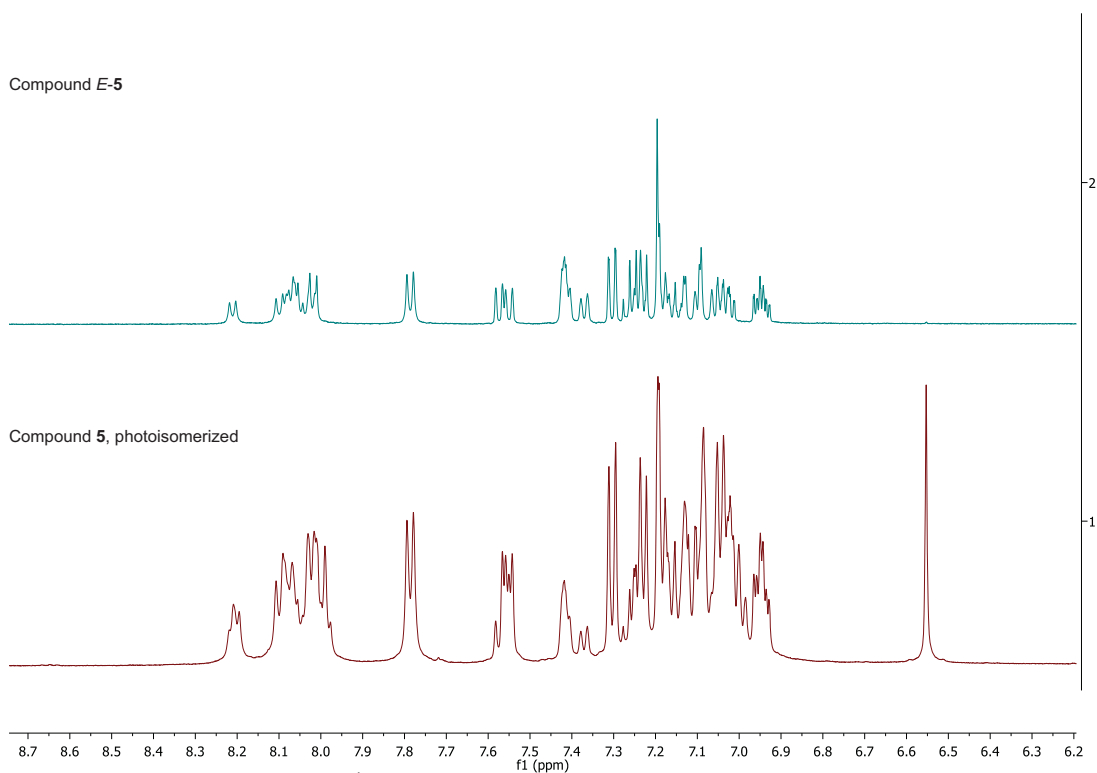
Figure S 16: Expansion of ^{1}H NMR spectrum of compound **5** (500 MHz, DMSO-d$_6$ solution). Top: *E*-isomer, bottom: photoisomer mixture.

7.2. Ac-Trigger-Phe-OH (6)

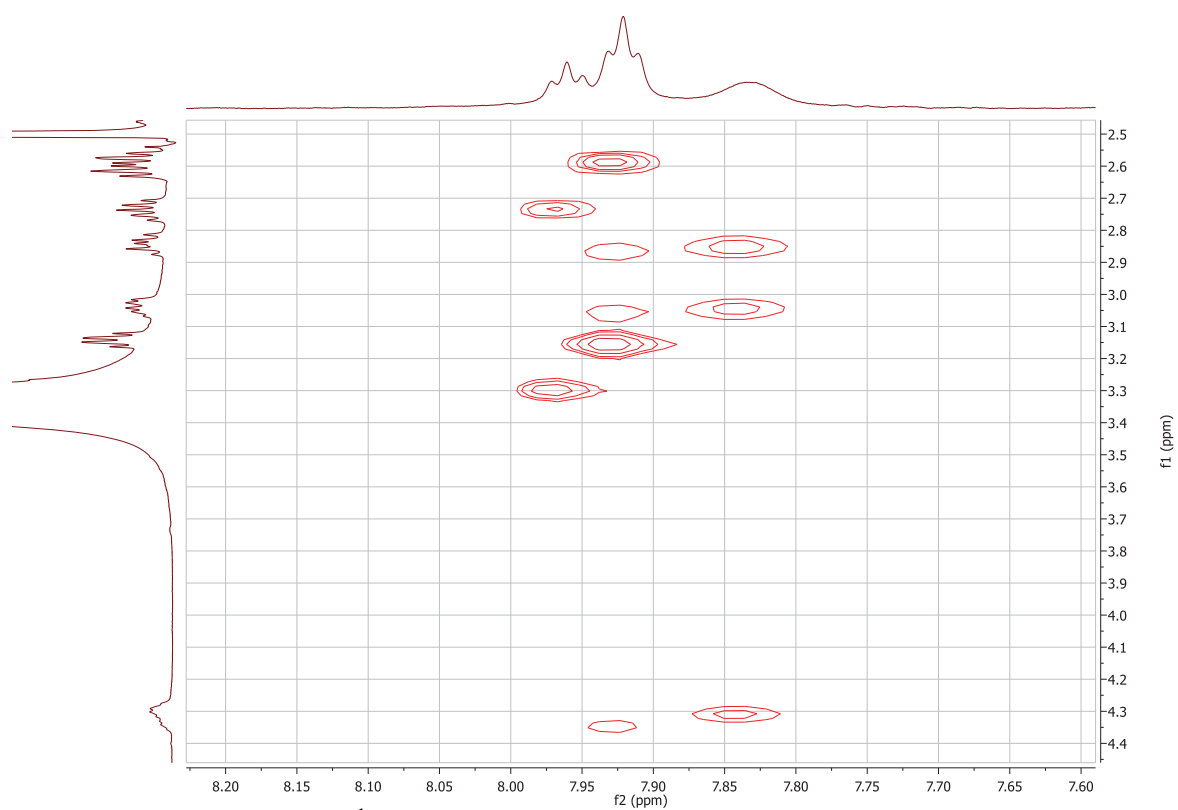Figure S 17: ^{1}H NMR spectrum of photoisomerized compound **6**, Ac-Trigger-Phe-OH (500 MHz, DMSO-d$_6$ solution).
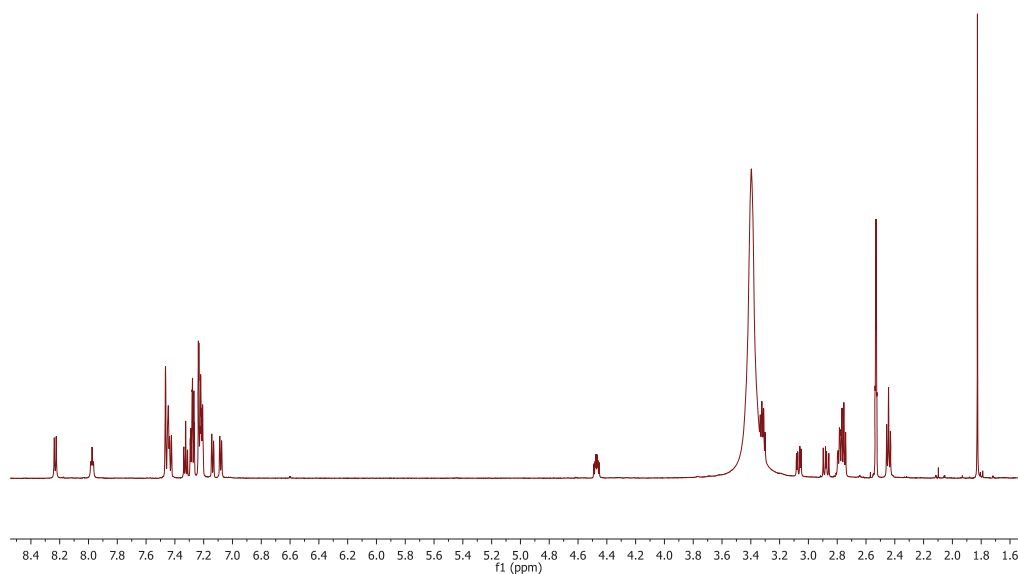
Figure S 18: ^{1}H NMR spectrum of compound **6**, Ac-Trigger-Phe-OH (600 MHz, DMSO-d$_6$ solution).

Compound *E*-**6**

Compound **6**, photoisomerized
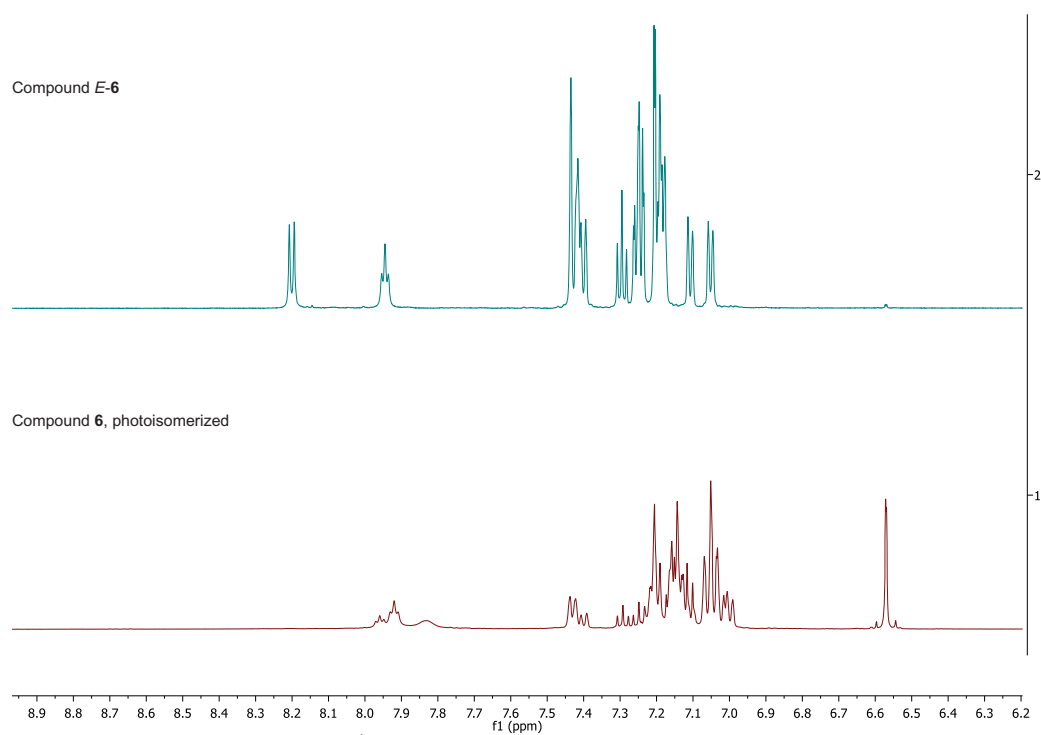
Figure S 19: Expansion of ^{1}H NMR spectrum of compound **6** (500 MHz, DMSO-d$_6$ solution). Top: *E*-isomer, bottom: photoisomer mixture.
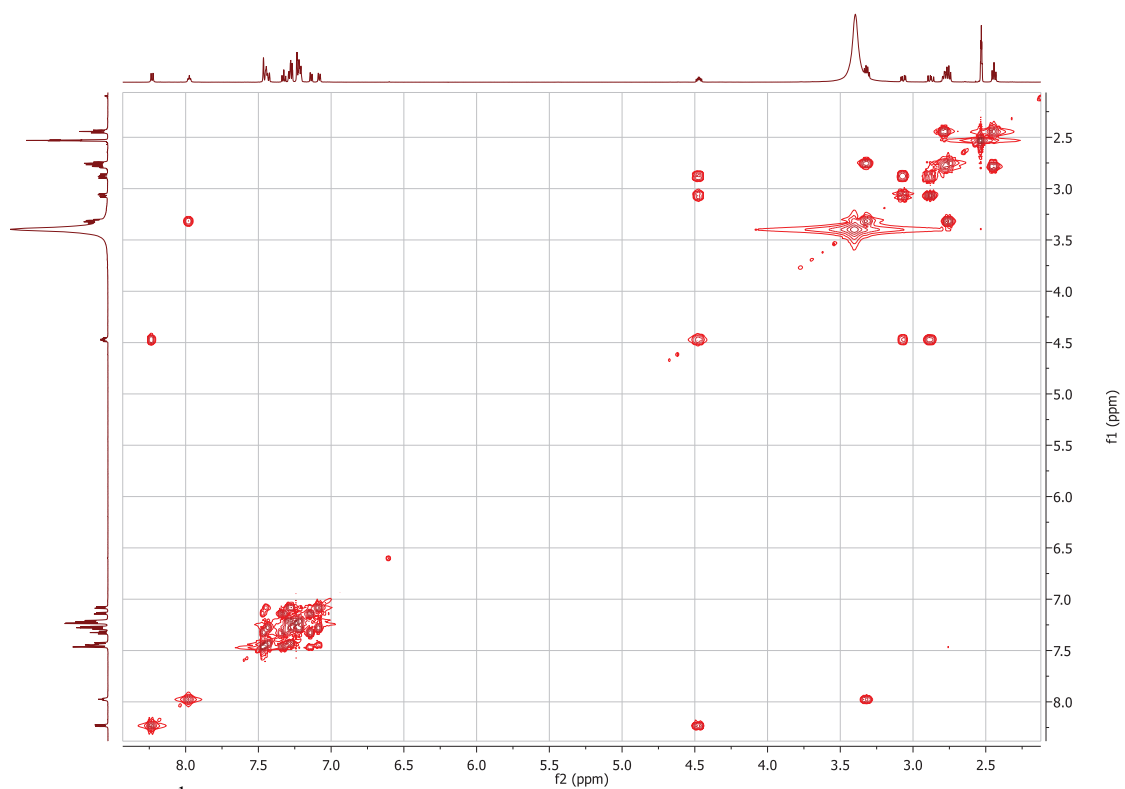
Figure S 20: ^{1}H COSY NMR spectrum of compound **6**, Ac-Trigger-Phe-OH (600 MHz, DMSO-d$_6$ solution).
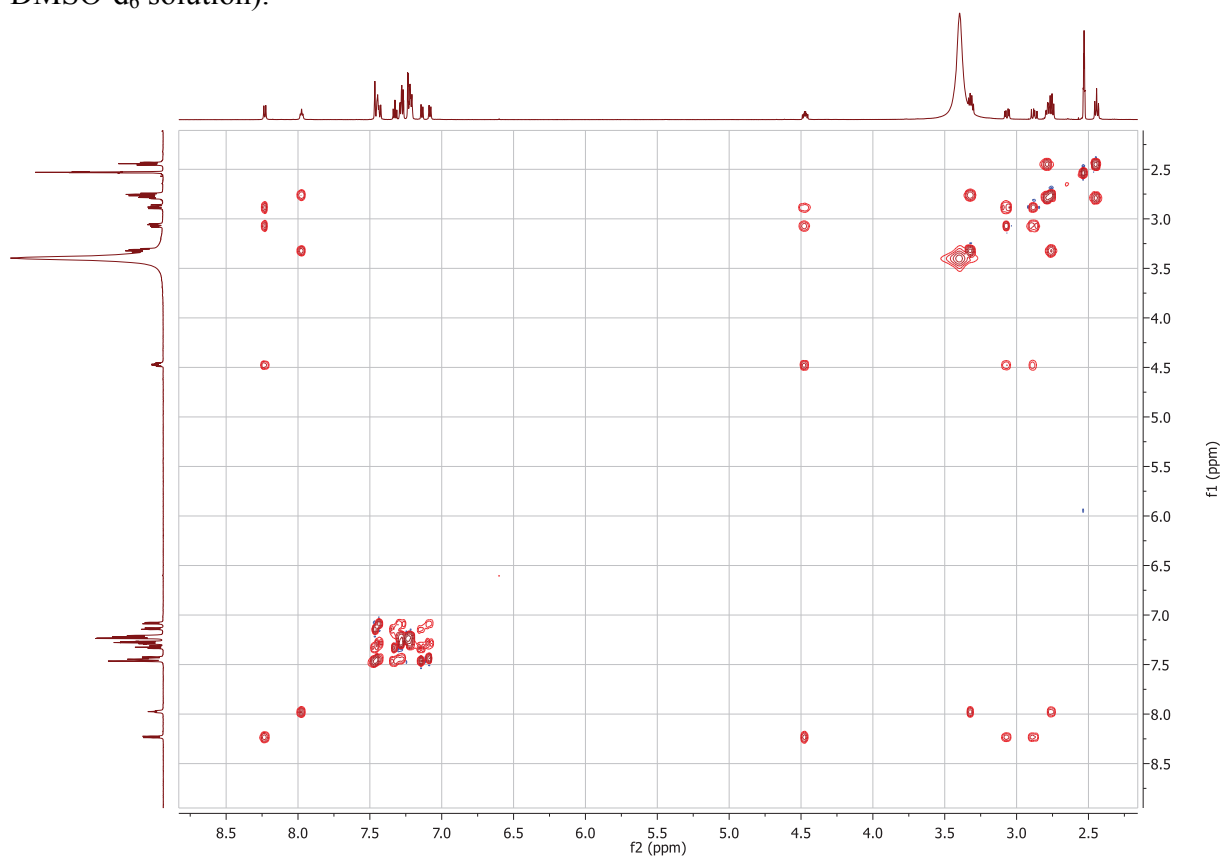
Figure S 21: ^{1}H TOCSY NMR spectrum of compound **6**, Ac-Trigger-Phe-OH (600 MHz, DMSO-d$_6$ solution).
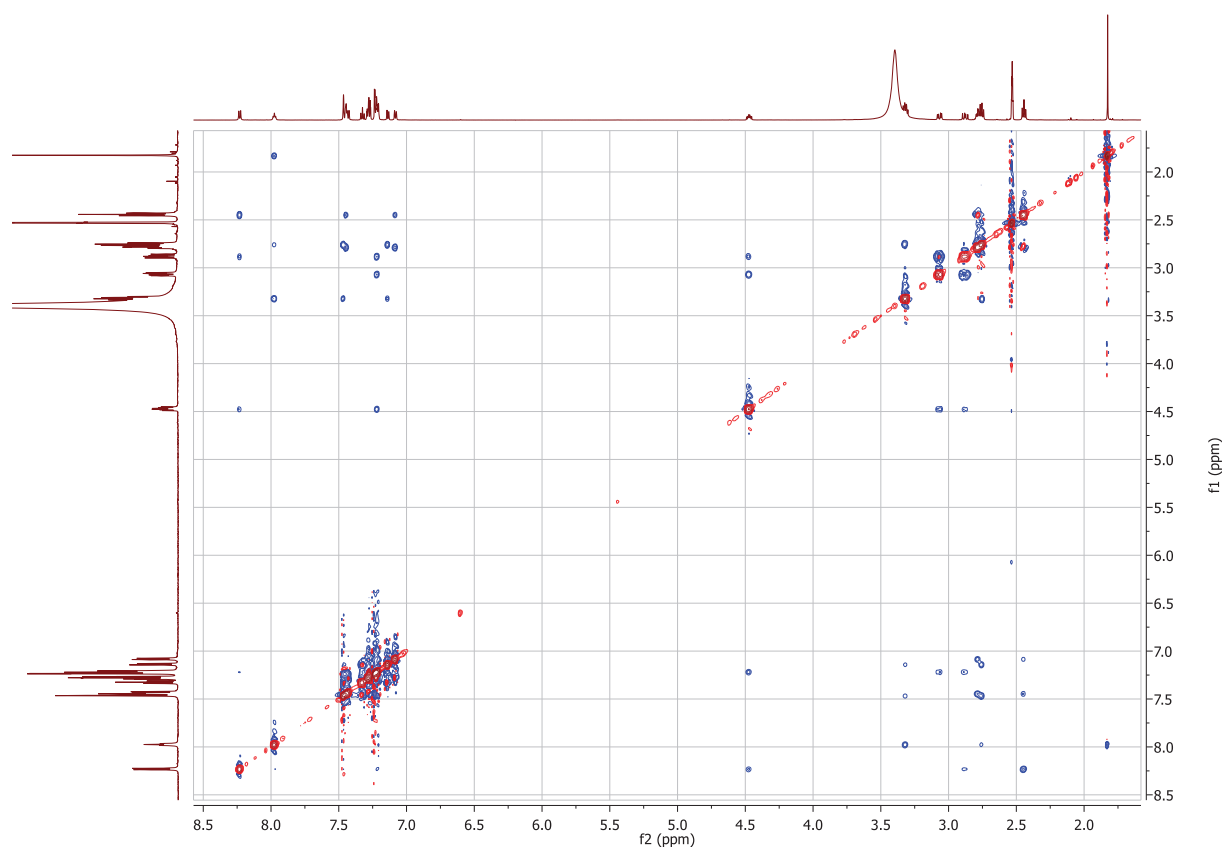
Figure S 22: ^{1}H ROESY NMR spectrum of compound **6**, Ac-Trigger-Phe-OH (600 MHz, DMSO-d[6] solution).
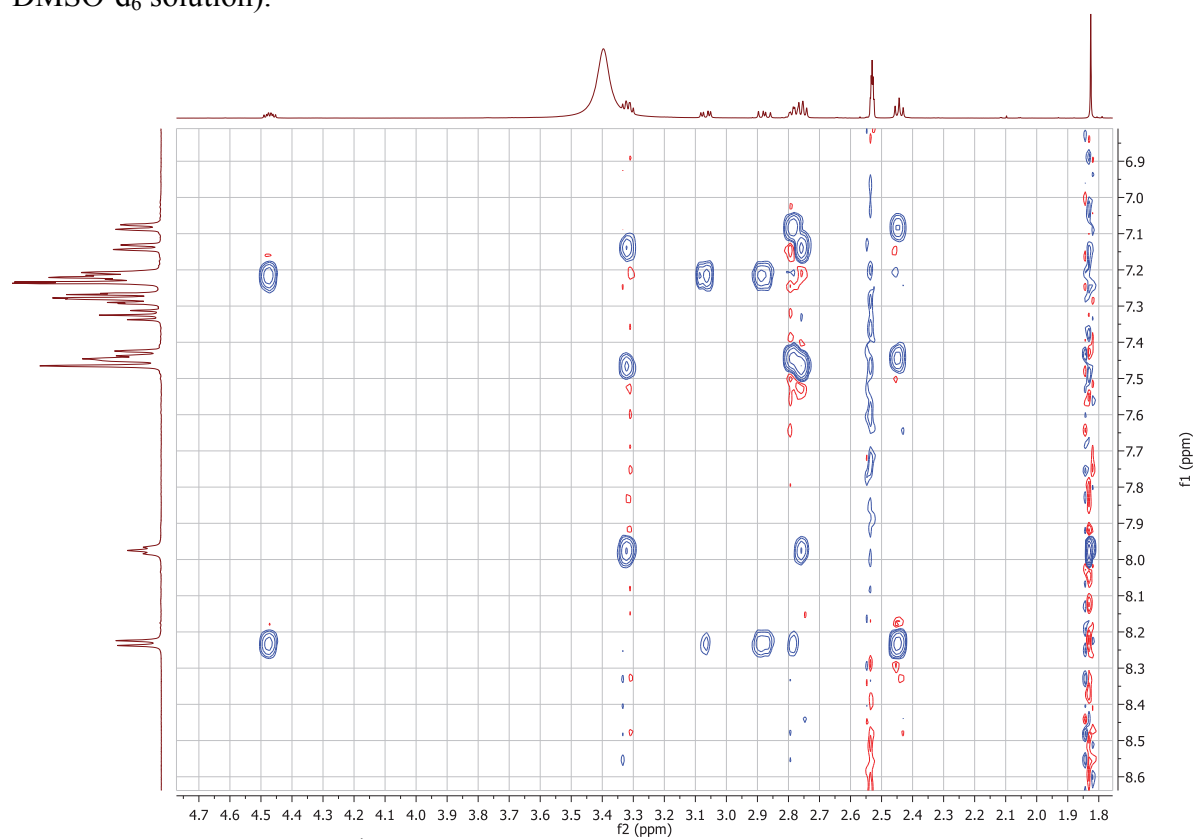
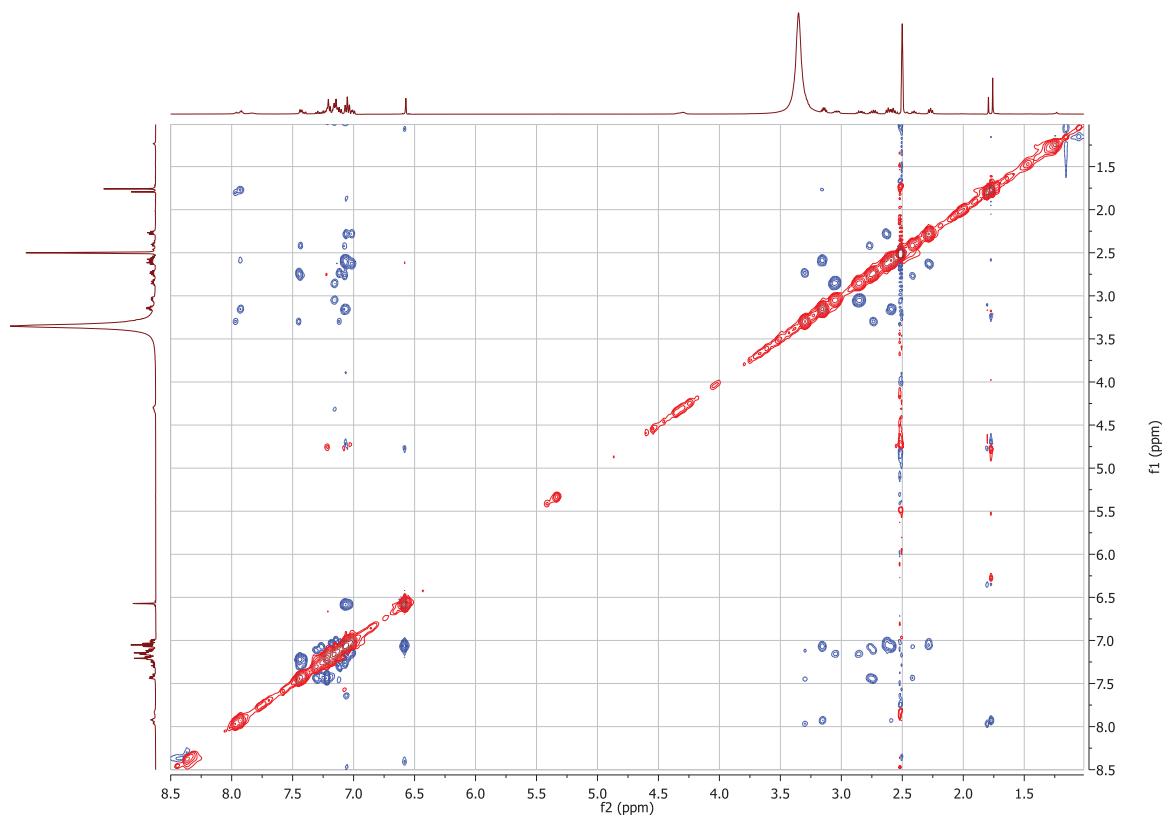Figure S 23: Expansion of ^{1}H ROESY NMR spectrum of compound **6**, Ac-Trigger-Phe-OH (600 MHz, DMSO-d[6] solution).
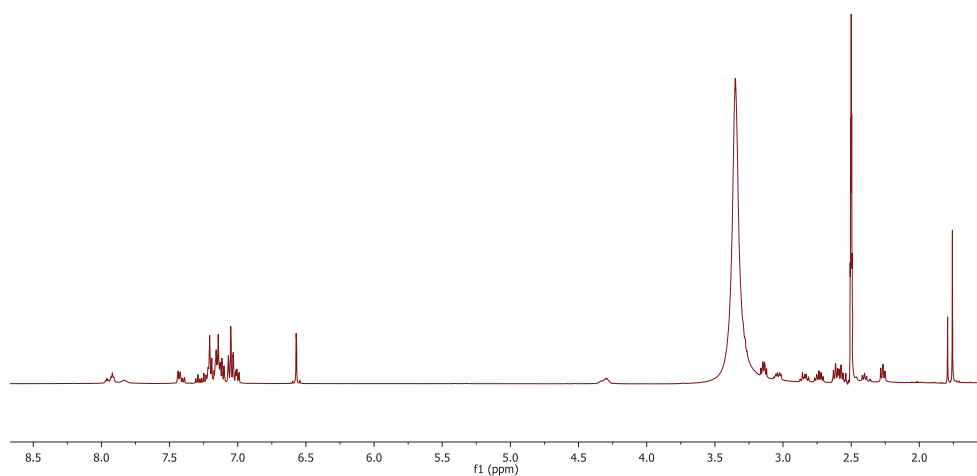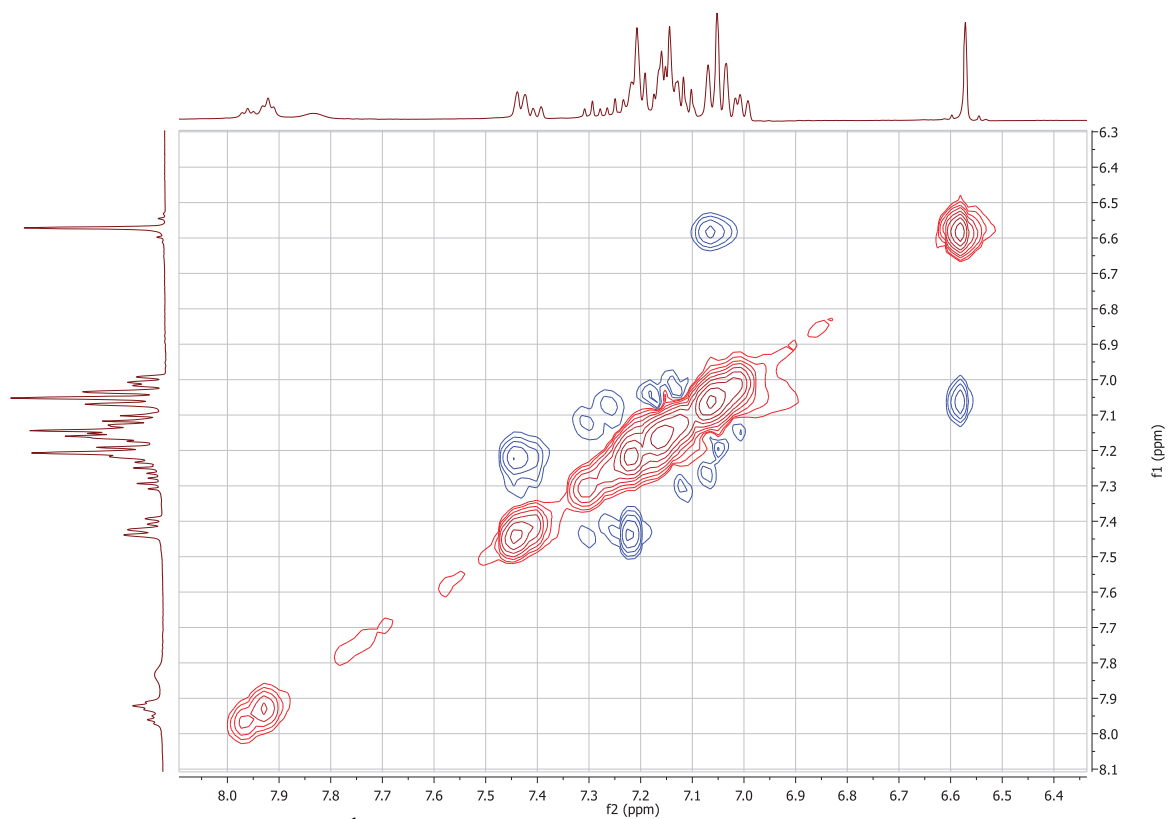
Figure S 24: ^{1}H NMR spectrum of photoisomerization of compound **6**, Ac-Trigger-Phe-OH (500 MHz, DMSO-d$_6$ solution).
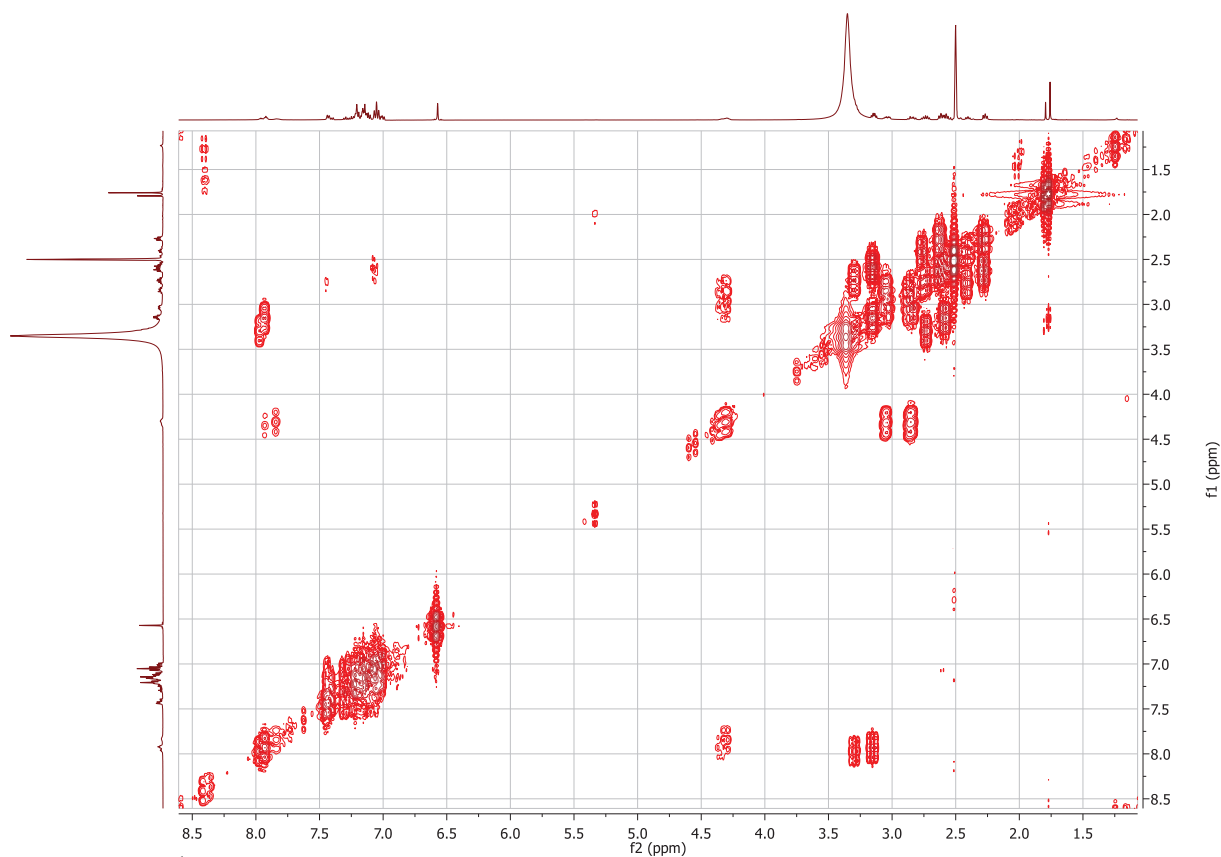
Figure S 25: ^{1}H COSY NMR spectrum of photoisomerization of compound **6**, Ac-Trigger-Phe-OH (500 MHz, DMSO-d$_6$ solution).
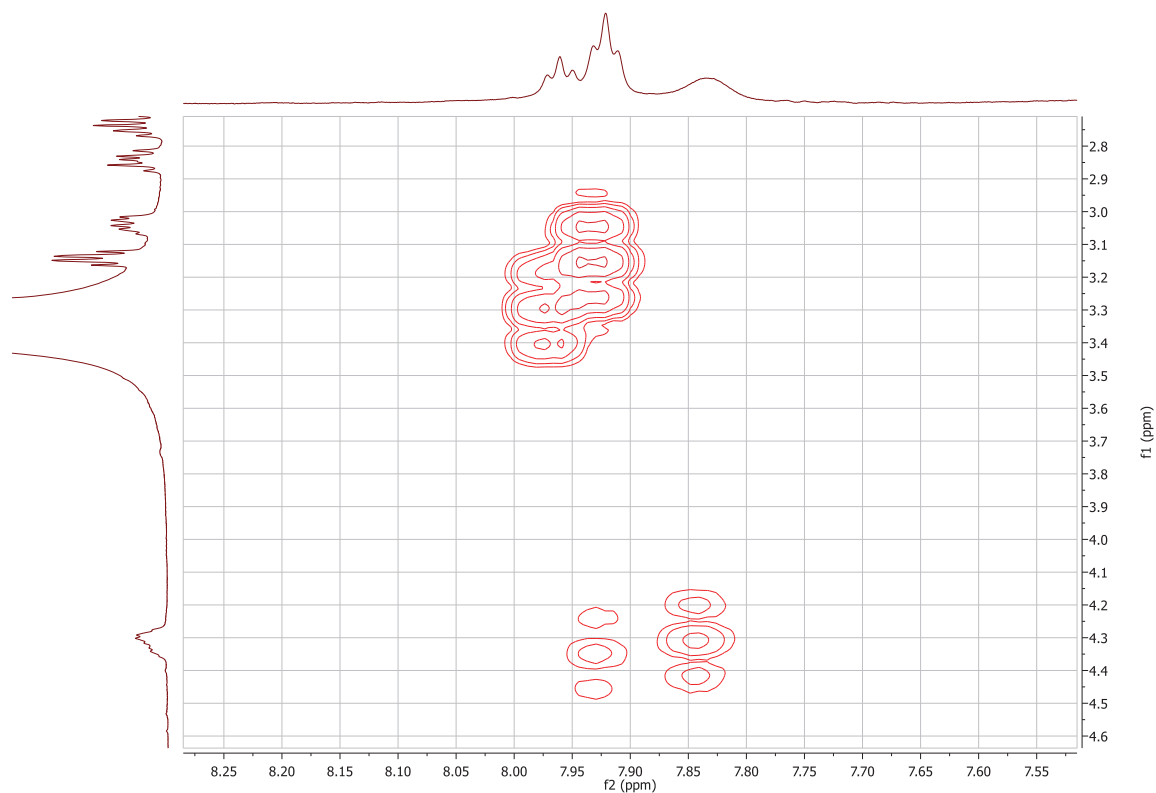
Figure S 26: Expansion of ^{1}H COSY NMR spectrum of photoisomerization of compound **6**, Ac-Trigger-Phe-OH (500 MHz, DMSO-d$_6$ solution).
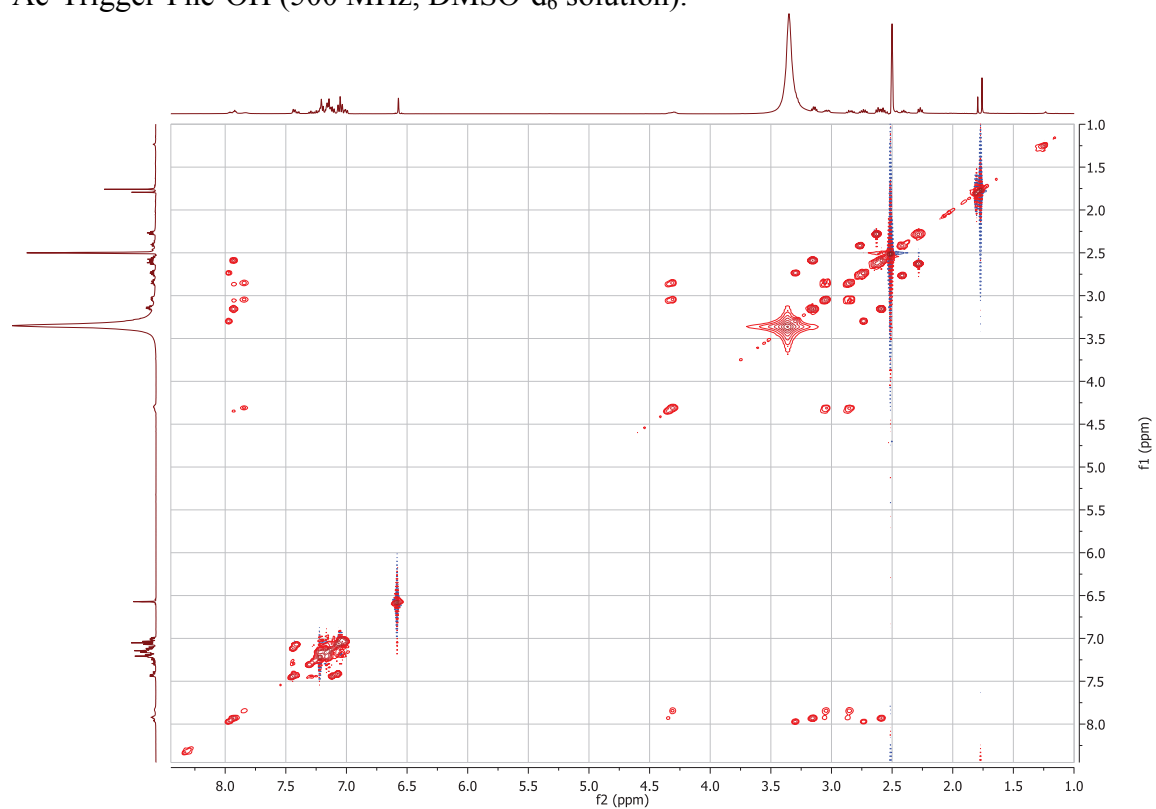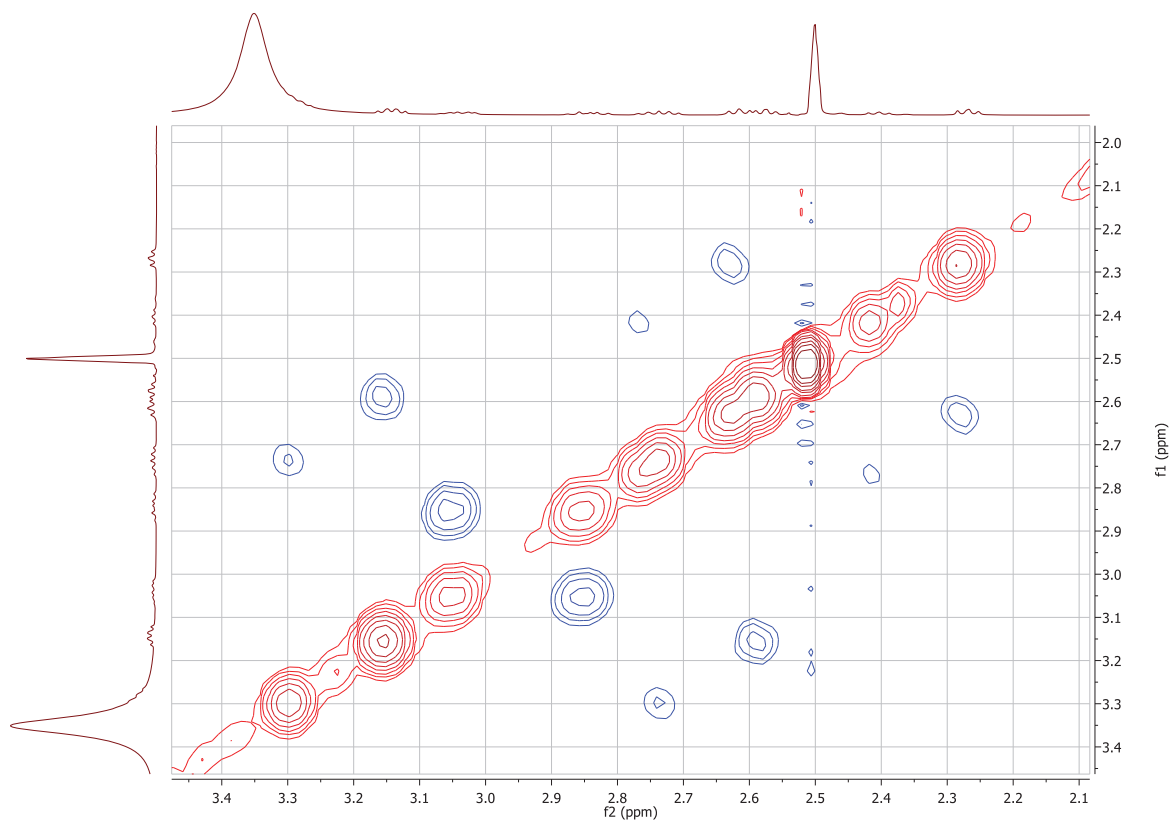

Figure S 27: ^{1}H TOCSY NMR spectrum of photoisomerization of compound **6**, Ac-Trigger-Phe-OH (500 MHz, DMSO-d$_6$ solution).
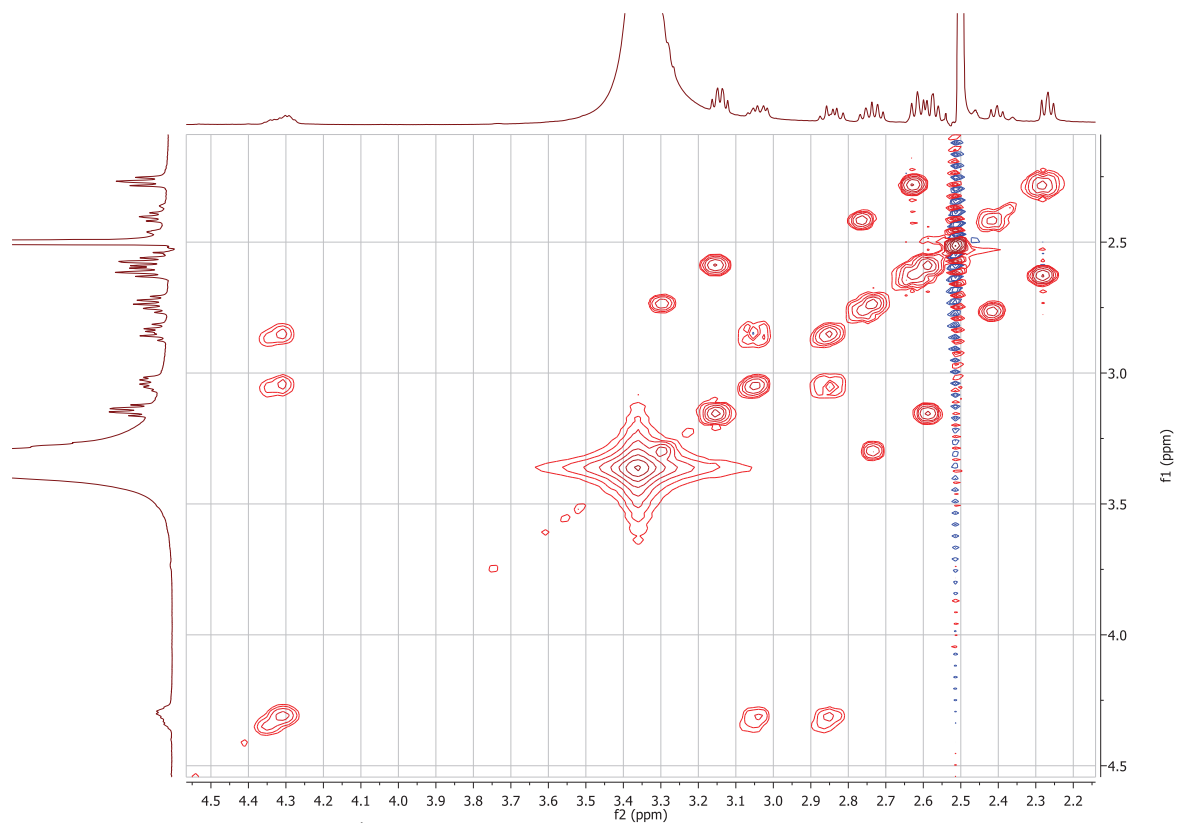
Figure S 28: Expansion of ^{1}H TOCSY NMR spectrum of photoisomerization of compound **6**, Ac-Trigger-Phe-OH (500 MHz, DMSO-d$_6$ solution).

Figure S 29: Expansion of ^{1}H TOCSY NMR spectrum of photoisomerization of compound **6**, Ac-Trigger-Phe-OH (500 MHz, DMSO-d$_6$ solution).

Figure S 30: ¹H ROESY NMR spectrum of photoisomerization of compound **6**, Ac-Trigger-Phe-OH (500 MHz, DMSO-d₆ solution).
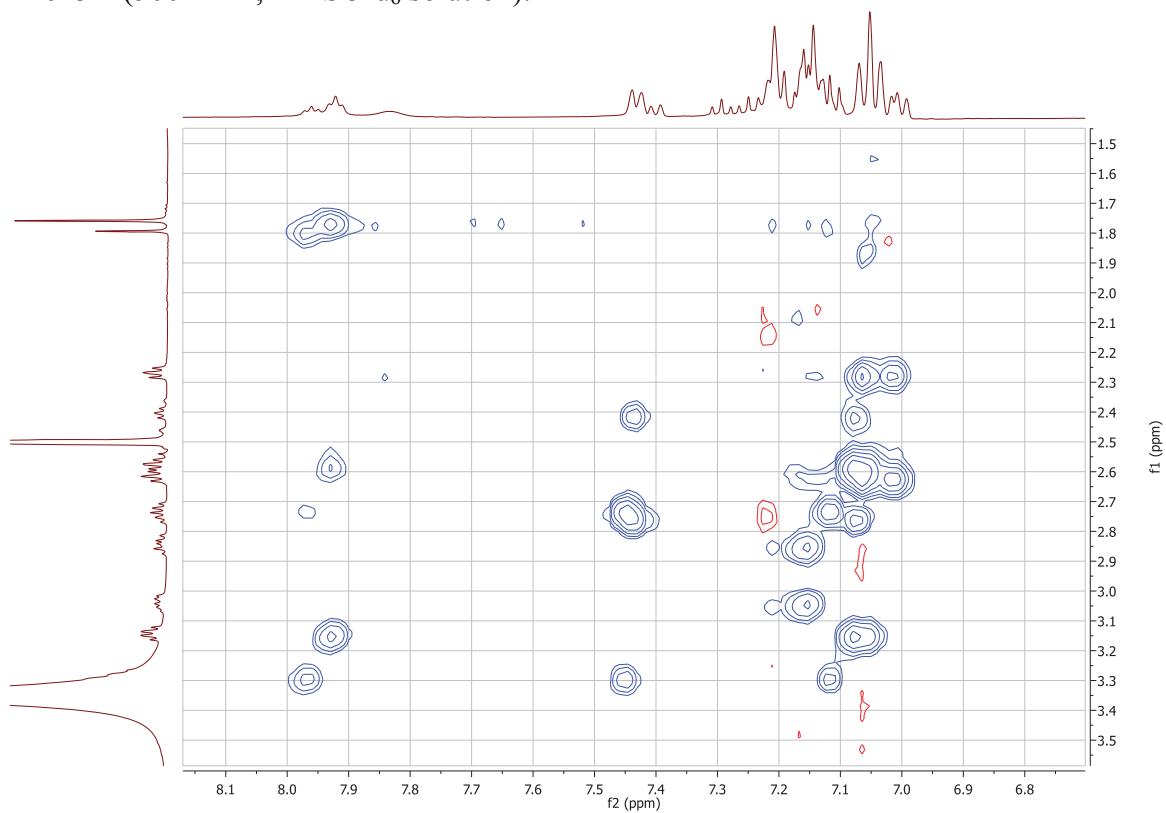
Figure S 31: Expansion of ¹H ROESY NMR spectrum of photoisomerization of compound **6**, Ac-Trigger-Phe-OH (500 MHz, DMSO-d₆ solution).

Figure S 32: Expansion of ^{1}H ROESY NMR spectrum of photoisomerization of compound **6**, Ac-Trigger-Phe-OH (500 MHz, DMSO-d$_6$ solution).

Figure S 33: Expansion of ^{1}H ROESY NMR spectrum of photoisomerization of compound **6**, Ac-Trigger-Phe-OH (500 MHz, DMSO-d$_6$ solution).

7.3. Ac-Trigger-Asp-Phe-OH (7)
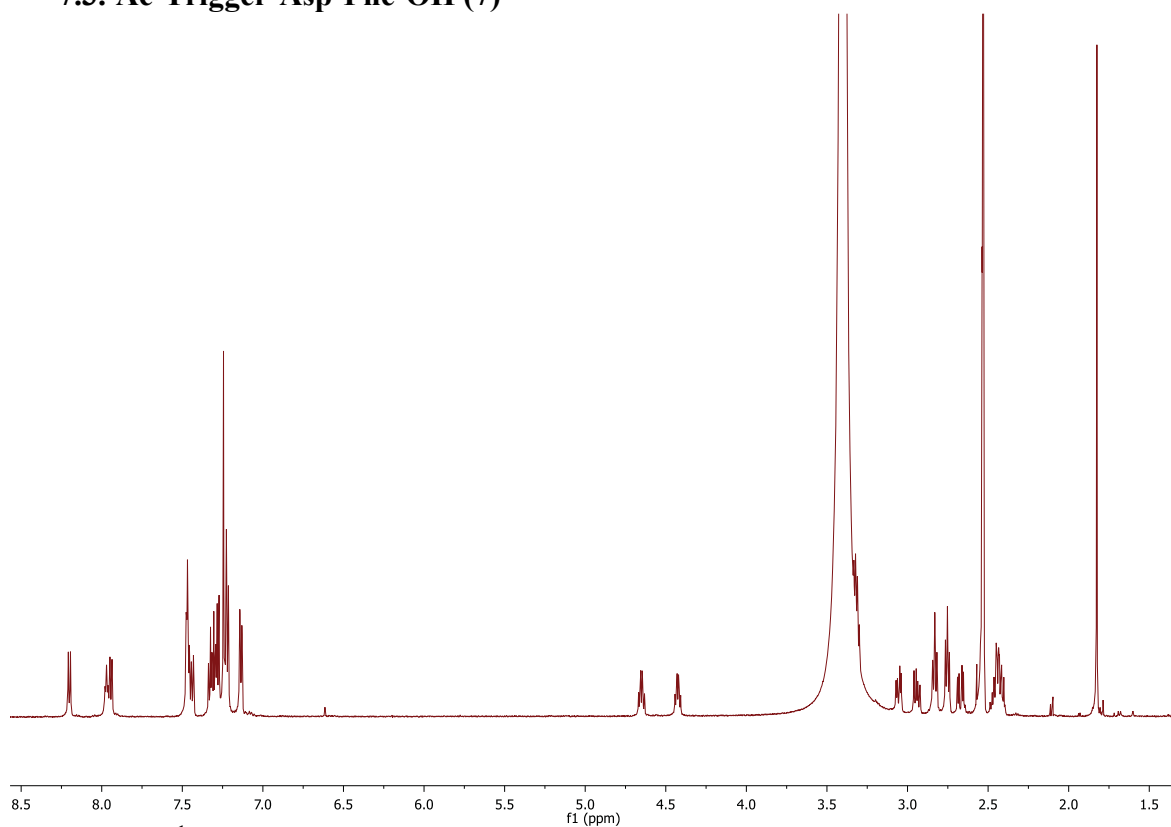
Figure S 34: ^{1}H NMR spectrum of compound **7**, Ac-Trigger-Asp-Phe-OH (600 MHz, DMSO-d$_6$ solution).
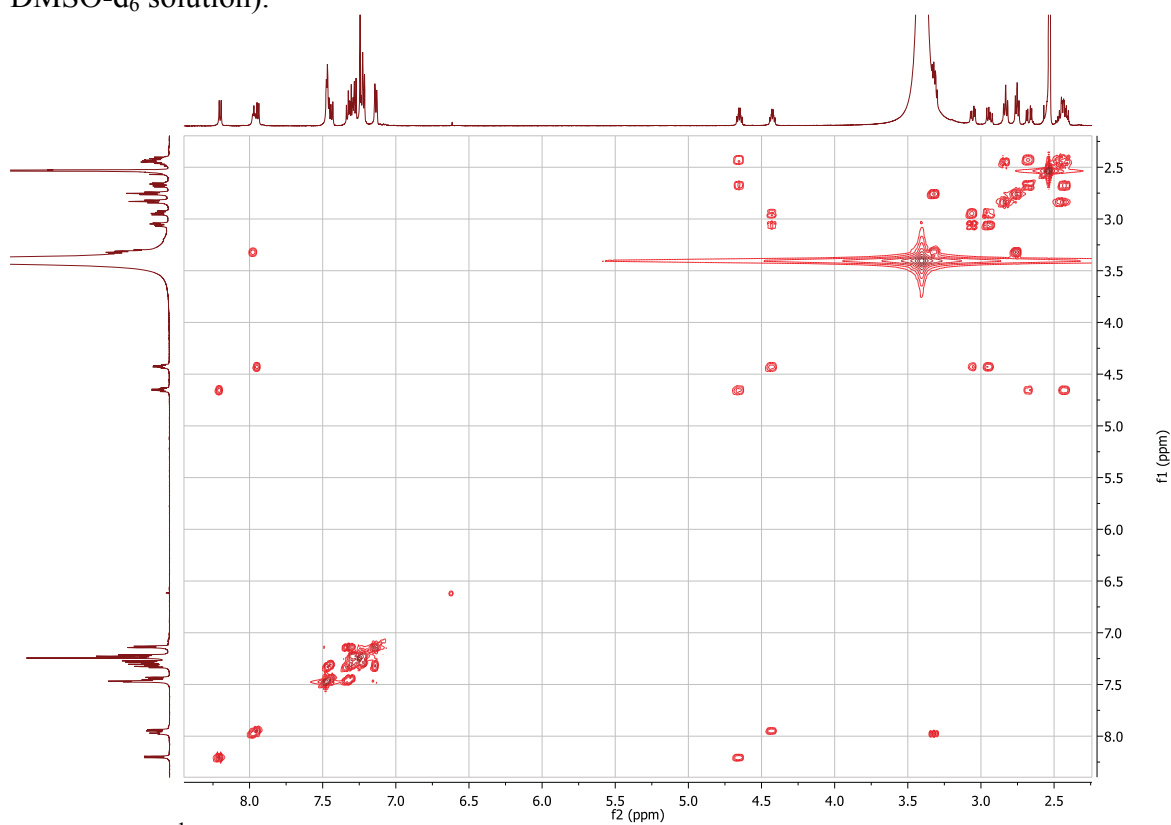
Figure S 35: ^{1}H COSY NMR spectrum of compound **7**, Ac-Trigger-Asp-Phe-OH (600 MHz, DMSO-d$_6$ solution).
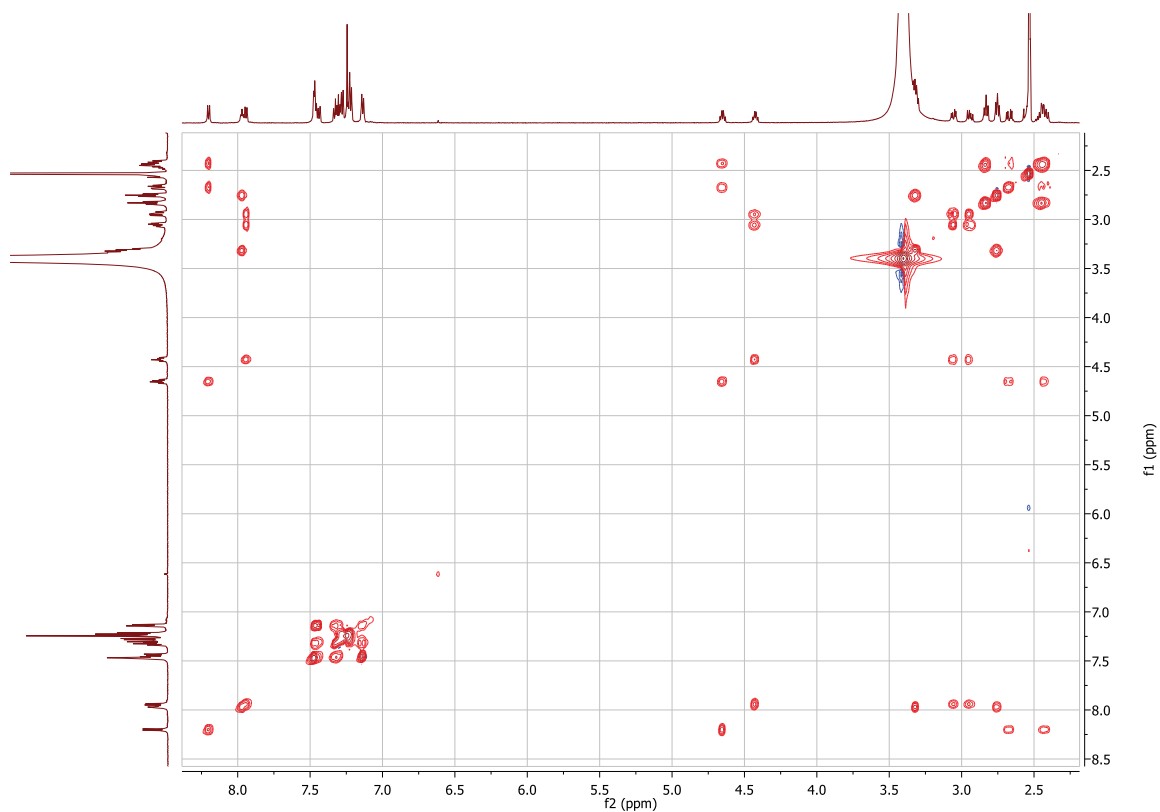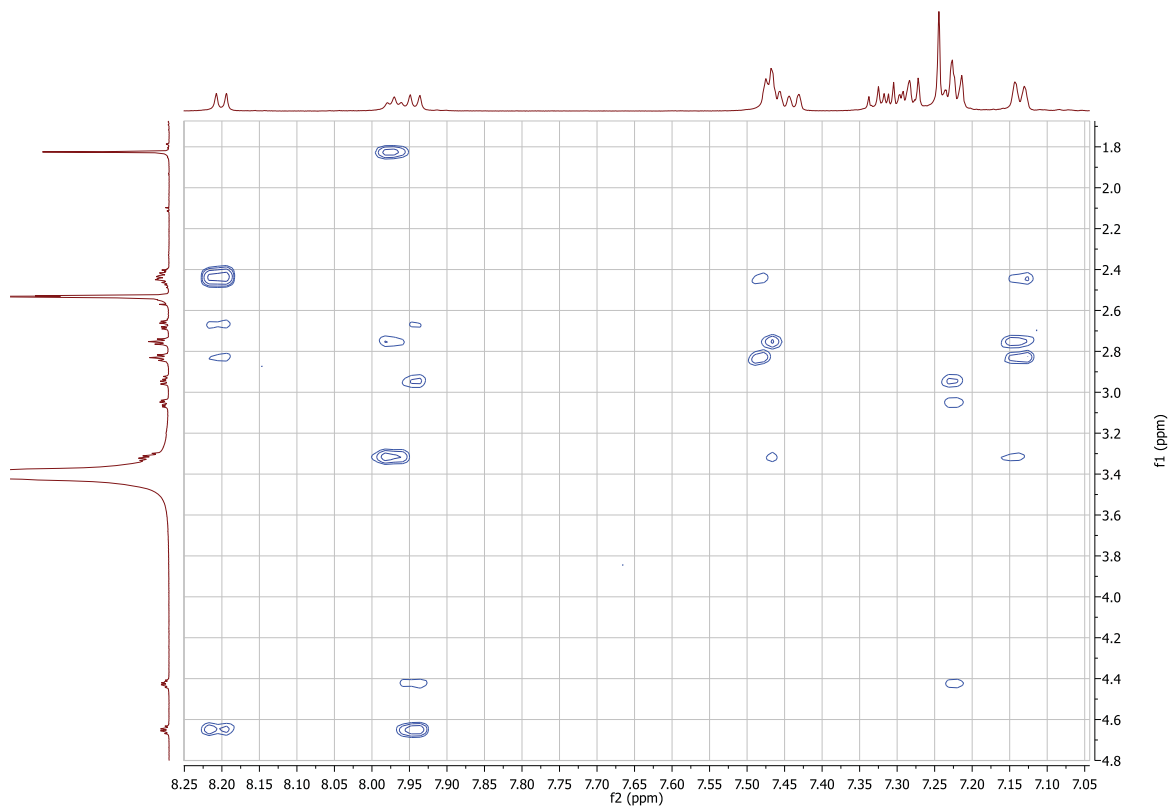
Figure S 36: ^{1}H TOCSY NMR spectrum of compound **7**, Ac-Trigger-Asp-Phe-OH (600 MHz, DMSO-d$_6$ solution).
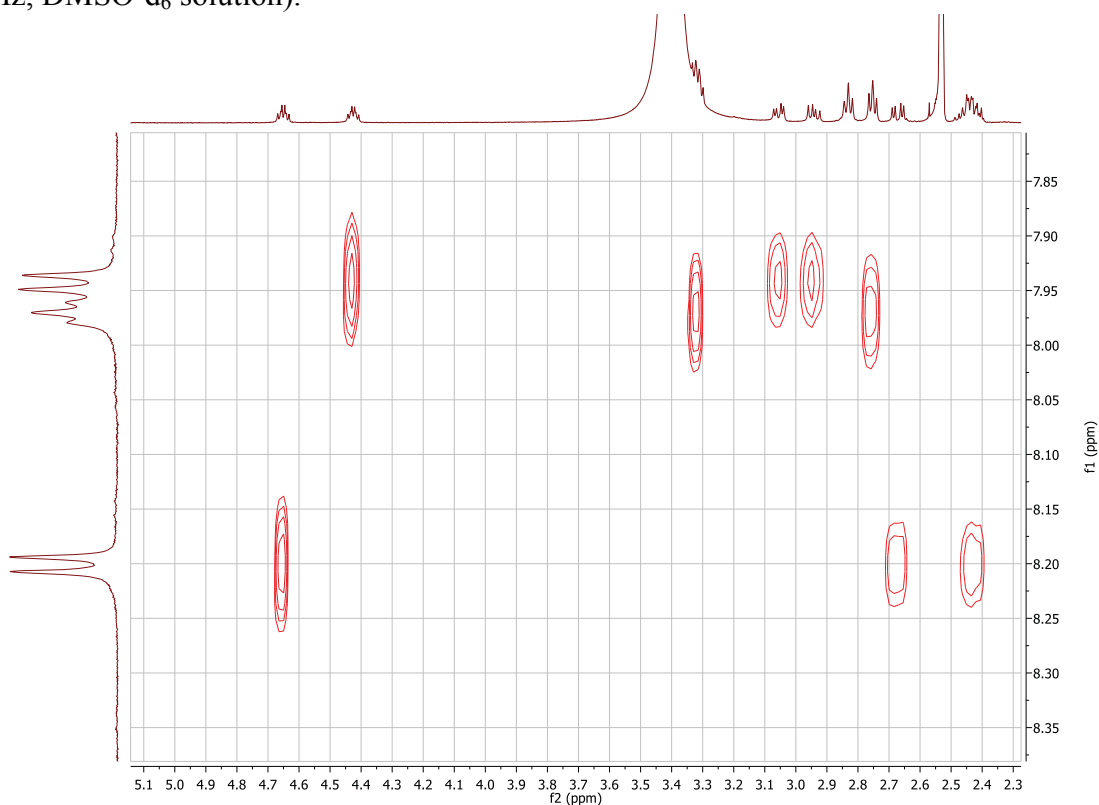
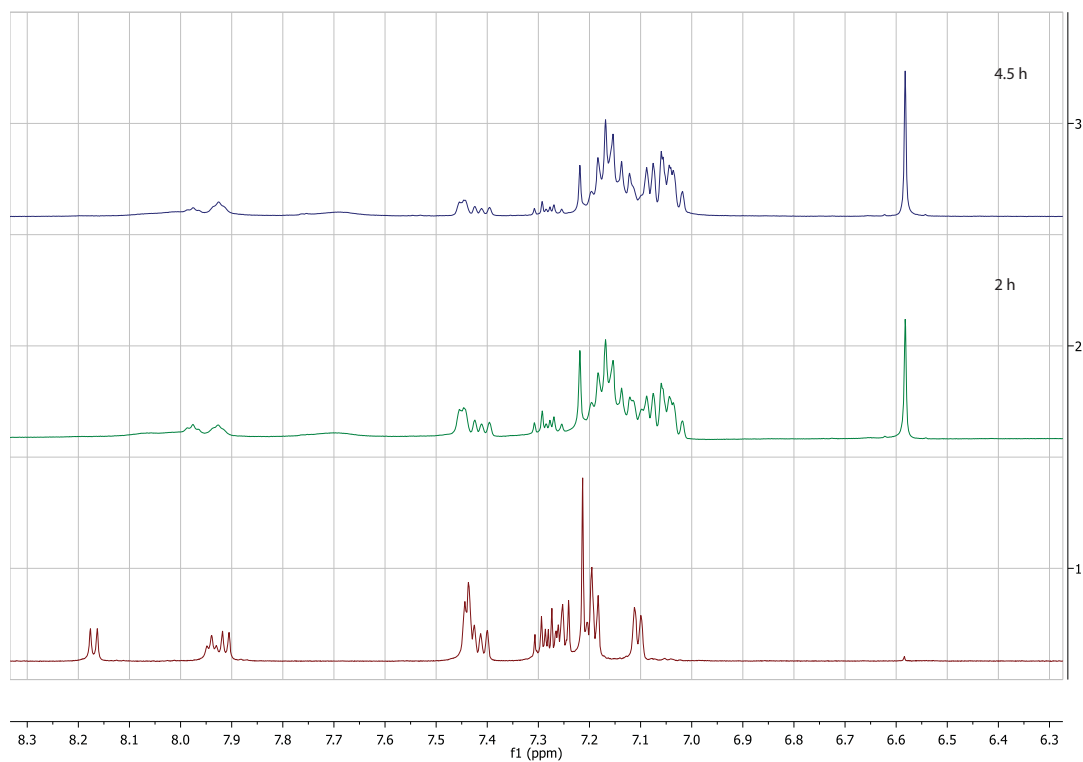Figure S 37: Expansion of ^{1}H TOCSY NMR spectrum of compound **7**, Ac-Trigger-Asp-Phe-OH (600 MHz, DMSO-d$_6$ solution).
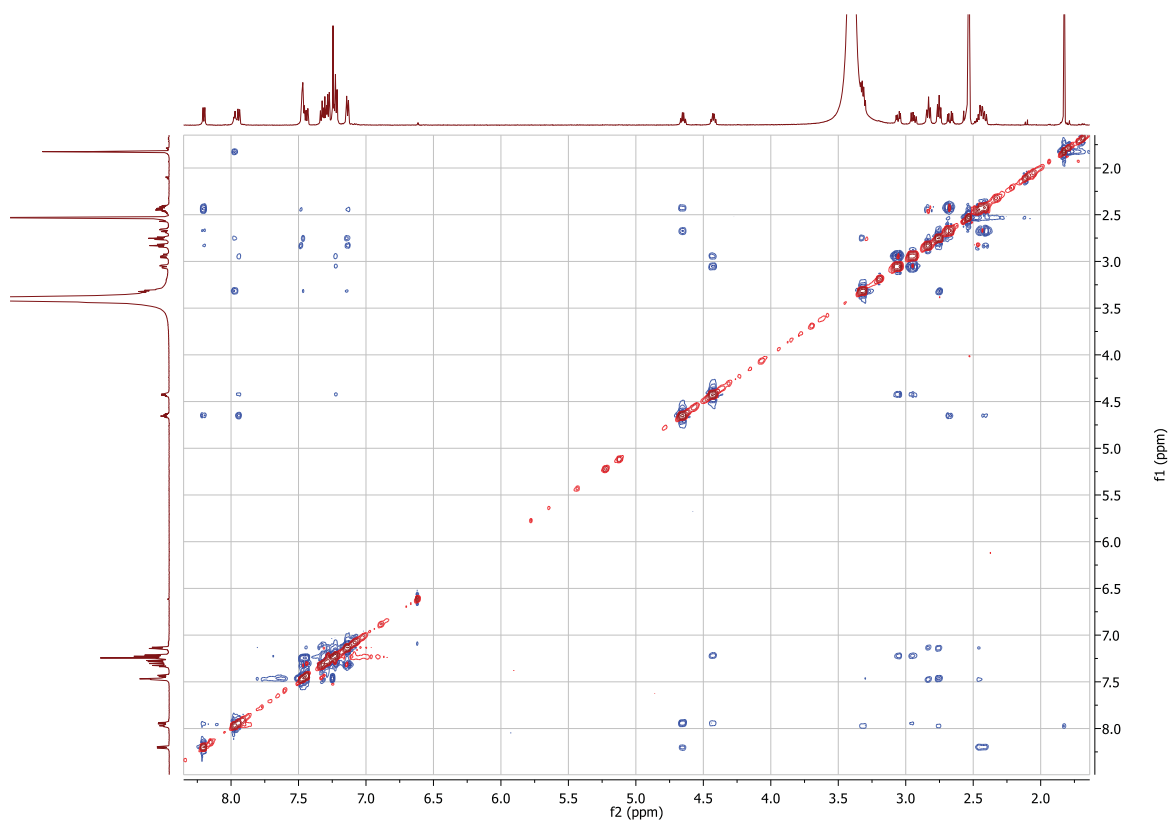
Figure S 38: ^{1}H ROESY NMR spectrum of compound **7**, Ac-Trigger-Asp-Phe-OH (600 MHz, DMSO-d$_6$ solution).

Figure S 39: Expansion of ^{1}H ROESY NMR spectrum of compound **7**, Ac-Trigger-Asp-Phe-OH (600 MHz, DMSO-d$_6$ solution).

Figure S 40: Expansion of ^{1}H NMR spectrum of photoisomerized compound **7**, Ac-Trigger-Asp-Phe-OH (500 MHz, DMSO-d$_6$ solution). Bottom: Starting material **E-7**.
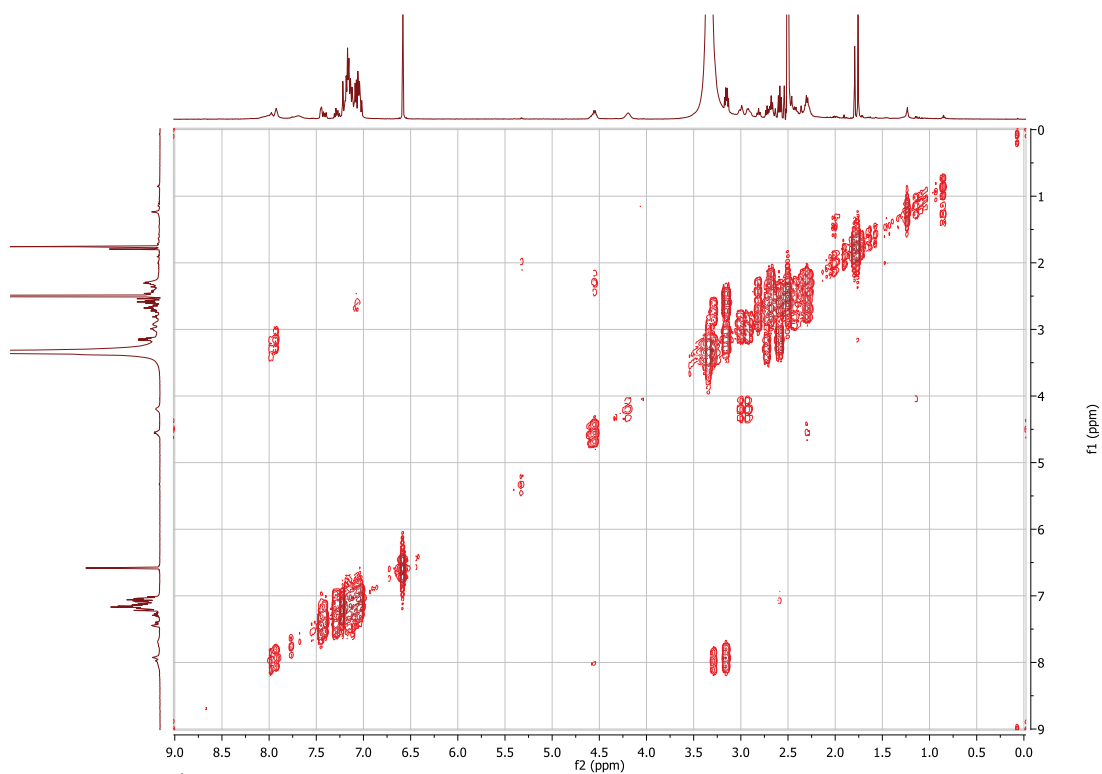

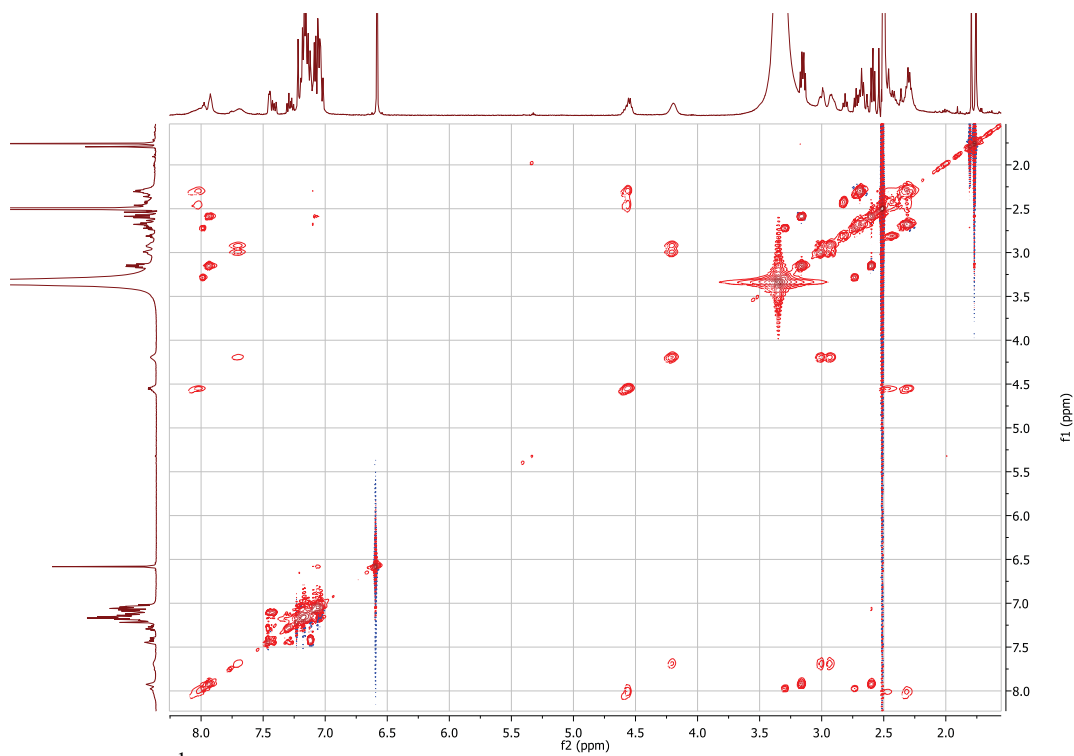Figure S 41: ^{1}H COSY NMR spectrum of photoisomerized compound **7**, Ac-Trigger-Asp-Phe-OH (500 MHz, DMSO-d$_6$ solution).

Figure S 42: ^{1}H TOCSY NMR spectrum of photoisomerized compound **7**, Ac-Trigger-Asp-Phe-OH (500 MHz, DMSO-d$_6$ solution).
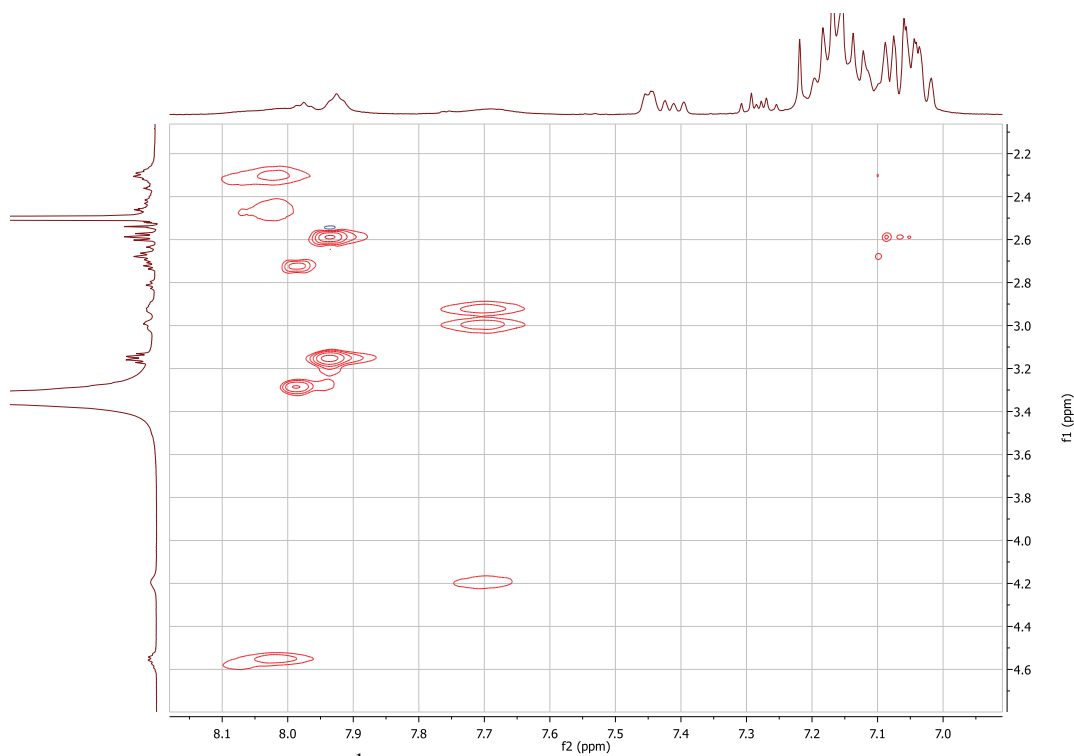

Figure S 43: Expansion of ^{1}H TOCSY NMR spectrum of photoisomerized compound **7**, Ac-Trigger-Asp-Phe-OH (500 MHz, DMSO-d$_6$ solution).
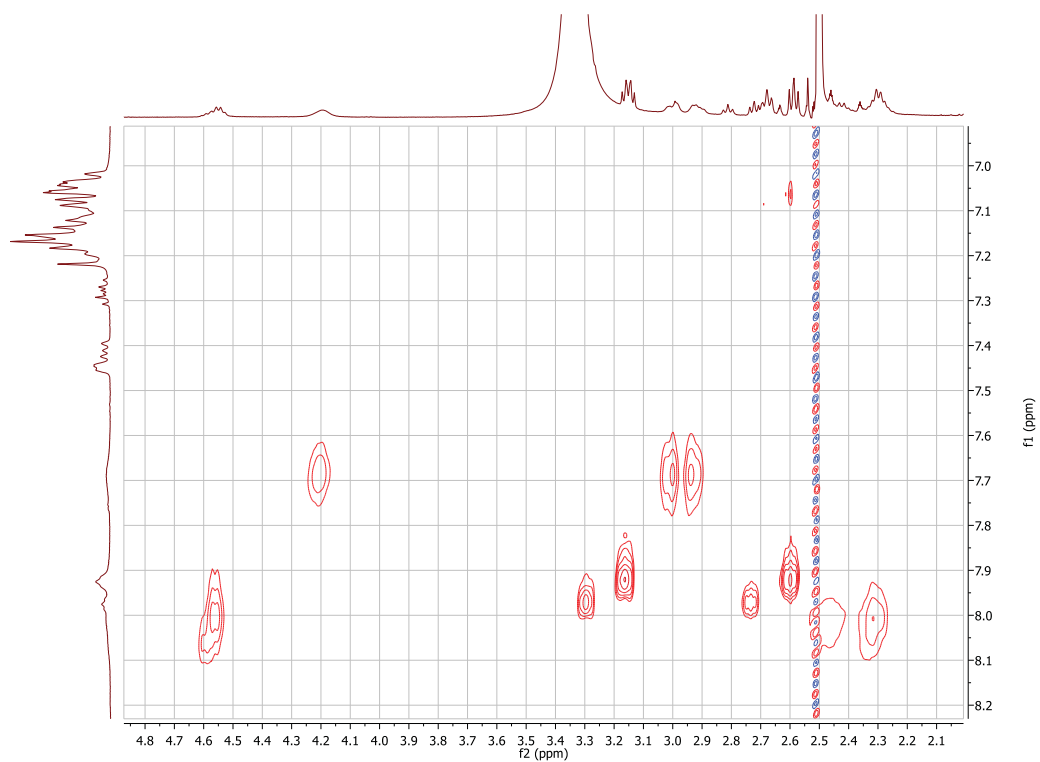
Figure S 44: Expansion of ^{1}H TOCSY NMR spectrum of photoisomerized compound **7**, Ac-Trigger-Asp-Phe-OH (500 MHz, DMSO-d$_6$ solution).
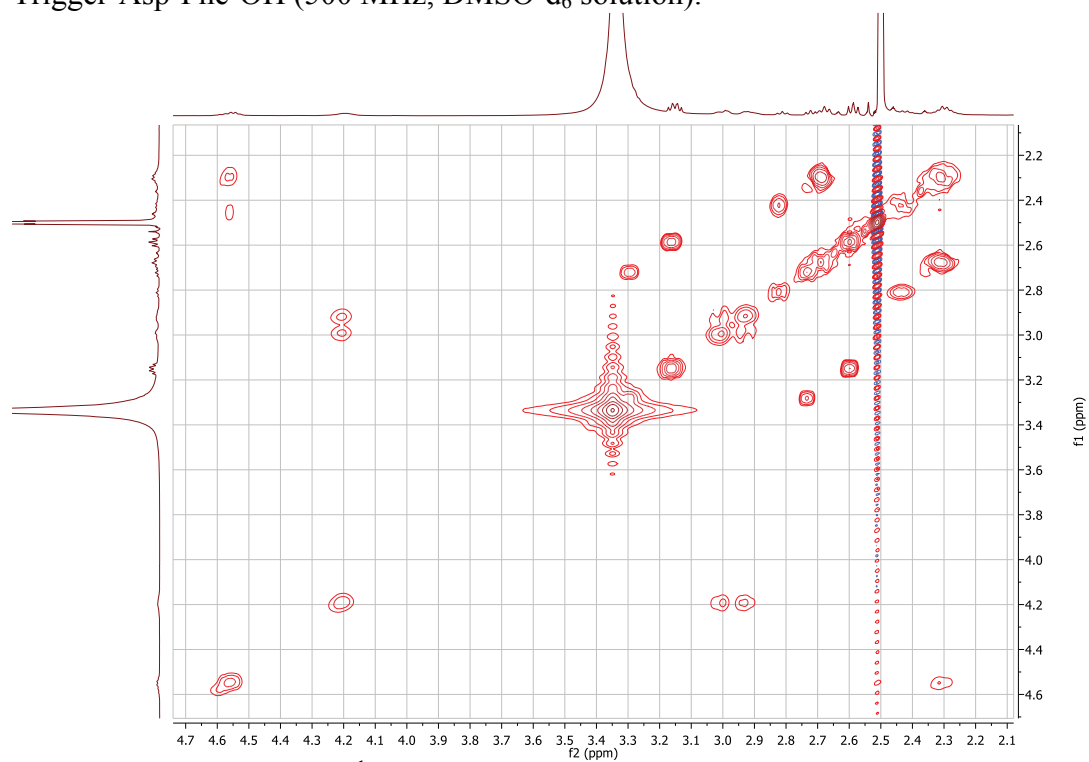

Figure S 45: Expansion of ^{1}H TOCSY NMR spectrum of photoisomerized compound **7**, Ac-Trigger-Asp-Phe-OH (500 MHz, DMSO-d$_6$ solution).
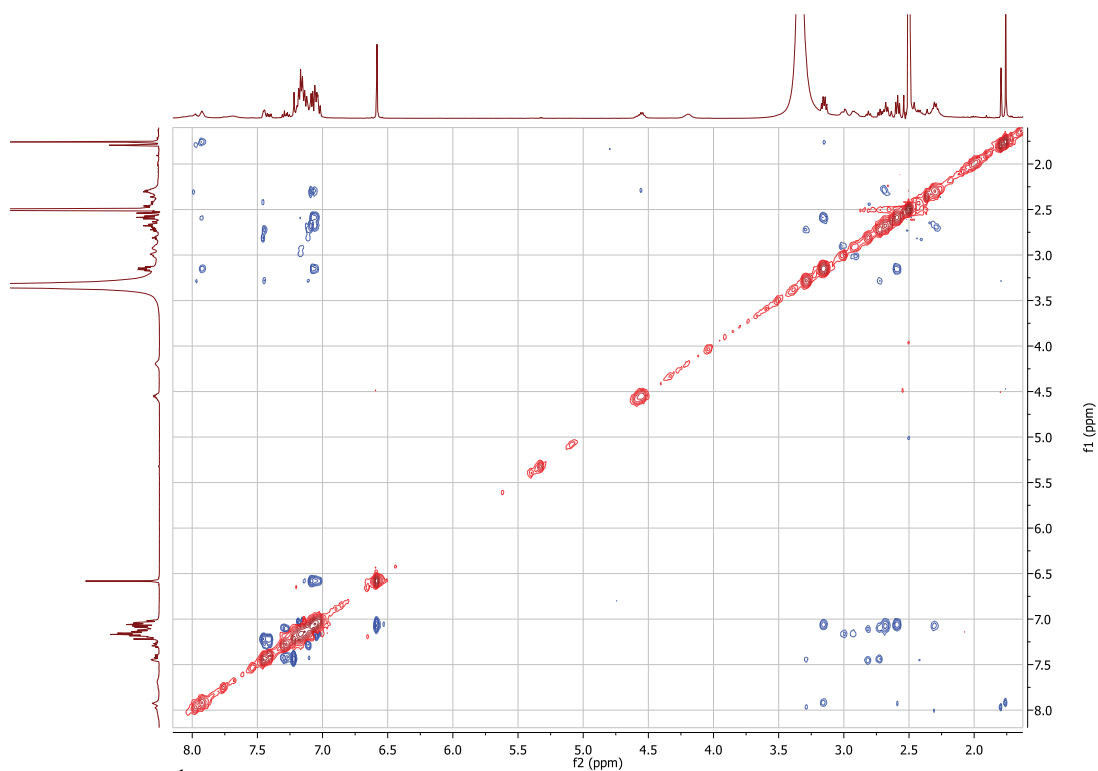
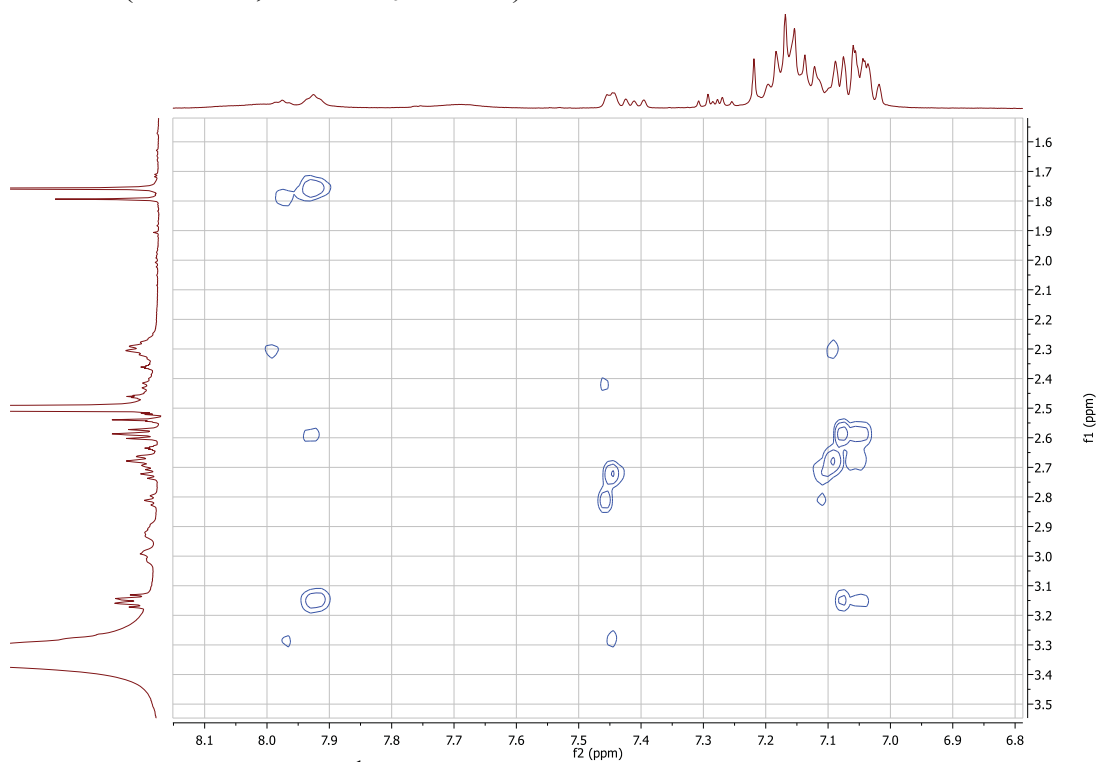Figure S 46: ^{1}H ROESY NMR spectrum of photoisomerized compound **7**, Ac-Trigger-Asp-Phe-OH (500 MHz, DMSO-d$_6$ solution).

Figure S 47: Expansion of ^{1}H ROESY NMR spectrum of photoisomerized compound **7**, Ac-Trigger-Asp-Phe-OH (500 MHz, DMSO-d$_6$ solution).
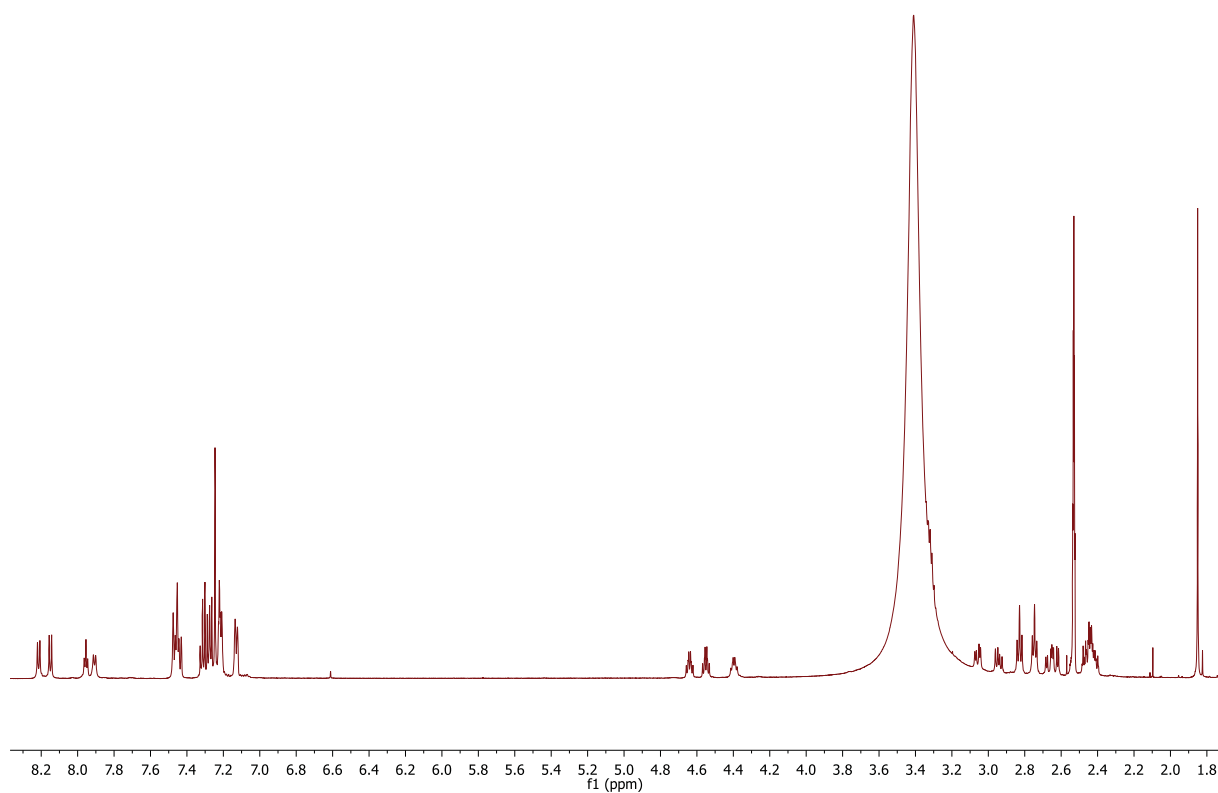
7.4. Ac-Asp-Trigger-Asp-Phe-OH (8)

Figure S 48: ^{1}H NMR spectrum of compound **8**, Ac-Asp-Trigger-Asp-Phe-OH (600 MHz, DMSO-d$_6$ solution).
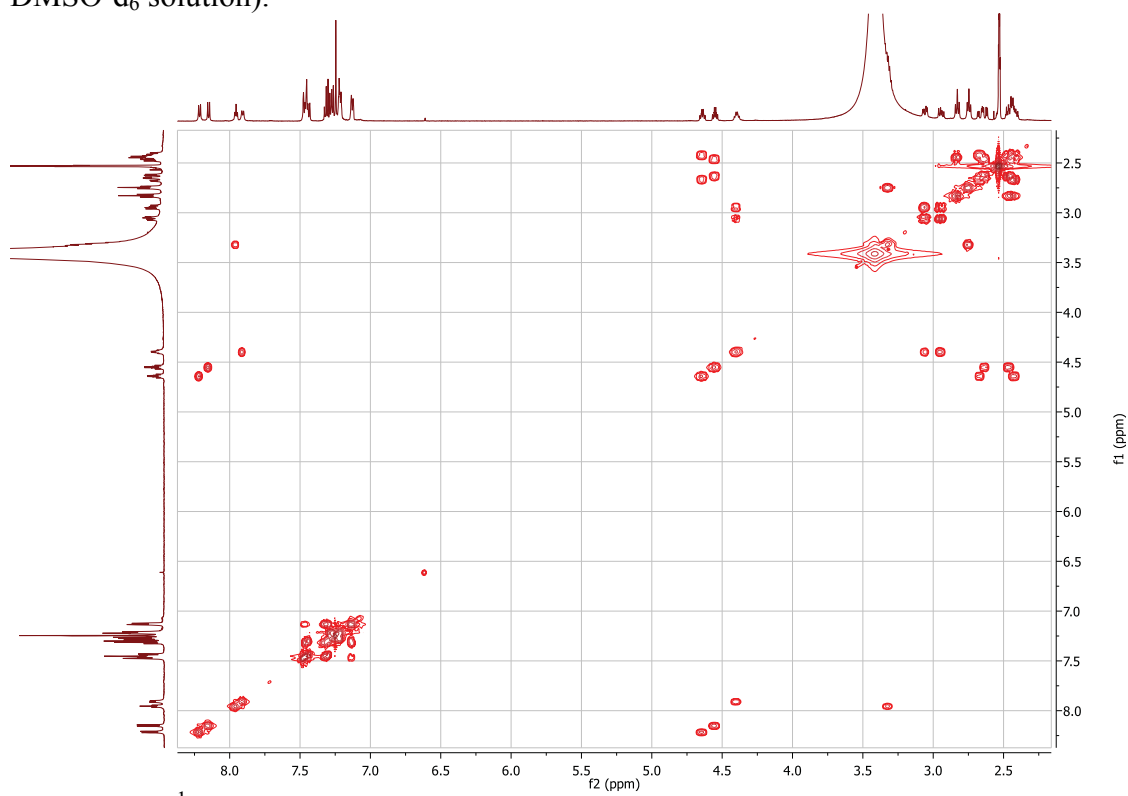

Figure S 49: ^{1}H COSY NMR spectrum of compound **8**, Ac-Asp-Trigger-Asp-Phe-OH (600 MHz, DMSO-d$_6$ solution).
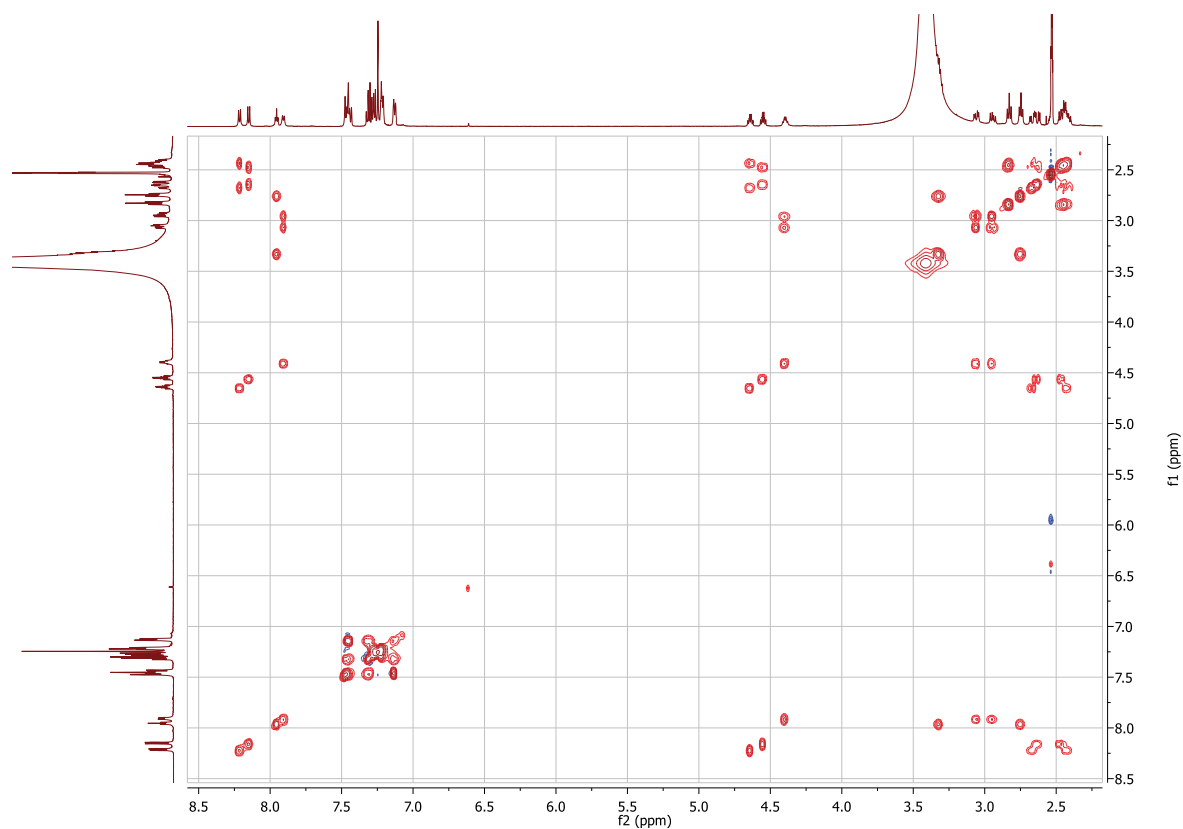
Figure S 50: ^{1}H TOCSY NMR spectrum of compound **8**, Ac-Asp-Trigger-Asp-Phe-OH (600 MHz, DMSO-d$_6$ solution).

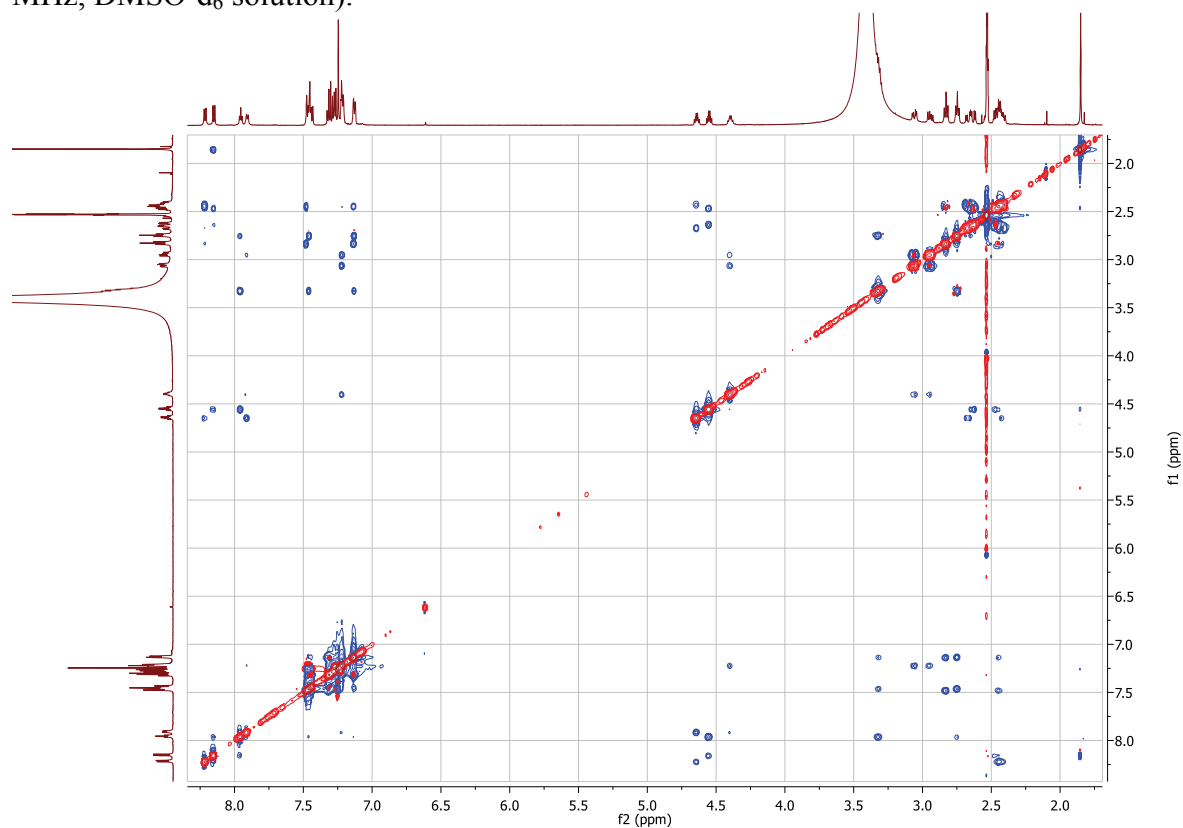Figure S 51: ^{1}H ROESY NMR spectrum of compound **8**, Ac-Asp-Trigger-Asp-Phe-OH (600 MHz, DMSO-d$_6$ solution).
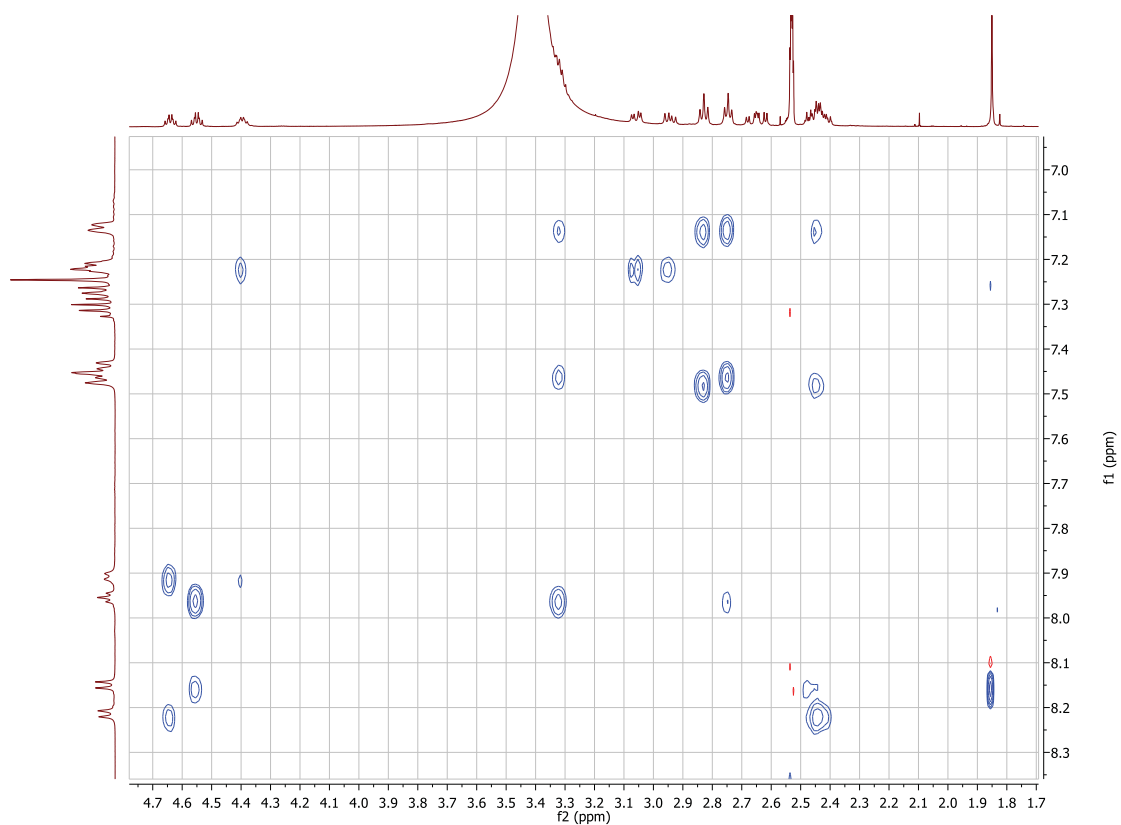
Figure S 52: Expansion of ¹H ROESY NMR spectrum of compound **8**, Ac-Asp-Trigger-Asp-Phe-OH (600 MHz, DMSO-d₆ solution).
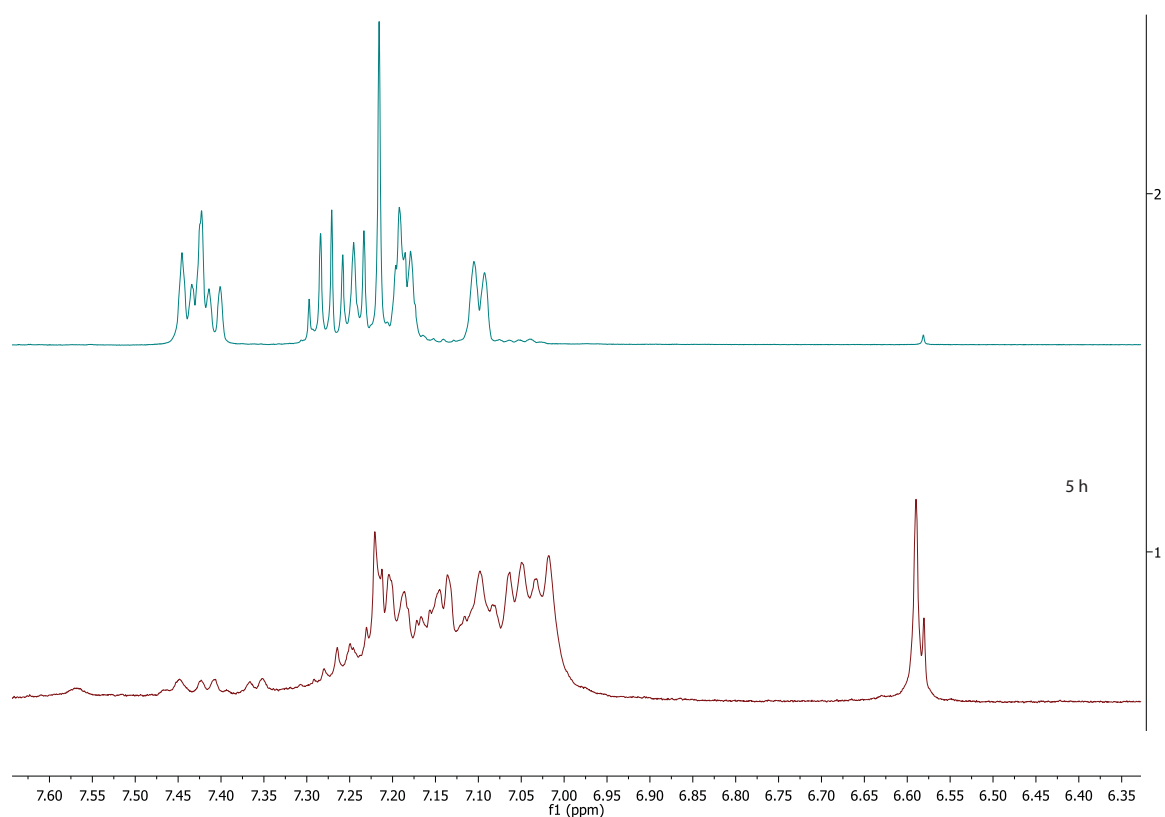
Figure S 53: Expansion of ¹H NMR spectrum of photoisomerized compound **8**, Ac-Trigger-Asp-Phe-OH (500 MHz, DMSO-d₆ solution). Top: Starting material **E-8**.

8. NH Proton Temperature coefficients

6	Ac-Trigger-Phe-OH
7	Ac-Trigger-Asp-Phe-OH
8	Ac-Asp-Trigger-Asp-Phe-OH

Figure S 54: Change of amide proton chemical shifts in compounds **6 – 8** in their respective *Z* and *E* configurations with varied temperature.

Figure S 55: Amide proton temperature coefficients for compounds **6 – 8**.

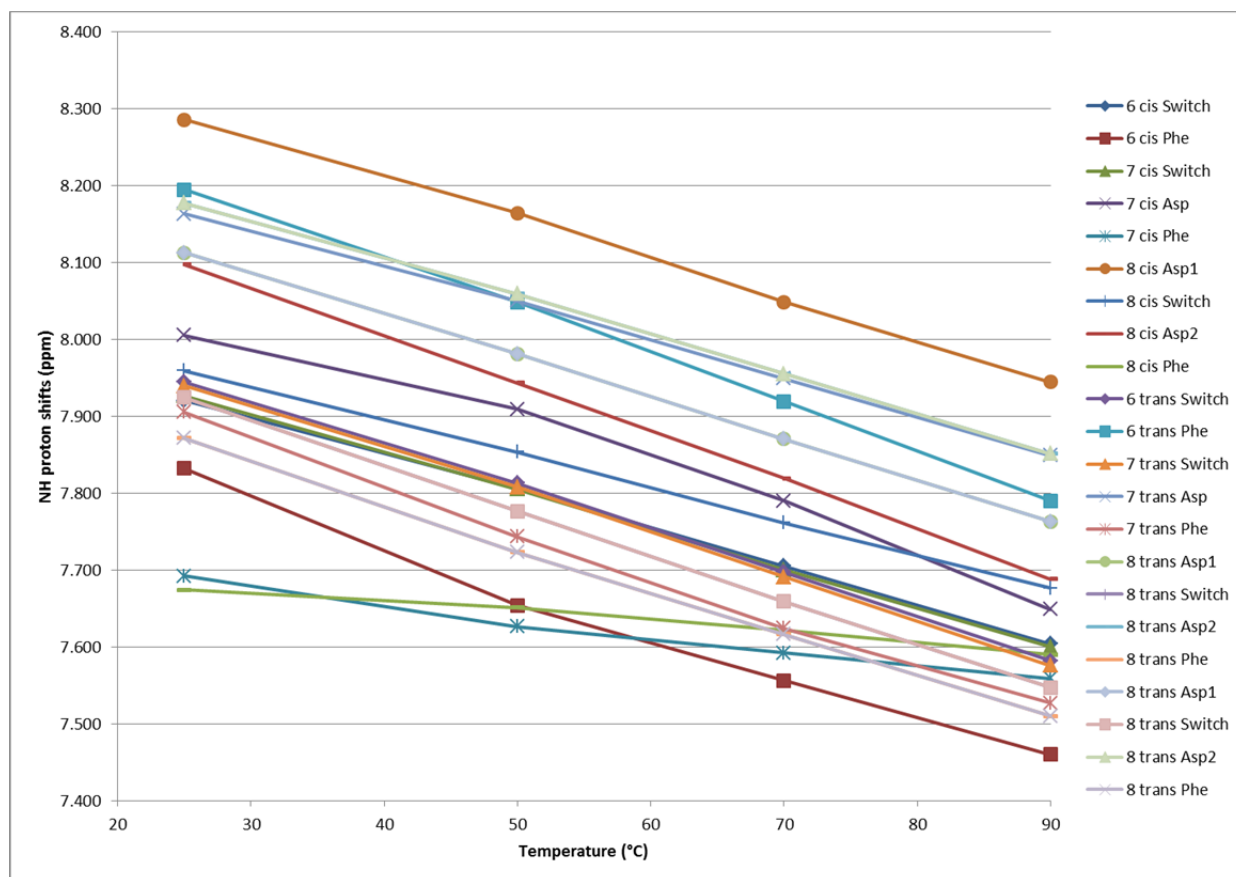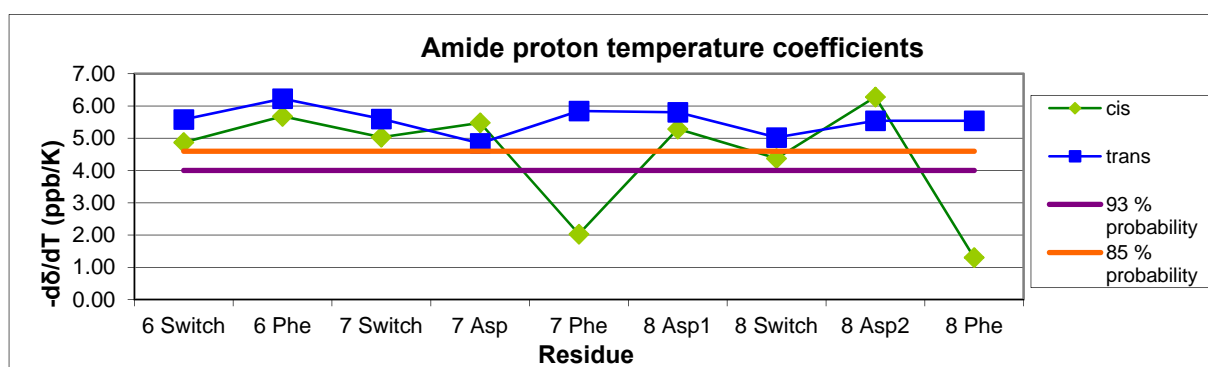Table S 4: Change of amide proton chemical shifts in compounds **6-8** in their respective *Z* and *E* configurations with varied temperature, and the calculated NH-proton temperature coefficients.

δ_{NH} *(ppm)*	25	50	70	90	-dδ/dT (ppb/K)	r2	P(H-bond)
6 Z Trigger	7,920	7,806	7,705	7,604	4,87	0,999	
6 Z Phe	7,832	7,654	7,556	7,460	5,68	0,989	
7 Z Trigger	7,926	7,805	7,700	7,600	5,03	1,000	
7 Z Asp	8,005	7,909	7,790	7,649	5,48	0,981	
7 Z Phe	7,692	7,626	7,592	7,559	2,03	0,984	>93%
8 Z Asp1	8,285	8,164	8,048	7,944	5,29	0,999	
8 Z Trigger	7,959	7,853	7,761	7,676	4,37	1,000	>85%
8 Z Asp2	8,097	7,943	7,819	7,688	6,28	1,000	
8 Z Phe	7,674	7,651	7,621	7,590	1,30	0,985	>93%
6 E Trigger	7,944	7,813	7,697	7,582	5,58	0,999	
6 E Phe	8,194	8,048	7,919	7,79	6,23	0,999	
7 E Trigger	7,939	7,808	7,691	7,576	5,60	0,999	
7 E Asp	8,163	8,05	7,949	7,849	4,84	0,999	
7 E Phe	7,905	7,743	7,624	7,527	5,85	0,996	
8 E Asp1	8,112	7,981	7,87	7,763	5,38	1,000	
8 E Trigger	7,924	7,776	7,659	7,547	5,81	1,000	
8 E Asp2	8,177	8,059	7,955	7,851	5,03	0,999	
8 E Phe	7,871	7,723	7,616	7,51	5,54	0,999	
8 E Asp1	8,112	7,981	7,87	7,763	5,38	1,000	
8 E Trigger	7,924	7,776	7,659	7,547	5,81	1,000	
8 E Asp2	8,177	8,059	7,955	7,851	5,03	0,999	
8 E Phe	7,871	7,723	7,616	7,51	5,54	0,999	

Table S 5: Summary of amide proton temperature coefficients for compounds **6-8**

-dδ/dT (ppb/K)	Z	E
6 Trigger	4,87	5,58
6 Phe	5,68	6,23
7 Trigger	5,03	5,60
7 Asp	5,48	4,84
7 Phe	2,03	5,85
8 Asp1	5,29	5,81
8 Trigger	4,37	5,03
8 Asp2	6,28	5,54
8 Phe	1,30	5,54

9. References

1. M. Erdélyi, A. Karlén, and A. Gogoll, *Chem. Eur. J.* **2006**, *12*, 403.
2. E. D. Matveeva, T. A. Podrugina, N. Yu. Morozkina, O. N. Zefirova, I. V. Seregin, S. O. Bachurin, R. Pellicciari, and N. S. Zefirov; *Russ. J. Org. Chem.* **2002**, *38*, 1769.
3. M. H. Roehrl, J. Y. Wang, G. Wagner, *Biochemistry* **2004**, *43*, 16056.
4. Y. Yokoyama; T. Koizumi; O. Kikuchi, *Chem. Lett.* **1991**, 2205.